

COLLINSVILLE SOLAR THERMAL PROJECT

SOLAR MIRROR CLEANING REQUIREMENTS

Report 3



ARENA



Australian Government
Australian Renewable Energy Agency

Prepared for
RATCH-Australia Corporation



This project is supported by funding from the Australian Government under the Australian Renewable Energy Agency (ARENA).

Chief Investigators

Paul Meredith, Global Change Institute

Craig Froome, Global Change Institute

Hal Gurgenci, School of Mechanical and Mining Engineering

John Foster, School of Economics

Tapan Saha, School of Information Technology and Electrical Engineering

Authors

Shengzhe Yu

Zhiqiang Guan

Hal Gurgenci, h.gurgenci@uq.edu.au

This report is one in a series of seven reports undertaken in relation to the Collinsville Solar Thermal Project. The series of reports included:

- 1. Yield forecasting*
- 2. Dispatch forecasting*
- 3. Solar mirror cleaning requirements*
- 4. Optimisation of operational regime*
- 5. Power system assessment*
- 6. Energy economics*
- 7. Fossil fuel boiler integration*

Copies of all reports can be found at www.gci.uq.edu.au

These reports are part of a collaborative research agreement between RATCH Australia and the Global Change Institute at The University of Queensland (UQ) partially funded by the Australian Renewable Energy Agency (ARENA). The research was primarily undertaken through the Energy Economics and Management Group, School of Economics, School of Mechanical and Mining Engineering and the Power and Energy Systems Group, School of Information Technology and Electrical Engineering.

1 Executive Summary

Dust particles on mirror surfaces deflect or scatter incident light rays. For a CSP solar mirror, even a small deflection will cause the rays to miss the receiver and not be collected. As a result, the solar power plant will lose production. Therefore, regular mirror cleaning forms an important part of the operation and maintenance (O&M) activities in solar thermal power plants to maintain high reflectivity of the mirrors.

Effective cleaning of the solar mirror can maintain high reflectivity with significant impact on the power plant economy. The influence of dust on the reflectance of solar mirrors is a complex function of dust deposition behaviour, the accumulation rates and the exposure conditions. Therefore, dust composition, particulate size of the dust, relative humidity, rainfall, wind, temperature, and the materials of the mirrors used are the most important parameters in optimizing solar mirror cleaning.

A dust monitor has been installed in Collinsville Power Station to collect the data of dust rates, relative humidity, wind condition and temperature for about a year in this study to determine the level of soiling at the Collinsville Energy Park. Dust samples were collected on filters which were inserted in the monitor. By analysing the real time dust data as well as the dust samples collected on site, the dust characterization was conducted. The following conclusions were made.

- The highest monthly average dust was about $31.5\mu\text{g}/\text{m}^3$ in October and the highest frequency was 898 for the density of $23\mu\text{g}/\text{m}^3$. In average, the dust was about $11\mu\text{g}/\text{m}^3$ in summer, $13\mu\text{g}/\text{m}^3$ in Winter, $14\mu\text{g}/\text{m}^3$ in Autumn and $18\mu\text{g}/\text{m}^3$ in Spring.
- The highest temperature was 44.3°C in summer noon (January period), and the lowest temperature was 3.7°C in the winter night (July period). The average temperature was about 27°C in summer and 15°C in winter.
- Over 90% of wind speeds are lower than 5 m/s during one-year monitoring period. The average wind speed during the one-year monitoring period was about 2 m/s. The high occurrences of wind direction were from the directions between 90° to 180° (South-East wind).
- The average size of dust particles is around $15\mu\text{m}$, and the compositions of the dust are mainly albite and silicon dioxide. Also, some typical particulates (sodium chloride; carnallite; aluminium oxide) were detected.
- The interaction of dust with different mirror materials needed to be quantified in the future work.
- Future study on the most widely used high pressure jet washing system should be focused on the optimum selection of parameters such as water pressure, water flow rate and nozzle type etc.

Contents

| | |
|---|----|
| Chief Investigators..... | 2 |
| Authors | 2 |
| 1 Executive Summary..... | 4 |
| Contents..... | 5 |
| Figures..... | 6 |
| Tables..... | 7 |
| 2 Introduction | 8 |
| 2.1 Plant description | 8 |
| 2.2 Scope of the study..... | 9 |
| 3. Literature review | 10 |
| 3.1 Dust and dust accumulation..... | 10 |
| 3.2 Impact of dust on the performance of solar thermal systems..... | 13 |
| 3.3 Mirror cleaning methods..... | 14 |
| 4. Dust monitoring device installed in Collinsville | 21 |
| 5. Results..... | 29 |
| 5.1 K-factor based on the in-situ calibration | 29 |
| 5.2 Time history of dust concentration | 29 |
| 5.2 Statistic results | 39 |
| 5.3 Estimated source (origin) of dust..... | 45 |
| 5.4 Dust particle size and properties..... | 51 |
| 6. Discussions and conclusions | 71 |
| 7. Suggestions for future work | 71 |
| 6.1 Interaction of Dust and Mirror surface degradation | 71 |
| 6.2 Optimising water spray cleaning | 73 |
| 8. References | 75 |
| Appendix A: Time History of Dust Concentration | 78 |
| Appendix B: Time History of Wind Speed..... | 80 |
| Appendix C: Time History of Wind Direction..... | 81 |
| Appendix D: Time History of Temperature..... | 82 |

Figures

| | |
|--|----|
| Figure 1. Proposed Collinsville Energy Park (3) | 9 |
| Figure 2. Average annual frequency of dust storm in Australia between 1957 to 1984 (5)... | 11 |
| Figure 3. Suspension of particles following an erosion event (8)..... | 12 |
| Figure 4. Quantity of dust accumulated on glass samples installed in eight different orientations with seven tilted angles in an arid location | 12 |
| Figure 5. Reduction in transmittance as a function of dust deposition density | 14 |
| Figure 6. Structures 1 to 4 (from left to right) at OPAC’s outdoor exposing area (25) | 15 |
| Figure 7. Normalized monochromatic specular reflectance for the different cleaning methods applied, after cleaning (25)..... | 15 |
| Figure 8. Normalized monochromatic specular reflectance for the different cleaning methods applied, after cleaning (25)..... | 16 |
| Figure 9. 3D diagram of water pressure and temperature testing results (26)..... | 16 |
| Figure 10. High-pressure water truck cleaning system (27)..... | 17 |
| Figure 11. Cleaning robot operating in GEMASOLAR (27)..... | 18 |
| Figure 12. PARIS prototype | 18 |
| Figure 13. The cleaning system in Shams 1 CSP plant (29) | 19 |
| Figure 14. Mr Twister used in SEGS | 19 |
| Figure 15. The Valent® cleaning system of Laitu Solar (31) | 20 |
| Figure 16. Novatec cleaning robot for Fresnel mirror (32)..... | 20 |
| Figure 17. Water washing system used in Kuraymat Solar Power plant (33) | 21 |
| Figure 18. Location of the dust monitor in Collinsville power station | 23 |
| Figure 19. The dust monitor installed in Collinsville | 24 |
| Figure 20. Light scatter due to airborne particulate | 25 |
| Figure 21. Dust sample collection with 47mm filter. | 26 |
| Figure 22. 034B wind sensor used in Collinsville..... | 26 |
| Figure 23. 3G modem used in the monitor | 27 |
| Figure 24. Relative humidity sensor used in Collinsville. | 27 |
| Figure 25. Time history of dust concentration for four typical periods in different seasons. | 32 |
| Figure 26. Time history of dust concentration in the period when dust sample was collected with filter (20/03/14 – 31/03/14) | 33 |
| Figure 27. Time history of dust concentration for three typical days..... | 34 |
| Figure 28. Time history of dust concentration for two typical weeks | 35 |
| Figure 29. Time history of dust concentration between 23/04/14 and 12/05/14..... | 35 |
| Figure 30. Wind speed and direction on 24/04/14, 05/05/14 and 11/05/14 | 36 |
| Figure 31. Monthly average temperature variation in Collinsville..... | 36 |
| Figure 32. Average dust concentration in Collinsville | 37 |
| Figure 33. Average wind speed during 24 hours and one-year period..... | 37 |
| Figure 40. Histogram of Wind Direction in April 2014..... | 42 |
| Figure 41. Distribution of wind speed in April 2014 | 42 |
| Figure 42. Relations of dust concentration and wind speed in October 2013..... | 43 |
| Figure 44. Relations of dust concentration and wind direction in October 2013..... | 44 |
| Figure 45. Relations of dust concentration and wind direction in May 2013..... | 45 |
| Figure 46. Relation of wind speed and high concentration in September 2013..... | 46 |
| Figure 47. Relation of wind speed and high concentration in October 2013..... | 46 |

| | |
|---|----|
| Figure 48. Relation of wind speed and high concentration in December 2013 | 47 |
| Figure 49. Relation of wind direction and high concentration in September 2013 | 47 |
| Figure 50. Relation of wind direction and high concentration in October 2013..... | 48 |
| Figure 51. Relation of wind direction and high concentration in December 2013 | 48 |
| Figure 52. Frequency of wind direction in September 2013 (>15µg/m ³)..... | 49 |
| Figure 53. Frequency of wind direction in October 2013 (>15µg/m ³) | 50 |
| Figure 54. Frequency of wind direction in December 2013 (>15µg/m ³)..... | 50 |
| Figure 55. Surrounding environment of dust monitor | 51 |
| Figure 56. Dust samples for property analysis..... | 52 |
| Figure 57. Electron image of the unused filter | 52 |
| Figure 58. Electron image of filter from December 13 | 54 |
| Figure 59. Electron image of filter from January 2014 | 56 |
| Figure 60. Electron image of dust collected in March 2014..... | 59 |
| Figure 61. Electron image based on the dust sample collected in April 14 | 64 |
| Figure 62. Electron image of dust sample from UQ monitor | 67 |
| Figure 66. Proposed mirror cleaning test in Gatton wind tunnel | 74 |
| Figure 67. PDPA located in Gatton wind tunnel..... | 74 |

Tables

| | |
|---|----|
| Table 1. A brief comparison of the two systems..... | 22 |
| Table 2. Data file shows information collected by the dust monitor | 28 |
| Table 3. Memory capacity of the E-Sampler..... | 30 |
| Table 4. Composition of the unused filter | 53 |
| Table 5. Dust composition in December 2013..... | 55 |
| Table 6. Composition of cubic dust particles collected in January 2014 | 56 |
| Table 7. Composition of stick dust particles collected in January 2014 | 57 |
| Table 8. Composition of other uneven dust particles in January 2014..... | 58 |
| Table 9. Composition of large particle size based on the dust sample collected in March 2014 | 60 |
| Table 10. Composition of cubic particles of the dust collected in March 2014 | 61 |
| Table 11. Composition of the stick particles based on the dust sample collected in March 2014 | 62 |
| Table 12. Composition of the uneven particles based on the dust sample collected in March 2014 | 63 |
| Table 13. Composition of large particles based on the dust sample collected in April 2014 | 65 |
| Table 14. Composition of fine particles based on the dust sample collected in April 2014. | 66 |
| Table 15. Composition of cube particle with the dust sample collected in UQ monitor | 68 |
| Table 16. Composition of the largest particle with the dust sample collected in UQ monitor | 69 |
| Table 17. Composition of the uneven particles with the dust sample collected in UQ monitor | 70 |

2 Introduction

The most common effect of a dust particle on mirror surfaces is to deflect or scatter incident light rays. For a CSP solar mirror, even a small deflection will cause the rays to miss the receiver and not be collected (1). As a result, the solar power plant will lose production. Therefore, regular mirror cleaning forms an important part of the operation and maintenance (O&M) activities in solar thermal power plants to maintain high reflectivity of the mirrors.

Studies show that the quantity of dust and its characteristic are site specific. Effects of dust on the reflectance of solar mirrors are a complex phenomenon. One of the most important factors is dust composition, and it will directly contribute to the rate and natural of dust accumulation on solar mirrors. Other factors include particulate size of the dust, the materials of the mirrors used, as well as exposure ambient conditions like relative humidity, rainfall, wind, and temperature. Therefore, effective cleaning (method and frequency) is site specific: it depends on the dust load and the dust property at the specific site.

2.1 Plant description

Collinsville Power Station is located 90km south-west of Bowen and 4km west of Collinsville, Queensland and is wholly owned by RATCH-Australia. The power station was operated until December 2012 fuelled by locally mined coal and with a total output of 180 MW (4x30 MW and 1x 60 MW generator units). The four 30 MW steam turbines were commissioned in 1968 and the 60 MW machine was later commissioned in 1976.

Carbon Monitoring for Action estimated Collinsville power station emitted 1.34 million tonnes of greenhouse gases each year as a result of burning coal (2). The plan to close the Collinsville Power Station raises the opportunity for solar power in Collinsville which is an ideal site for base load solar power generation as it is very close to a skilled workforce, and with high voltage power lines connecting to the coastal grid. In 2010, as part of the Australian Government's Solar Flagship Project, RATCH-Australia is actively investigating options to redevelop the site into Collinsville Energy Park with one or more new forms of electricity generation, including solar thermal, solar photovoltaic and gas generation. The Collinsville coal-fired power station is now closed and is under care and maintenance by RATCH-Australia.

The proposed new Collinsville Energy Park includes two stages of development: In the stage 1 development, the Solar Photovoltaic (PV) Power Station will involve a 20 - 30 MW solar panel based facility at the site; while the stage 2 will involve a 30 MW hybrid solar thermal power station. The locations of the Solar Photovoltaic (PV) and the hybrid solar thermal (CSP technology) stations are shown in Figure 1 (3).

As of 20 February 2013, Ratch Corporation (the operator of the plant) is partnering with the University of Queensland to investigate replacing all the coal-fired power generators with solar thermal generators. Mirror cleaning is part of this study.



Figure 1. Proposed Collinsville Energy Park (3)

It should be noted that there is an open-cut coal mine owned by the NCA Joint Venture near the Collinsville power plant. Medium volatile hard coking coal and medium volatile thermal coal is mined from the open-cut. Run of Mine (ROM) coal production is 6.0 million tonnes per annum (Mtpa). The operating dust from the open-cut coal mine is a major concern for the solar mirror cleaning.

2.2 Scope of the study

Since the effective mirror cleaning (method and frequency) is site specific, dust in Collinsville need to be characterised and its ambient conditions need to be identified before an effective mirror cleaning method can be selected.

An analysis of dust rates and dust property were undertaken in this study to determine the level of soiling at the Collinsville Energy Park. The results should lead to the development of a cost effective cleaning system for the proposed Collinsville hybrid solar thermal station.

The following forms the scope of this study. A dust monitor was installed in Collinsville site to collect real time dust concentration, wind speed, wind direction, humidity and temperature. Dust samples (for size analysis) were collected on filters which can be inserted in the monitor. After the real time dust data as well as the dust samples have been collected on site, the dust characterisation will be conducted. The followings list the steps involved in the study:

1. Installation of dust monitor in Collinsville
2. Calibration, maintenance of the equipment
3. Dust characterisation:
 - a. Time history of dust concentration during the monitoring periods.
 - b. Dust particle size and properties
 - c. Impact of weather conditions on the dust.
4. Report on dust characterisation and the requirements related to the solar mirror cleaning.

Once the mirror cleaning issues related to dust were identified specific to the Collinsville site, other studies on the effective cleaning of the solar mirror can be recommended.

3. Literature review

Dust deposition on solar mirrors result in power loss for CSP plants. Effective cleaning of the solar mirror can maintain high reflectivity with significant impact on the power plant economy.

The mirror fouling in a CSP/gas hybrid plant can be classified as: dirt, dust and debris; smog and ash; moss and fungus; pollens and leaves; bird and animal droppings; etc. Dirt, dust and debris may be the dominant sources for a CSP/gas power plant. Any cleaning method has to address the significant characteristics of dust such as typically size, distribution, density, shape, composition, chemistry and charge.

Although there are several commercially available cleaning systems for the solar industry using different mechanism in general, it has been identified that automatically controlled high pressure jet washing methods are more cost-effective and are mostly suitable for CSP plants (4).

3.1 Dust and dust accumulation

The influence of dust on the reflectance of solar mirrors is a complex function of dust deposition behaviour, the accumulation rates and the exposure conditions. Effective cleaning of solar mirrors is strongly dependent on dust composition, particulate size of the dust, relative humidity, rainfall, wind, temperature, and the materials of the mirrors used.

Atmospheric dust (aerosols), based on different regions in the world, has a variety of size, constituent and shape and are believed to be the main dust source for solar mirror fouling.

Dust storms tend to foul the mirror surfaces by particulate deposition. There are five regions which have high risk of strong dust storms in Australia (5). Central Queensland is one of them as shown in Figure 2. Collinsville Energy Park has a low risk of strong dust storm and has annual frequency of less than 1/2 according this study. In addition to storm dust, normal airborne dust can also be a problem.

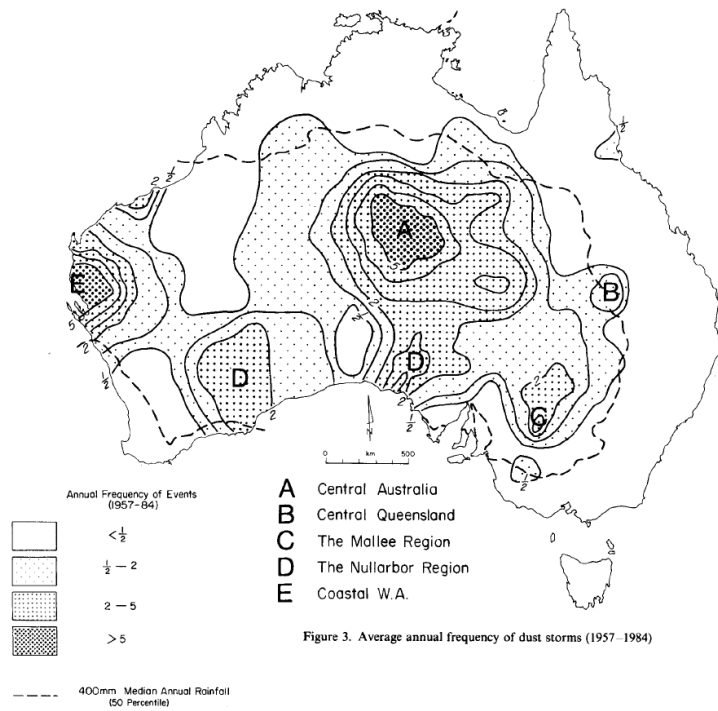


Figure 2. Average annual frequency of dust storm in Australia between 1957 to 1984 (5)

The physical mechanism driving the release of dust from a source into an airstream was studied by several researchers (6, 7). When soils have no adequate protection against wind shear, a particle may dislodge and have a negative effect on the processes of creep and saltation (7). When top soil under the collision of larger particles with other particles during saltation processes and the disturbance, the finer particulates then release to the passing airstream and become airborne (6). The entrainments of particles into the atmosphere are transported by wind.

Previous study showed (8) that the particle sizes range from 20 to 70 μm has short-term suspension and the long-term suspension particles must be less than 20 μm as shown in Figure 3. The particle size deposit on solar mirror should be less than 70 μm if the airborne dust is the main cause for mirror fouling according to this study.

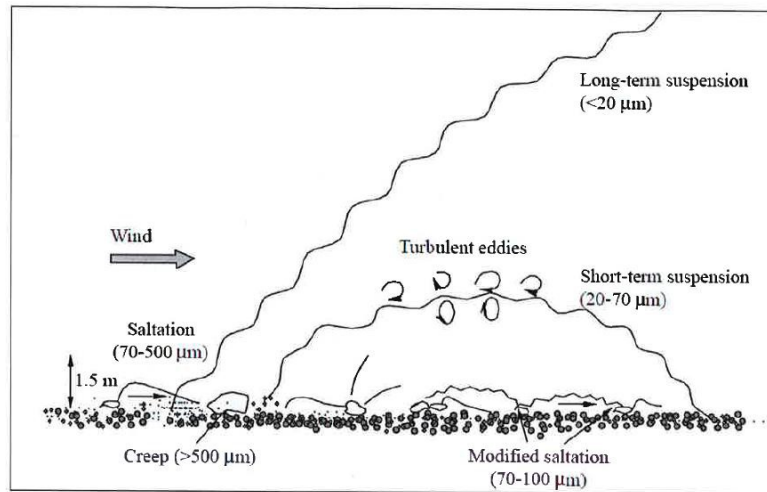


Figure 3. Suspension of particles following an erosion event (8)

Particles are accumulated when falling onto surfaces through gravity, are attracted and held by electrostatic charges, and can be lifted and carried by wind or water droplets. The dust accumulation on the glass samples in a natural condition was investigated by Hamdy et al (9). In the study, eight glass samples were exposed in a natural condition outdoors during the months of December 2004 to June 2005 each with seven different tilt angles. The resulting monthly average of the total suspended particles deposited on the glass surfaces is shown in Fig. 4. They concluded that the dust accumulation decrease as the tilt angle of the glass increases, which is due to dust particles tend to roll from the surface.

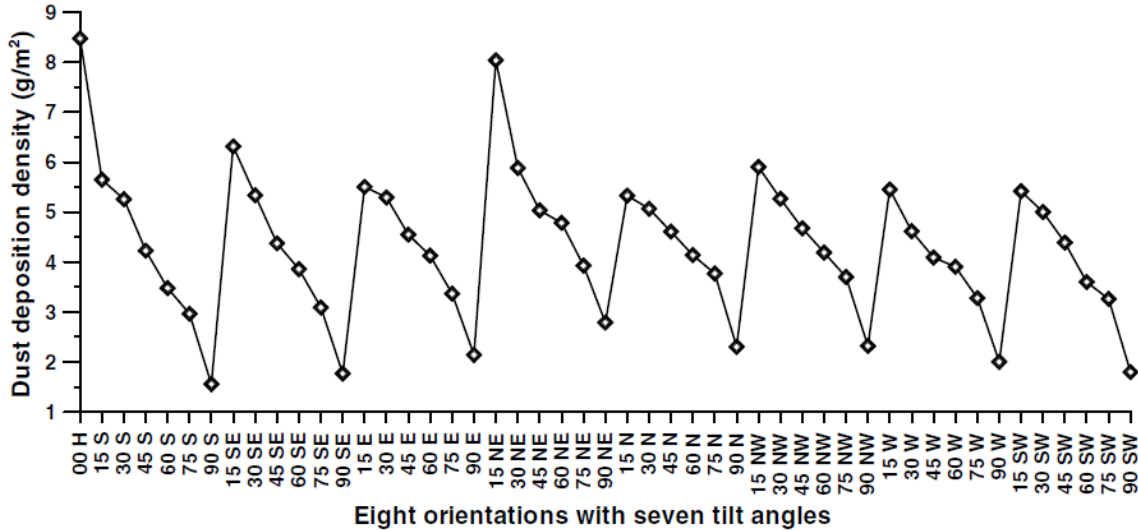


Figure 4. Quantity of dust accumulated on glass samples installed in eight different orientations with seven tilted angles in an arid location

3.2 Impact of dust on the performance of solar thermal systems

Effect of dust on the performance of various solar thermal systems has been carried out by many researchers. The effects of dust accumulation on flat plate solar heat collectors were explored by Hottel and Woertz (10) in 1942 in USA. During the 3-months exposure of the solar heat collectors, the dirt accumulation led to an average of 1% loss of incident solar radiation when the glass plate was placed with the tilt angle of 30°C. Up to 5% reduction of solar radiation was observed by Dietz in 1963 (11) when the tilt angle of the glass plate was oriented from 0°C and 50°C.

Garg (12) found that the normal transmittance of direct solar radiation of glass or plastic sheets at different angles of tilt reduced from 90% to about 45%.

During the 6-month tests conducted in Saudi Arabia, Nimmo and Saed (13) recorded a 26% reduction in efficiency for thermal collectors. Sayigh (14) carried out the similar experiments in the same country in 1978 and found a 30% performance reduction in flat-plate collectors after only three days without cleaning. Sayigh et al (15) later conducted more-extensive tests in Kuwait in 1985. After the mirror samples were exposed in the Kuwait desert up 38-day, the reduction in transmittance of the glass plates was 64%, 48%, 38%, 30% and 17% corresponding to the tilt angles of 15°C, 30°C, 45°C, and 60°C respectively. A range from 2.8% per month to 7% per month of reduction on the solar-thermal mirrors were reported by Said (16) after evaluating the effects of dust accumulation over a year on a flat-plate solar thermal and a evacuated-tube collector panel.

El-Nashar (17) conducted experiments to compare the performance of evacuated-tube and flat-plate types solar-thermal over different periods, extending from one month to a year. The performance of the evacuated-tube decreases more than 10% / month during the summer and 6%/month during the winter. The performance reduction was about 30% without cleaning for the entire year.

Niknia, et al (18) reported that an amount of 1.5 g/m² dust can reduce the instantaneous performance of parabolic trough collectors (PTC) up to 60% and the average performance during the dust deposition up to 37%. Spain experience showed that, in summer, reflectivity rapidly decreases at a rate of about 0.0025% per day during the first two weeks after washing the PTC system (19). Strachan et al (20) studied the effect of dust on the degradation of heliostat efficiencies. On the average, soiling reduced mirror reflectivity of the heliostats by 6.3 and 8.8% respectively for the two types of heliostats in their study. Blackmon (21) observed that the reflectance loss was 7.17% and 10.95% for the glass and acrylic mirrors of the heliostat respectively after a storm.

Hamdy et al (9) presented the reduction in transmittance as a function of dust deposition density as shown in Figure 5. They concluded that the reduction in transmittance is directly caused by the accumulation of dust on the glass surface. As the dust deposition increases, the transmittance reduction increases but with a progressively decreasing rate until reaching its upper limit. Thereafter, the effect of dust deposition vanishes.

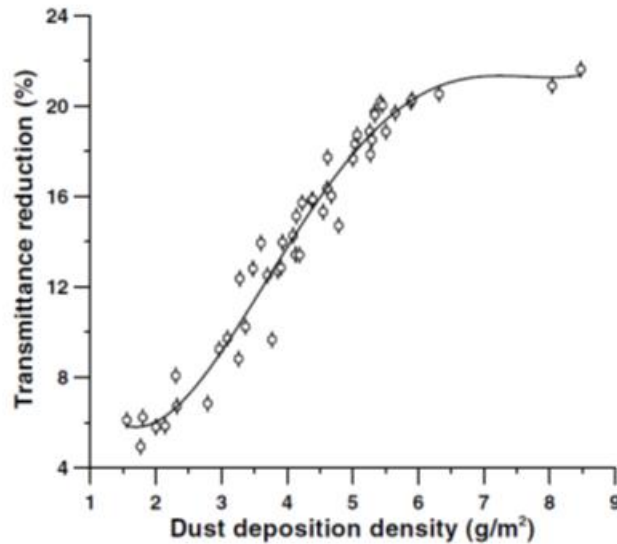


Figure 5. Reduction in transmittance as a function of dust deposition density

Deffenbaugh et al (22) developed predictive models of parabolic trough solar performance by incorporating a factor that accounts for dust and dirt accumulation on the optical surfaces.

3.3 Mirror cleaning methods

Any cleaning method has to address the significant characteristics of dust. There has been a significant amount of research concerning soiling mechanisms for collector materials and the effectiveness of different cleaning procedures on test samples.

Morris (23) conducted tests to determine the nature of the soil which is irreversibly deposited on solar collectors during environmental exposure and the cleaning methods of removing this soil. Roth and Anaya (24) found that the small particles adhere strongly to the mirror surface and are less easily removed by natural cleaning forces.

Blackmon and Curcija (21) observed the effectiveness of a natural cleaning by rain, snow, and frost. They made the following conclusions based on the dust-related degradation of the mirror surfaces: nightly parking positioning is effective in protecting the mirrors from dust deposition; the most effective cleaning method is by spray using treated-water; the acrylic-protected surfaces are more difficult to clean than glass-surface mirrors; the dust accumulation on the acrylic surfaces is more rapid, these surfaces tend to retain the dust due to attractive forces and probably roughness; the degradation rates depend very strongly on weather conditions for both glass and plastic surfaces; and surfaces in the dry climate condition demand more cleaning and maintenance.

The effect of weather conditions on the effectiveness of cleaning can be clearly identified from the results obtained by Fernández-García et al (25) during their study on different cleaning methods for CSP plants. In the study, four metallic test benches each with 20 reflector samples (as shown in Figure 6) were exposed to real outdoor conditions in a semi-desert climate for 2-year to compare the effectiveness of several cleaning methods, including natural cleaning. The test periods of 2-years were divided into 6 periods with each about 3 months for different cleaning methods. Each cleaning was applied every two weeks.

The results (Figure 7) showed that the reflectance is recovered to more than 96% of its maximum value during the whole extension of the study, except in the summer of 2012, when the cleaning methods applied in structure 1 and 3 could not really clean the reflector samples.



Figure 6. Structures 1 to 4 (from left to right) at OPAC's outdoor exposing area (25)

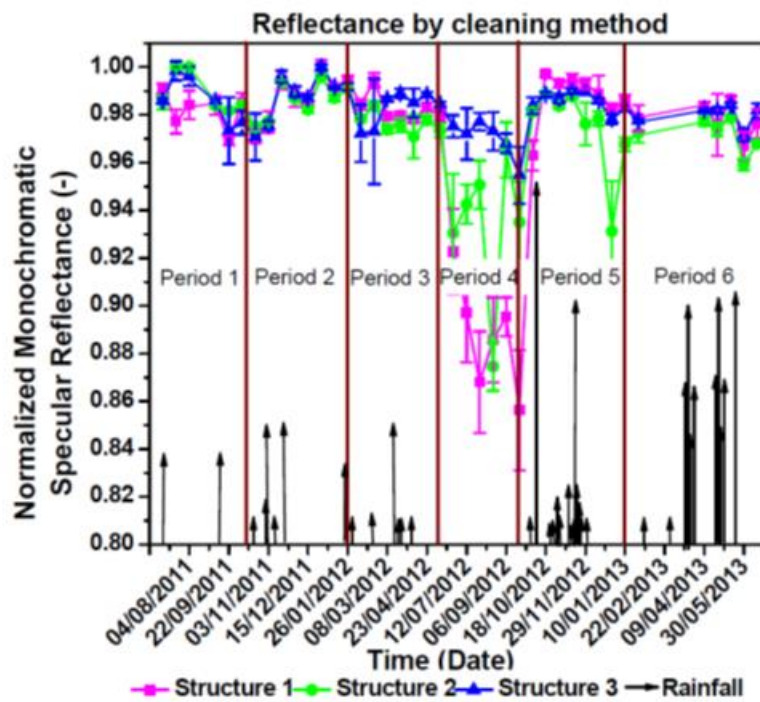


Figure 7. Normalized monochromatic specular reflectance for the different cleaning methods applied, after cleaning (25)

Fernández-García, et al (25) also found the effectiveness of natural cleaning without any intervention of artificial cleaning as shown in Figure 8. Reflectance was recovered up to around 90 % of its maximum value during the rainy season but reaching very low values in summer seasons (both in 2011 and in 2012) due to the very dry ambient.

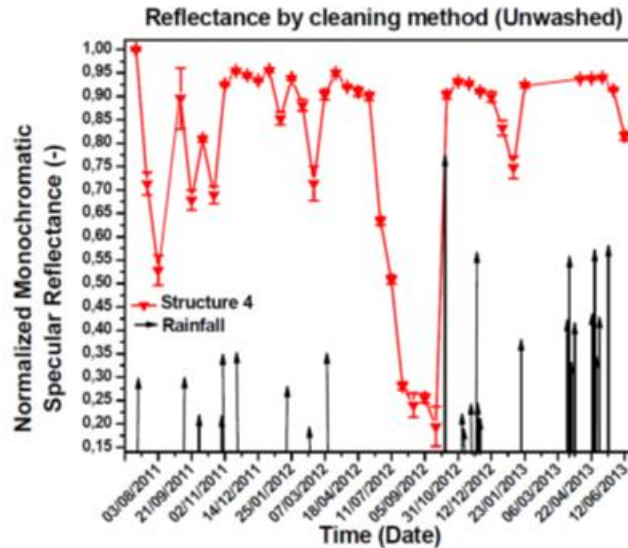


Figure 8. Normalized monochromatic specular reflectance for the different cleaning methods applied, after cleaning (25)

Aránzazu et al (26) tried to optimize a spray cleaning system for CSP plants by conducting tests on a parabolic-trough collector (PTC) testing loop at the Plataforma Solar de Almería (PSA), Spain. The three main parameters, quality, pressure and temperature of the pressurized water, were studied in detail to optimize the system. They concluded that water quality is an important selection criterion in the solar mirror cleaning - the bigger is the hardness of the water used, the lower the mirror reflectance can be achieved after cleaning. In terms of water pressure and temperature, they found that the optimum combination was low washing water temperatures and medium washing water pressures. In figures, that means washing parameters around 125 bar and 50°C as indicated in Figure 9.

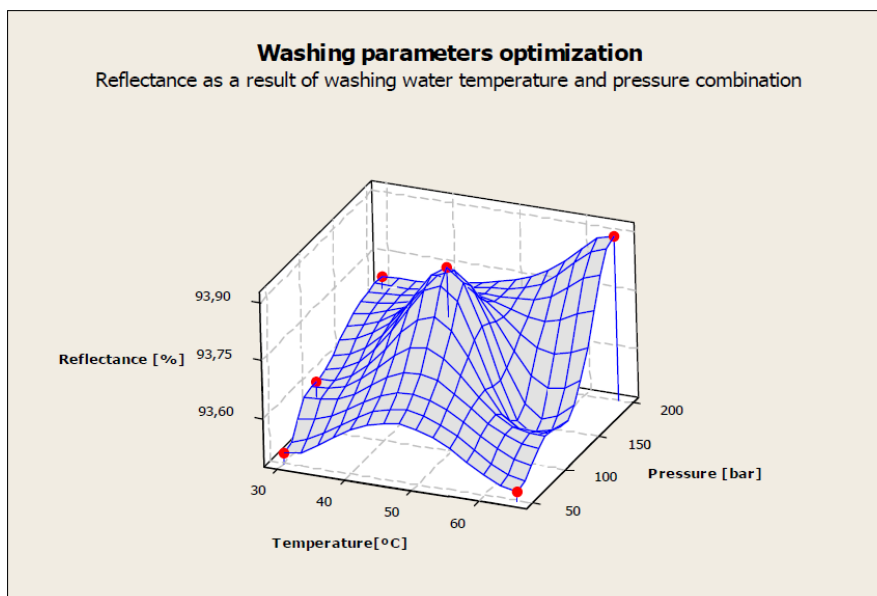


Figure 9. 3D diagram of water pressure and temperature testing results (26)

Commercially operating CSP plants typically use one or more of the following mirror wash systems:

- Mechanically controlled high-pressure jet washing
- Mechanically controlled brush washing
- Deluge style washing
- Manual brush washing
- Manual high-pressure jet washing
- Robot washing

The cleaning systems for heliostat plants include the truck system used at the GEMASOLAR Power Plant in Spain (27). GEMASOLAR Plant used Torresol Energy developed high-pressure water truck (Figure 10) to clean its 2,650 heliostats with total reflective area of more than 300,000 m². Depending on the dirtiness of the solar field, the truck can work at different cleaning speeds and water pressures.



Figure 10. High-pressure water truck cleaning system (27)

In order to reduce the water consumption while maximizing the cleanliness factor, SENER has developed a cleaning system called Heliostat Cleaning Team Oriented Robot (HECTOR) for heliostats based on a fleet of small, individual cleaning robots using brushing and wiping (27). A fleet of robots (Figure 11) is able to clean the full solar field with minimum water consumption and high effectiveness while reducing the operational costs.



Figure 11. Cleaning robot operating in GEMASOLAR (27)

PARIS-Autonomus cleaning system is developed by SENER for Parabolic Troughs cleaning (28). PARIS is a wet mechanical cleaning using rotary brushes. The PARIS is a 4x4 m, low weight vehicle and is characterized for being autonomous, performing an unmanaged cleaning. The wet brush cleans the trough by moving the brushes vertically as shown in Figure 12 (28).



Figure 12. PARIS prototype

An unspecified cleaning system was posted in internet by Dave Levitan (29). The web site shows a photo of the cleaning system, which was claimed that only two systems were used to clean the entirety of the Shams 1 concentrating solar power plant in the desert near Abu Dhabi. The wet brush cleans the trough mirror horizontally which is different from the PARIS system (Figure 13).



Figure 13. The cleaning system in Shams 1 CSP plant (29)

US Solar Energy Generating System (SEGS) plant at Kramer Junction in the Mojave Desert uses an automated washing system known as Mr Twister, to clean parabolic reflective panels (30). In this system, a rotating hydraulically driven arm sprays high-pressure water at the parabolic trough mirror, which is oriented to allow cleaning access (Figure 14).



Figure 14. Mr Twister used in SEGS

The Spanish company Laitu Solar developed an automatic cleaning system Valent®, which is unique in that it uses two parabolic shaped rotating brushes and a pressurised water system both fully integrated in order to achieve effective cleaning of the surface of the parabolic collector as well as of the absorber tube in solar thermal plants (31). This truck mounted wash system with curved rotation brush (Figure 15) allows the brush to adapt to the mirror's shape and remain in full contact with the reflecting surface at all times.



Figure 15. The Valent® cleaning system of Laitu Solar (31)

Novatec Solar has a robot cleaning system for Fresnel mirror cleaning (32). The robot automatically cleans the mirror surface uses wiper and a minimal quantity of water. Novatec claimed that it uses about 98% less water than typical parabolic trough-cleaning system.



Figure 16. Novatec cleaning robot for Fresnel mirror (32)

A high-pressure water cleaning system, mounted at the Kuraymat Solar Power plant in Egypt (Figure 17), uses a truck with a water tank. 20 loops of mirror can be cleaned every day by 2 washing trucks. This means the solar field can be completely cleaned every two day. Rate of consumable water is about 30 M³/day (33).



Figure 17. Water washing system used in Kuraymat Solar Power plant (33)

Other cleaning methods are also under the development. Boston University developed a self-cleaning coating on the surface of solar cells. The system uses a transparent, electrically sensitive material, which is coated on glass or transparent plastic sheet covering the panel. Sensors measure dust levels on the panel surface and energize the material when dust concentration reaches a pre-determined level. The electric charge transmits a dust-repelling wave over the material surface, lifting away dust and transporting it off the screen's edge (34).

Cuddihy also suggested that performance losses caused by soiling could be minimised by using surface coatings that have low affinity for soil retention and a maximum susceptibility to natural cleaning and are readily cleanable by simple and inexpensive maintenance cleaning techniques (35).

In terms of the cost and efficiency of cleaning methods, it has been identified that brush washing is typically five times slower than spray cleaning, but requires much less water (36).

4. Dust monitoring device installed in Collinsville

As mentioned before, dust load, dust composition, and the ambient conditions are all important factors related to mirror cleaning of CSP plants. Therefore, measurements of these parameters are a critical step toward the study of dust-related fouling of solar mirrors in CSP plants.

Historically, a wide variety of dust sampling instruments have been developed for occupational health and safety (OHS) and environmental science etc. While some measurement technologies depend on dust settlement, others operate by filtration of dust, by measuring light transmissivity (light opacity technology), by measuring Beta ray attenuation, by electrical and thermal precipitation of dust, and by measuring the light scattering caused by dust.

The advantages and limitations of various dust monitoring technologies have been reviewed by Pluschke in 2011 (37). RATCH had also hired THIESS Service PTY LTD to

compare the two monitoring products for the dust monitoring in Collinsville Energy Park: the Thermo Scientific FH62 C14 Beta Attenuation Monitor; and the Ecotech E-Sampler Light Scattering Monitor. THIESS found while the FH62 C14 Beta Attenuation Monitor meets the Australian Standard AS3580 as a compliance dust monitor, the Ecotech E-Sampler was a cost effective system for providing real time dust readings but it does not meet the Australian Standard AS3580 as a compliance dust monitor. Since this dust monitor is not for the OHS purpose, compliance with the Australian Standard AS3580 is not required in this study. A brief comparison made by THIESS on these two dust monitoring systems is listed in Table 1.

Table 1. A brief comparison of the two systems

| | Thermo Scientific FH62 C14 | Ecotech E-Sampler |
|---|---|---|
| Recognised in Australia as a compliance monitor under AS3580 | Yes | No |
| Smallest data / reading resolution | 15 minutes | 1 minute |
| Range | 0-5000ug/m ³ or 0-10000ug/m ³ | 0-500ug/m ³ or 0-1000ug/m ³ or 0-10000 ug/m ³ or 0-65000 ug/m ³ |
| Resolution | +/- 1 ug/m ³ | +/- 3 ug/m ³ or 2% of reading |
| Operating temperature | -30 to 60 deg C | -10 to 50 deg C |
| Battery bank size @ 12v | 3000Ah | 100Ah |
| Solar array size | 2200 Watts | 125 Watts |

A final decision has been made to use Met One’s E-sampler for continuous particulate monitoring in Collinsville power plant. The E-sampler incorporates dual technology that combines light scattering technology and gravimetric method, each with strengths and weakness (38). The light scattering technology uses light scatter from suspended particulate to provide a continuous real-time measurement of airborne particulate. Gravimetric method uses a 47 mm filter system for filtration of dust. The 47 mm filter system serves two functions in this instrument. The first function is to provide calibration factor for the measurement of light scattering. The second function is to provide airborne particulate sample for size and property analysis. After the sample air has been measured by the light scatter system, it is collected on a 47 mm filter. The filter can be sent to the laboratory for concentration, size and physical/chemical analysis.

The monitoring system was installed in Collinsville in 16 May 2013. The location of the dust monitor is shown in Figure 18 provided by RATCH. The system includes the E-Sampler, a solar power panel, a wind speed and direction sensor, and a mounting frame as shown in Figure 19. A humidity sensor was added in April 2014.

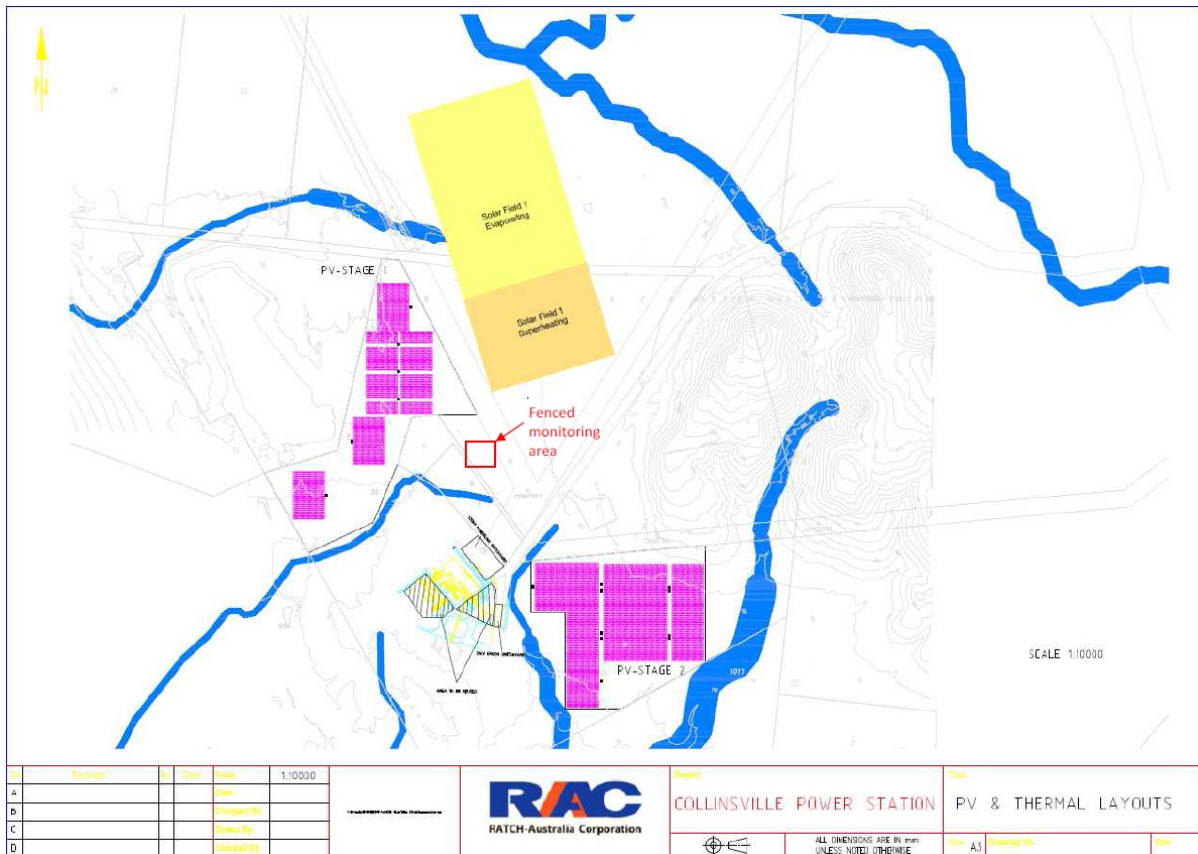


Figure 18. Location of the dust monitor in Collinsville power station



Figure 19. The dust monitor installed in Collinsville

The E-Sampler is a light scattering technology (38). An internal visible laser diode is collimated and directed through sample air. This sample air is drawn into the E-Sampler by an internal rotary vane pump. When particulate laden sample air intersects the laser beam a portion of the light is scattered. The scattered light is collected at a near forward angle and focused on a photo diode that converts the light to an electric signal proportional to the amount of scattered light (see Figure 20). Particulate weight per unit volume ($\mu\text{g}/\text{m}^3$ or mg/m^3) is recorded by the E-Sampler.

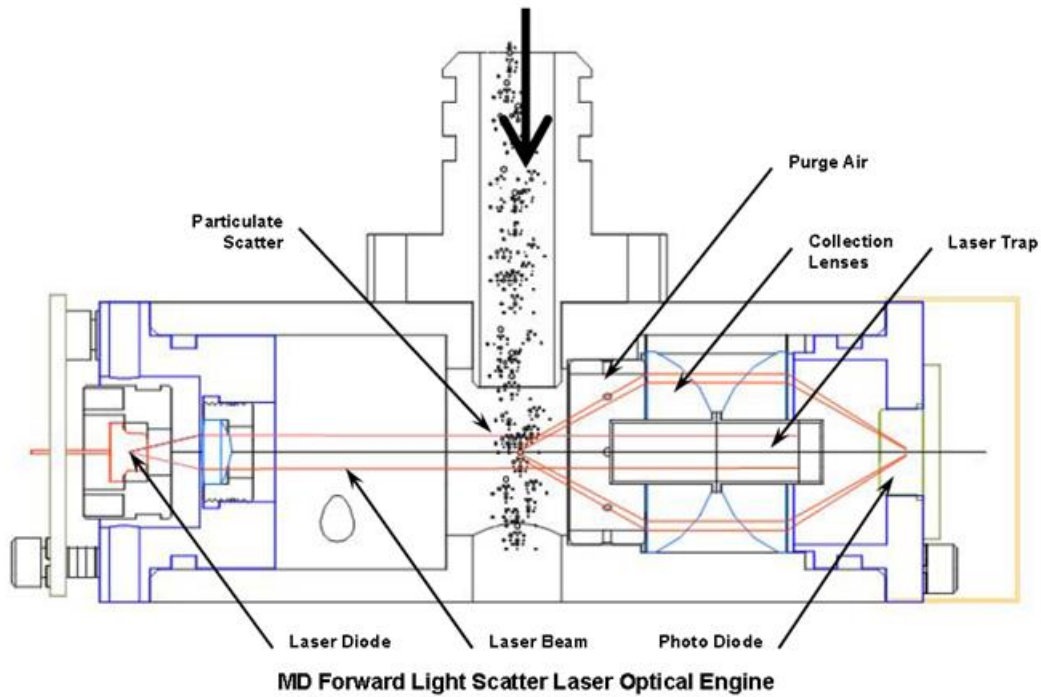


Figure 20. Light scatter due to airborne particulate

Downstream of the nephelometer measurement is the 47 mm filter. The filter media can be selected depending on laboratory analysis. One of the uses for the 47 mm filter element is a gravimetric calibration of the continuous light scatter measurement since all light scatter devices have inherent difficulties when converting light scatter to mass. Index of refraction and mean particle diameter can affect the amount of light scattered from the same amount of mass. The simplest solution is to compare the light scatter concentration for a set period of time with a gravimetric concentration over the same period of time. Comparing the concentrations will yield a K-factor that can be entered into the E-Sampler. All subsequent concentration values will be adjusted by this K-factor (38). The other use of the filter is to collect the dust sample for the dust size and properties analysis.

The 47 mm filter can be easily inserted as shown in Figure 21 and the dust sample can be collected for its physical and chemical properties analysis in lab.

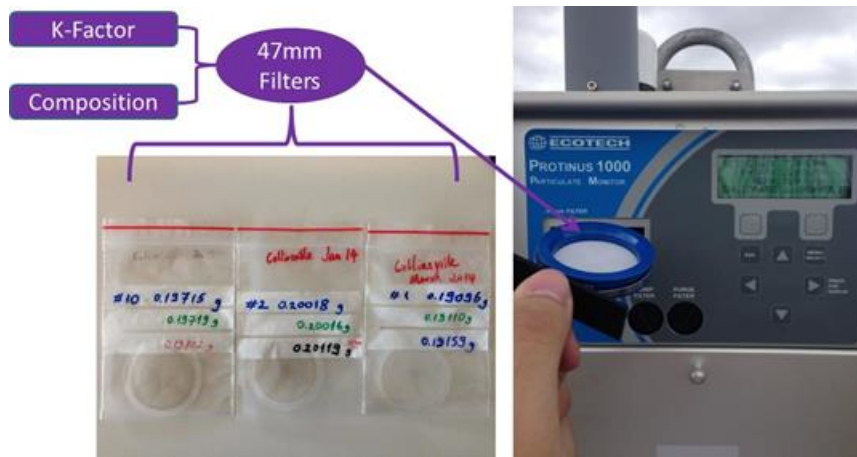


Figure 21. Dust sample collection with 47mm filter.

The wind speed and direction are measured in a single sensing unit 034B wind sensor from Met One Instruments, Inc. as shown in Figure 22. The speed measurement range of the sensor is 0 - 75 m/s with the accuracy of $\pm 1.1\%$.



Figure 22. 034B wind sensor used in Collinsville.

The solar panel is for charging a 12 volt, 110 amp-hour battery that powers the E-sampler. The battery can last about 67 hours for the continuous operation of the E-Sampler and will need the solar panel to recharge for the remote applications.

The data are downloaded remotely through a 3G modem as shown in Figure 23. Telstra data only SIM card and a DynDNS account are used to map the IP address of the 3G modem to a URL. All data can be downloaded in the offices located anywhere.



Figure 23. 3G modem used in the monitor

A relative humidity sensor is added in April 2014 to monitor the ambient humidity in Collinsville. Model 083E/593A relative humidity sensor (see Figure 24) is used in this system and the accuracy of the sensor is about $\pm 2\%$ from 0 to 100% relative humidity.



Figure 24. Relative humidity sensor used in Collinsville.

The following digital data are collected from the dust monitor: date and time, dust concentration ($\mu\text{g}/\text{m}^3$), wind speed, wind direction, temperature and humidity. At certain periods, the dust samples are collected on the filter. Table 2 shows a data file collected from the Collinsville monitor.

Table 2. Data file shows information collected by the dust monitor

The screenshot shows the 'Comet' software interface. On the left, there is a 'Station Info' panel with the following details: Name: dustgather2, Product: E-Sampler, ID: (blank), Version: (blank). Below this is 'Connection Info' with IP Addr: dustgather2.dyndn and IP Port: 3001. At the bottom left, there are 'Data Options' with buttons for 'Retrieve Current' and 'Open Previous'. The main area displays a data table with tabs for 'Data', 'Chart', and 'Direct Connect'. The table has 11 columns: Time, Conc(MG/M3), Flow(l/m), AT(C), BP(PA), RHx(%), RHl(%), WS(M/S), WD(Deg), BV(V), and Alarm. The data rows show a steady increase in concentration from 0.000 at 11:10:00 to 0.010 at 15:00:00, with other parameters like flow and temperature remaining relatively stable.

| Time | Conc(MG/M3) | Flow(l/m) | AT(C) | BP(PA) | RHx(%) | RHl(%) | WS(M/S) | WD(Deg) | BV(V) | Alarm |
|----------------------|-------------|-----------|-------|--------|--------|--------|---------|---------|-------|-------|
| 23-APR-2014 11:10:00 | 0.000 | 0.0 | 22.6 | 99236 | 83 | 75 | 2.7 | 178 | 14.1 | 0 |
| 23-APR-2014 11:20:00 | 0.006 | 1.3 | 22.0 | 99236 | 80 | 70 | 2.6 | 167 | 14.0 | 0 |
| 23-APR-2014 11:30:00 | 0.012 | 2.0 | 22.0 | 99216 | 81 | 62 | 2.3 | 155 | 13.0 | 0 |
| 23-APR-2014 11:40:00 | 0.011 | 2.0 | 22.1 | 99197 | 81 | 55 | 2.4 | 164 | 12.9 | 0 |
| 23-APR-2014 11:50:00 | 0.011 | 2.0 | 22.4 | 99197 | 80 | 51 | 2.8 | 171 | 13.2 | 0 |
| 23-APR-2014 12:00:00 | 0.009 | 2.0 | 22.7 | 99177 | 81 | 49 | 2.4 | 162 | 14.1 | 0 |
| 23-APR-2014 12:10:00 | 0.014 | 2.0 | 23.0 | 99158 | 80 | 52 | 2.8 | 156 | 14.0 | 0 |
| 23-APR-2014 12:20:00 | 0.013 | 2.0 | 23.1 | 99138 | 81 | 50 | 2.9 | 172 | 14.0 | 0 |
| 23-APR-2014 12:30:00 | 0.014 | 2.0 | 23.2 | 99138 | 80 | 50 | 3.3 | 173 | 13.6 | 0 |
| 23-APR-2014 12:40:00 | 0.013 | 2.0 | 23.5 | 99118 | 78 | 49 | 3.6 | 166 | 13.8 | 0 |
| 23-APR-2014 12:50:00 | 0.014 | 2.0 | 23.4 | 99118 | 78 | 50 | 3.5 | 168 | 13.6 | 0 |
| 23-APR-2014 13:00:00 | 0.012 | 2.0 | 23.2 | 99099 | 79 | 50 | 3.3 | 174 | 13.8 | 0 |
| 23-APR-2014 13:10:00 | 0.014 | 2.0 | 23.2 | 99099 | 78 | 50 | 2.9 | 170 | 13.6 | 0 |
| 23-APR-2014 13:20:00 | 0.015 | 2.0 | 23.1 | 99079 | 80 | 51 | 2.9 | 168 | 13.1 | 0 |
| 23-APR-2014 13:30:00 | 0.016 | 2.0 | 22.6 | 99060 | 83 | 50 | 3.1 | 154 | 12.8 | 0 |
| 23-APR-2014 13:40:00 | 0.017 | 2.0 | 22.5 | 99040 | 84 | 50 | 2.7 | 170 | 13.1 | 0 |
| 23-APR-2014 13:50:00 | 0.017 | 2.0 | 22.5 | 99021 | 84 | 51 | 3.2 | 158 | 13.5 | 0 |
| 23-APR-2014 14:00:00 | 0.018 | 2.0 | 22.6 | 99021 | 84 | 50 | 2.9 | 161 | 13.7 | 0 |
| 23-APR-2014 14:10:00 | 0.010 | 2.0 | 22.6 | 98982 | 83 | 50 | 3.0 | 155 | 13.6 | 0 |
| 23-APR-2014 14:20:00 | 0.008 | 2.0 | 22.8 | 98962 | 83 | 49 | 3.1 | 155 | 13.5 | 0 |
| 23-APR-2014 14:30:00 | 0.008 | 2.0 | 22.8 | 98962 | 83 | 52 | 2.5 | 152 | 13.0 | 0 |
| 23-APR-2014 14:40:00 | 0.010 | 2.0 | 22.9 | 98962 | 84 | 51 | 1.5 | 170 | 12.7 | 0 |
| 23-APR-2014 14:50:00 | 0.010 | 2.0 | 23.0 | 98962 | 84 | 50 | 1.4 | 171 | 12.7 | 0 |
| 23-APR-2014 15:00:00 | 0.010 | 2.0 | 23.0 | 98943 | 85 | 50 | 1.8 | 148 | 13.0 | 0 |

5. Results

The real time data covered the time interval from May in 2013 to May 2014 except three months data missing. From November 2013 to March 2014, Telstra charged RATCH a very high amount of SIM card fee and was unable to explain the reason of the charge, which forced RATCH to terminate the Telstra service. Therefore, no data were collected during this period through the internet. UQ later purchased a new Telstra SIM card to continue the remote data downloading since then.

Dust concentration, ambient weather conditions during the monitoring periods and the dust samples collected by four filters are presented in this section. To guarantee the accuracy of the dust concentration obtained by light scattering technology, in-situ calibration was carried out to provide 'K-factor' for the monitor. The so-called 'K-factor' was defined as the ratio of the dust concentration obtained by particle deposition on the 47mm filter and the total concentration measured by the light scattering method of the instrument at the same time interval.

5.1 K-factor based on the in-situ calibration

The factory calibrated K-factor is one which is based on the vendor's laboratory calibration and was a default K-factor used by the E-Sampler monitor. Since the dust composition in Collinsville may be quite different from the vendor's laboratory, a calibration is necessary for light scattering technology to give the accurate dust concentration. In this case, only the first three 47mm (with 2 μ m filtration) Teflo filters have been used for the calibration. These three filters were installed to collect the dust samples for total 60 days (20 days each) to obtain the K-factor. The three K-factors based on each filter were 4.05, 4.89 and 4.56, respectively. The average value of 4.5 was used as K-factor for the system.

5.2 Time history of dust concentration

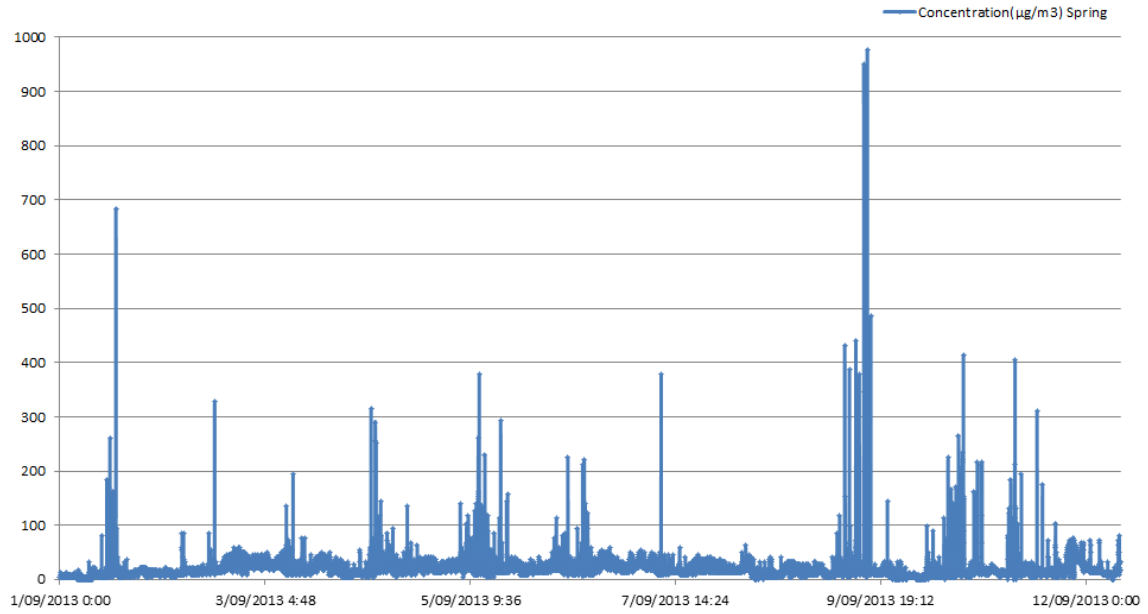
The E-sampler takes readings at a frequency of 1 Hz and outputs the averages over intervals that can be selected as 1, 5, 15, 30 or 60 minutes. Although the E-Sampler measures the particulate concentration and updates the display each second, the fastest average period that can be logged in memory is 1 minute. Since the unit contains memory for 4369 data records, the memory will fill up faster the shorter the average interval is set to, as shown in the table 3 below (38). When the memory is full, the unit over-writes the oldest data. This memory issue has no effect on the remote data downloading as only as the downloading time is set up less than 3 days for 1 minute average output or before the memory becomes full for other outputs average set up. It is better to use lower average time for wind/dust correlation. In our monitoring period, 5 minute output average was used. However, 15 minutes average time was used when the three filters was installed for calibration, which leaves enough time for dust accumulating on the filter while one does not need to worry the data downloading.

Table 3. Memory capacity of the E-Sampler

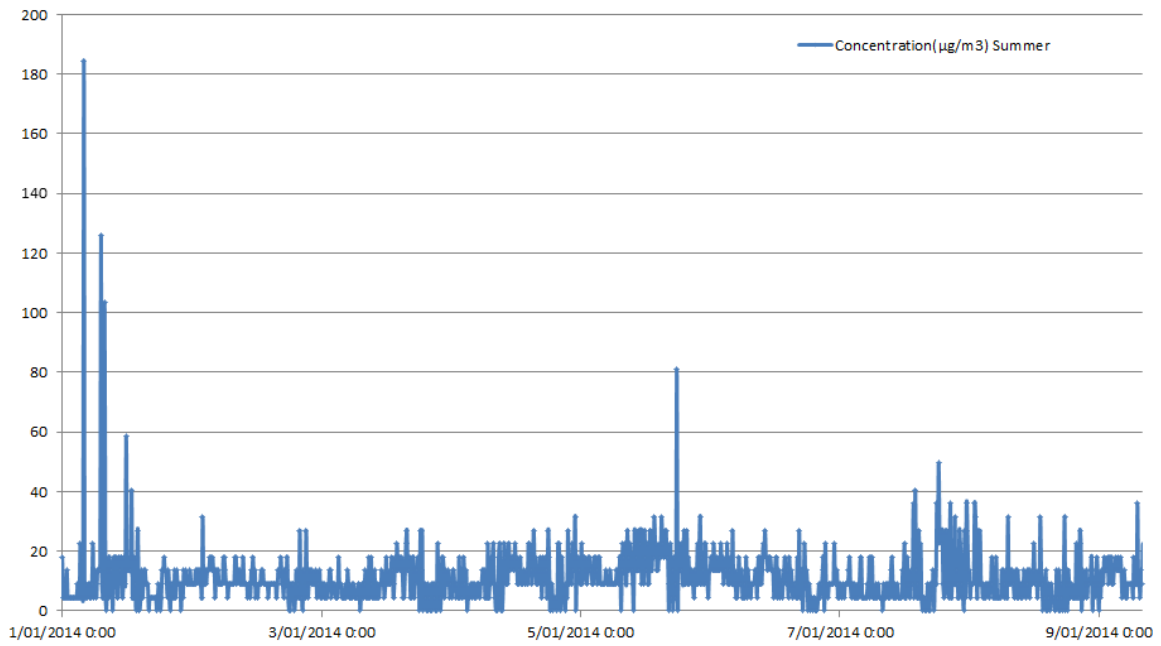
| Real-Time Average Setting | Records Stored Per Hour | Memory Capacity (Days) |
|---------------------------|-------------------------|------------------------|
| 1 min | 60 | 3.03 |
| 5 min | 12 | 15.1 |
| 10 min | 6 | 30.3 |
| 15 min | 4 | 45.5 |
| 30 min | 2 | 91 |
| 60 min | 1 | 182 |

The time history of dust concentration for all data collected is presented in Appendix A. Four typical periods in different seasons, which are 01/09/13-18/09/13 (spring), 01/01/14-09/01/14 (summer), 01/04/14-10/04/14 (autumn) and 05/08/13-14/08/13 (winter), are plotted in Figure 25. Although the maximum dust concentration of $1472\mu\text{g}/\text{m}^3$ was detected in a short period in winter, the average dust concentration was about $13\mu\text{g}/\text{m}^3$ in this winter period. There were some high dust concentrations in spring but the average dust concentration was about $18\mu\text{g}/\text{m}^3$, which is the highest in average in those four periods. The average dust concentration in autumn period was $14\mu\text{g}/\text{m}^3$ and $11\mu\text{g}/\text{m}^3$ in summer period.

Concentration($\mu\text{g}/\text{m}^3$) Spring



Concentration($\mu\text{g}/\text{m}^3$) Summer



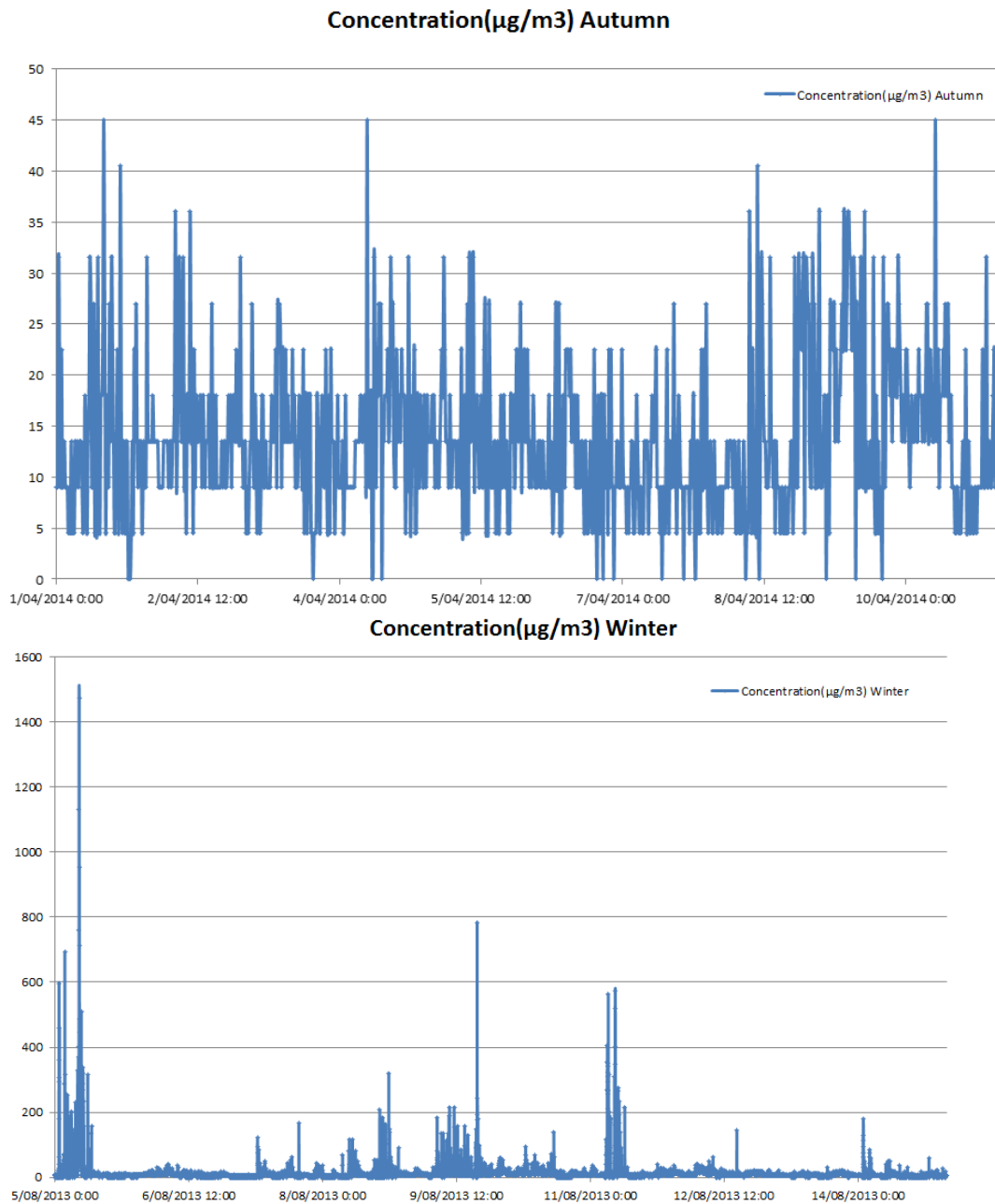


Figure 25. Time history of dust concentration for four typical periods in different seasons

From 20/03/14 to 31/03/14, since one filter was installed and the dust sample was collected during this period. Therefore, the time history of dust concentration during this period is also processed and is shown in Figure 26. The highest dust concentration during this period was about $108\mu\text{g}/\text{m}^3$. The average dust concentration was about $14\mu\text{g}/\text{m}^3$.

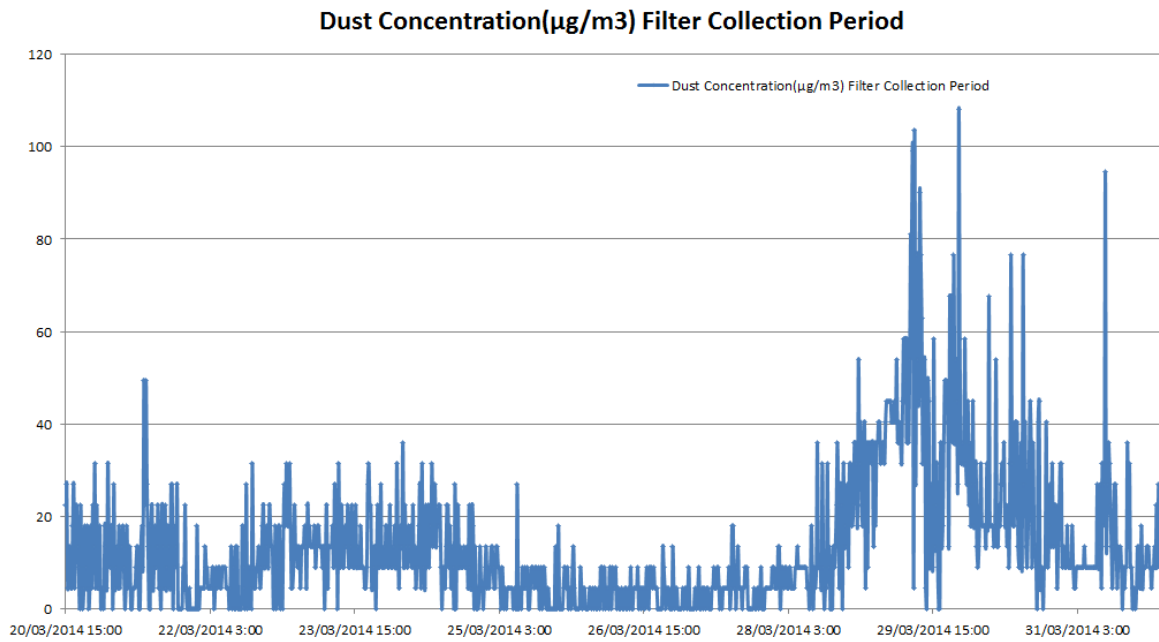


Figure 26. Time history of dust concentration in the period when dust sample was collected with filter (20/03/14 – 31/03/14)

The dust concentrations recorded in the period from 23/04/14 to 12/05/14 were closed to the average value of the whole period ($15\mu\text{g}/\text{m}^3$) and were analysed in detail. The time histories of the dust concentration during this period are shown in Figures 27-29. Figure 27 presents daily time history for three different days and it seems that higher dust concentration happened from 4:00am to 12:00 pm during that period. More than $20\mu\text{g}/\text{m}^3$ was observed quite often on the 5th of May in the morning. Figure 26 shows weekly time history for two different weeks from April to May 2014. Some high dust concentration ($>30\mu\text{g}/\text{m}^3$) can be clearly identified from the figure. Figure 29 presents the data collected between 23/04/14 and 12/05/14. It can be seen that the highest dust concentrations of $278\mu\text{g}/\text{m}^3$ and $139\mu\text{g}/\text{m}^3$ were at the time: 6:20AM 01/05/14 and 9:40AM 01/05/14. The dust concentrations were lower than $30\mu\text{g}/\text{m}^3$ in most of time.

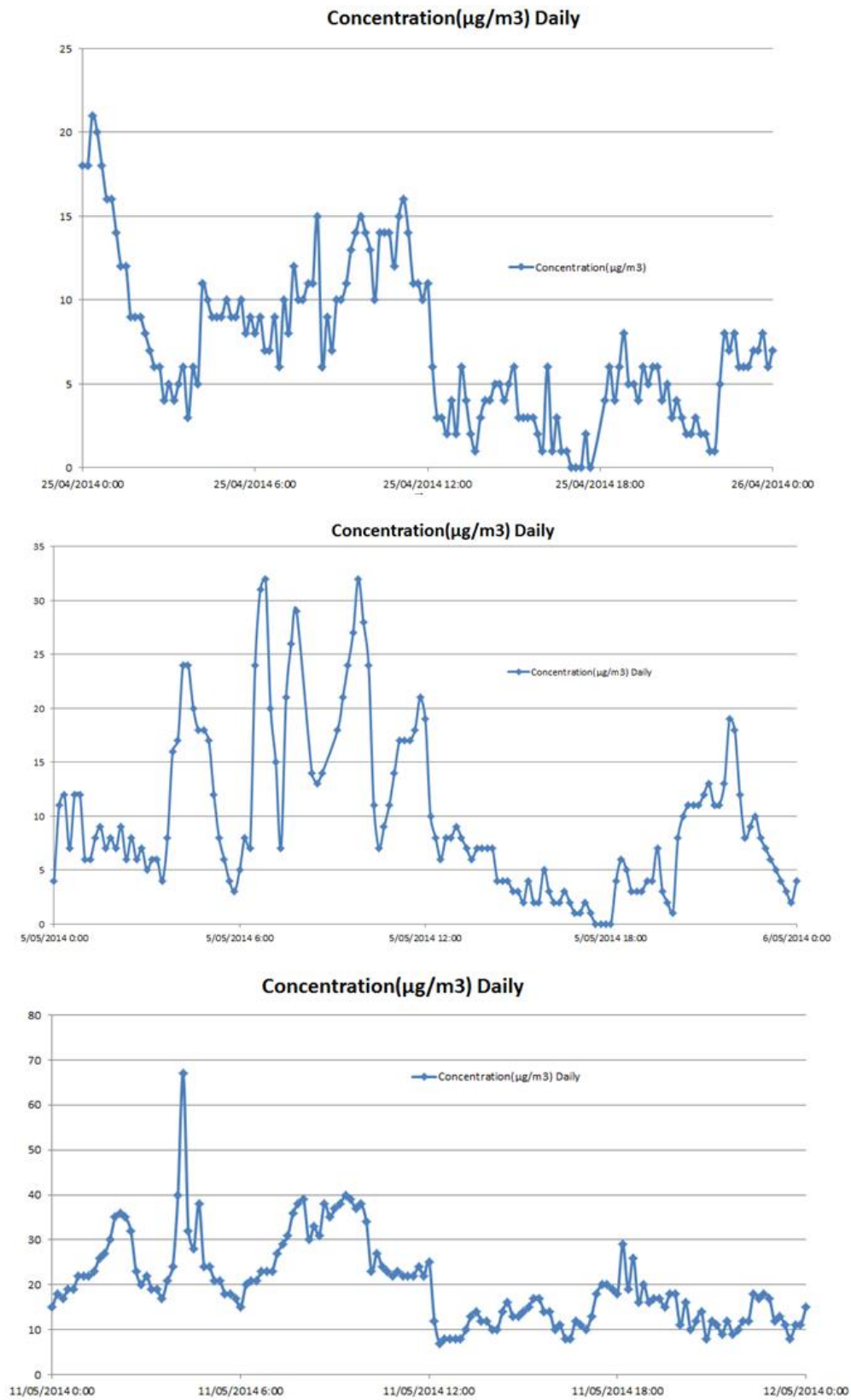


Figure 27. Time history of dust concentration for three typical days

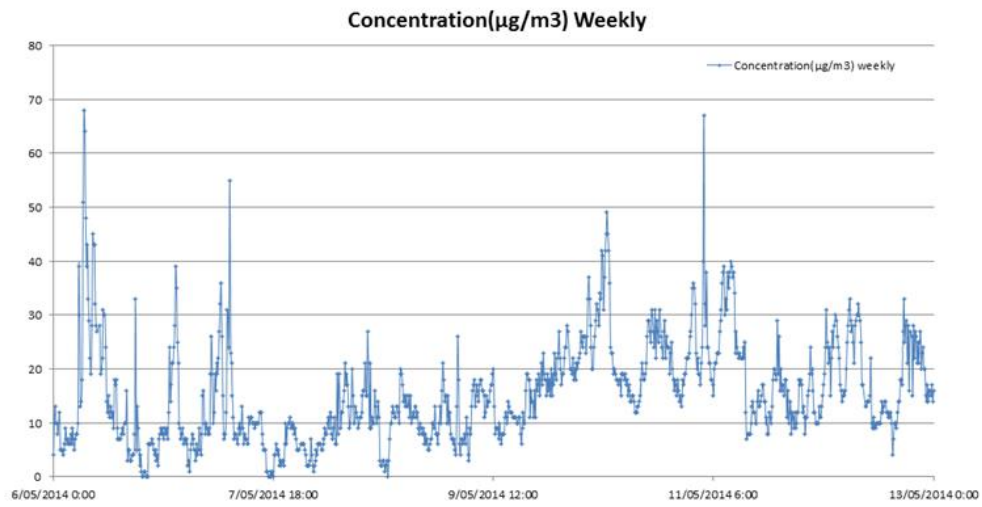
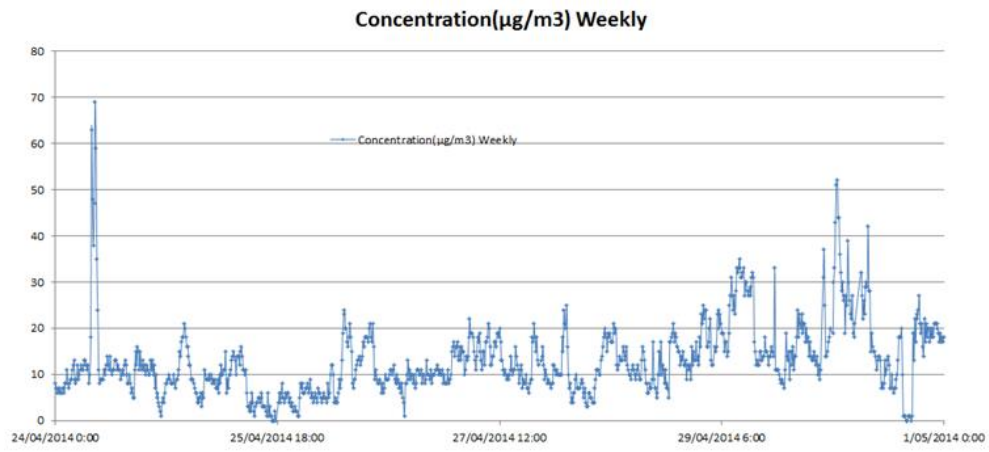


Figure 28. Time history of dust concentration for two typical weeks

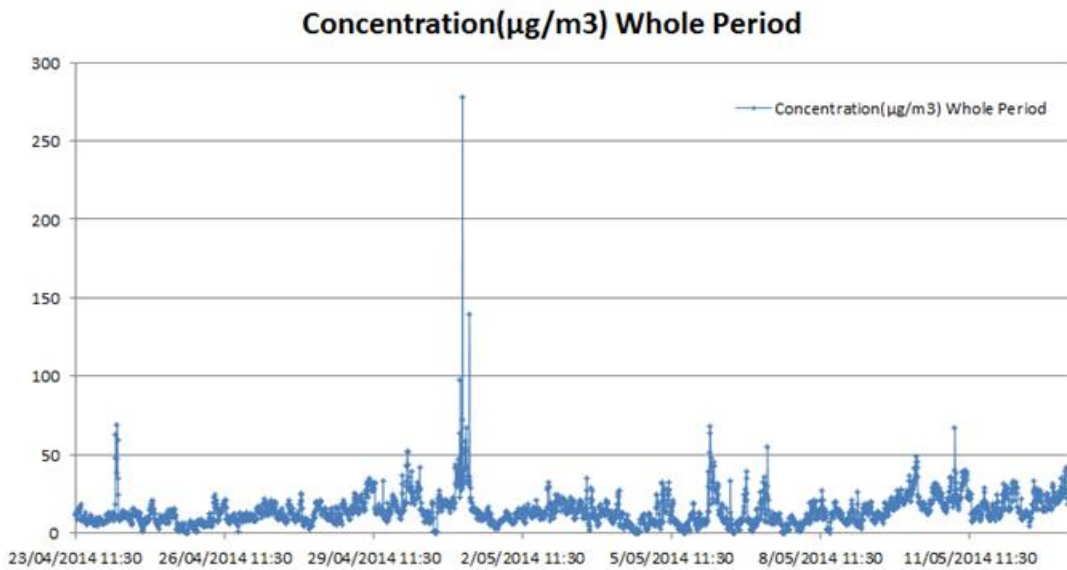


Figure 29. Time history of dust concentration between 23/04/14 and 12/05/14

The time histories of wind speed and wind direction are plotted in Figure 30 for three different days during the periods from 23/04/14 to 12/05/14. The daytime wind speeds were higher than the night wind.

The average temperature of each month in Collinsville was shown in Figure 31. Based on the raw temperature data collected (see appendix D), the highest temperature was 44.3°C in summer noon (January period), and the lowest temperature was 3.7°C in the winter night (July period). The average temperature was about 27°C in summer and 15°C in winter.

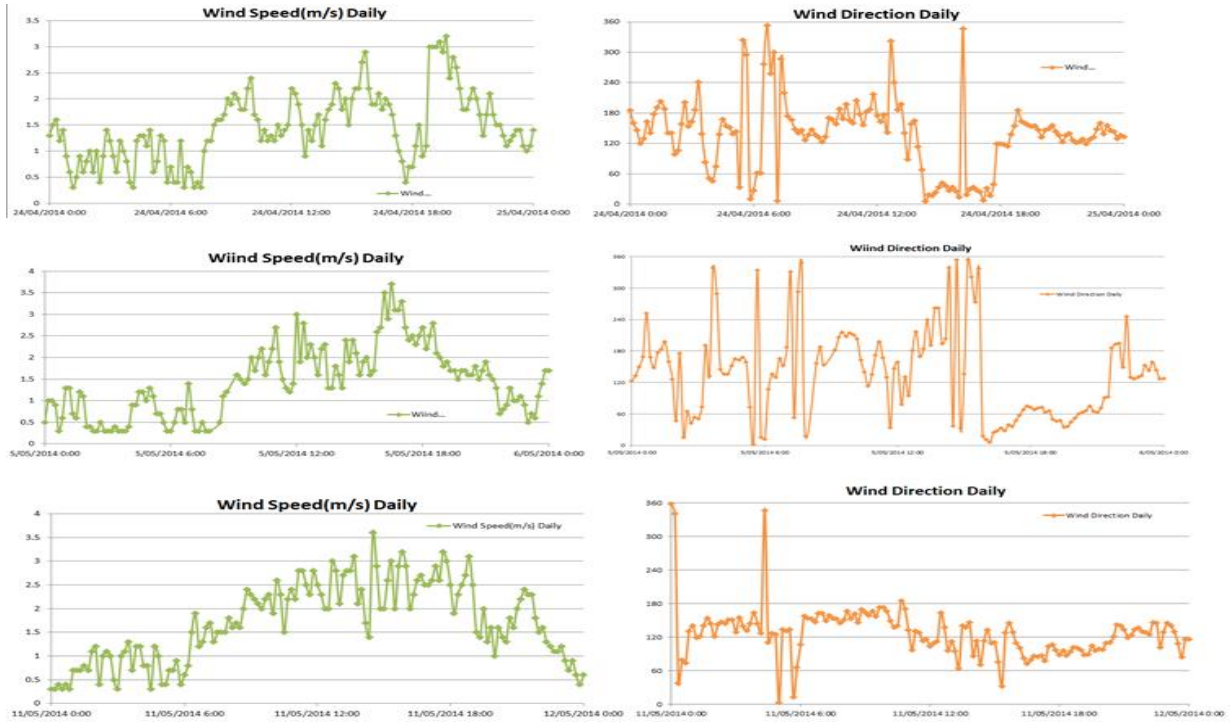


Figure 30. Wind speed and direction on 24/04/14, 05/05/14 and 11/05/14

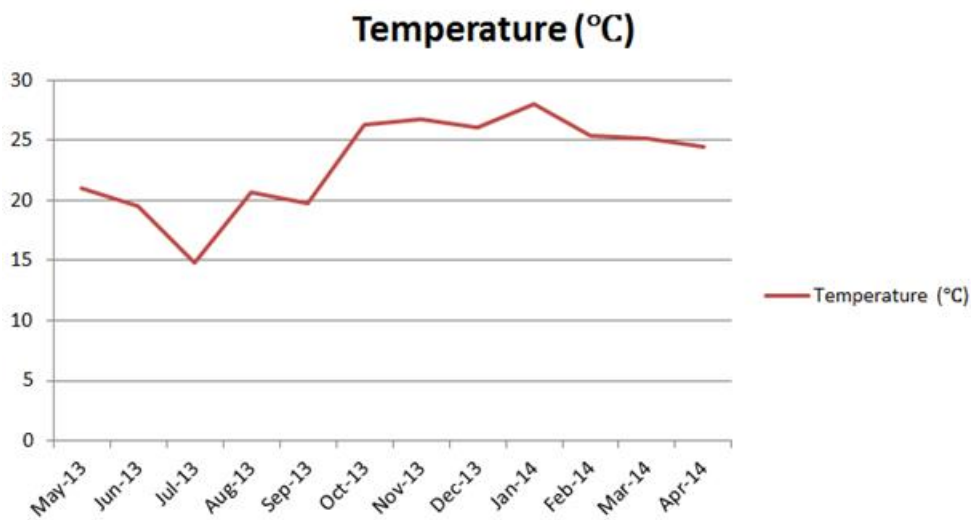


Figure 31. Monthly average temperature variation in Collinsville

Figure 32a shows hourly average of dust concentrations on 16/10/2013 and the hourly average of wind speed was presented in Figure 33a for the same day. From this one day's data, the dust concentration was higher from midnight to the early morning (8:00am) but the wind speed was lower during that period.

The monthly average of dust concentrations and wind speed in the whole monitoring period are shown in Figures 32b and 33b, respectively. Total twelve data points (one point for each month) were presented in each figure. Due to the Telstra SIM card issues as mentioned before, manual downloads were conducted during the periods from November 2013 to March 2014 with some data lost. The manual downloaded data included: only one day data in November which was 30/11/2013; a full month data in December (from 01/12/13 to 31/12/13); nine days data in January (01/01/2014 to 09/01/14); about two weeks data in February (03/02/2014 to 14/02/14); and about 10 days data in March (20/03/14 to 31/03/14). From 23/04/14, new SIM card was installed and the data was downloaded through internet.

It shows that October had the highest average dust concentration. The average wind speed in this month is also high and was about 2.7m/s.

The wind direction setting was followed through the manual provided by the manufacturer of the dust monitor which was as follows: 0° - North; 180° - south; 90° - East; and 270° - West. The wind direction related to the reading of the monitor is shown in Figure 34, which will be used in next section.

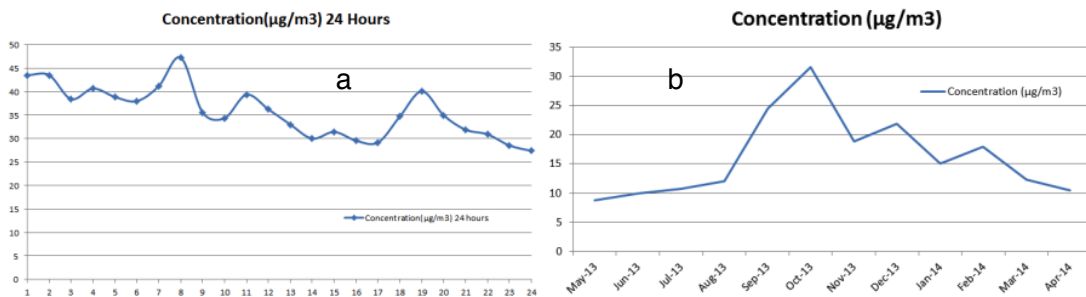


Figure 32. Average dust concentration in Collinsville

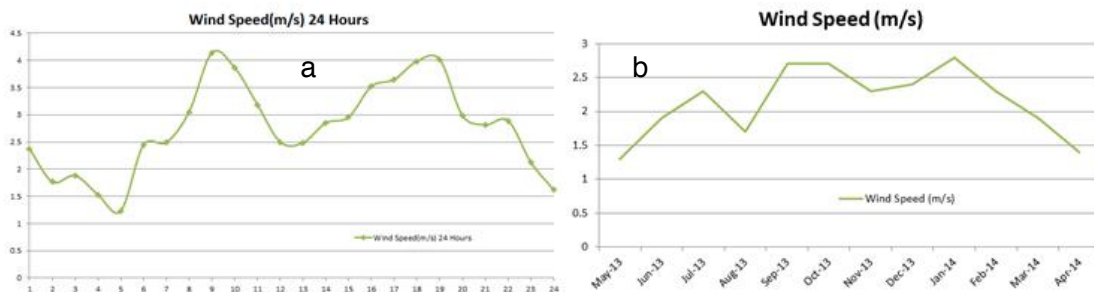


Figure 33. Average wind speed during 24 hours and one-year period

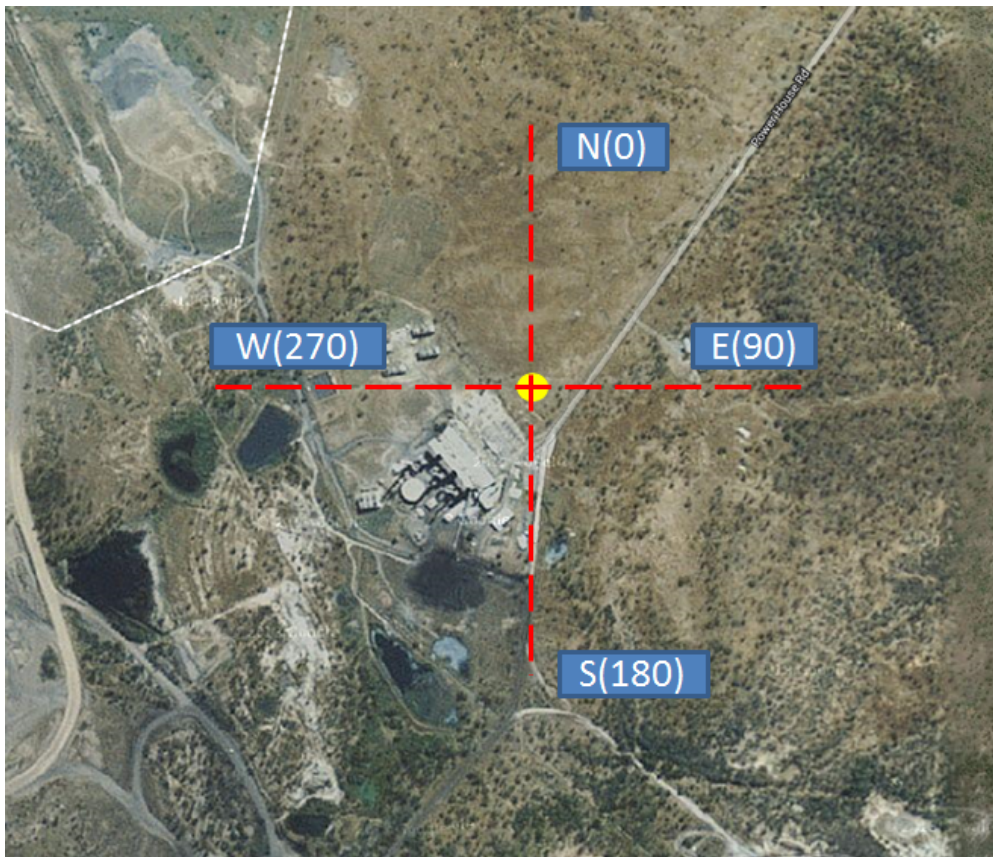


Figure 34. Setting of wind direction

5.2 Statistic results

The histogram plot of dust concentration during one-year monitoring period is shown in Figure 35. The frequency showing the dust concentrations of more than $100\mu\text{g}/\text{m}^3$ is very low. The highest occurrence of dust concentration is about $10\mu\text{g}/\text{m}^3$. To have a more close view on the occurrence of dust concentration, Figure 36 plots the statistic data collected in April (23/4/14 – 30/4/14), which has the average dust concentration close to the average in one-year period. It can be seen that over 90% of the dust concentration are lower than $25\mu\text{g}/\text{m}^3$.

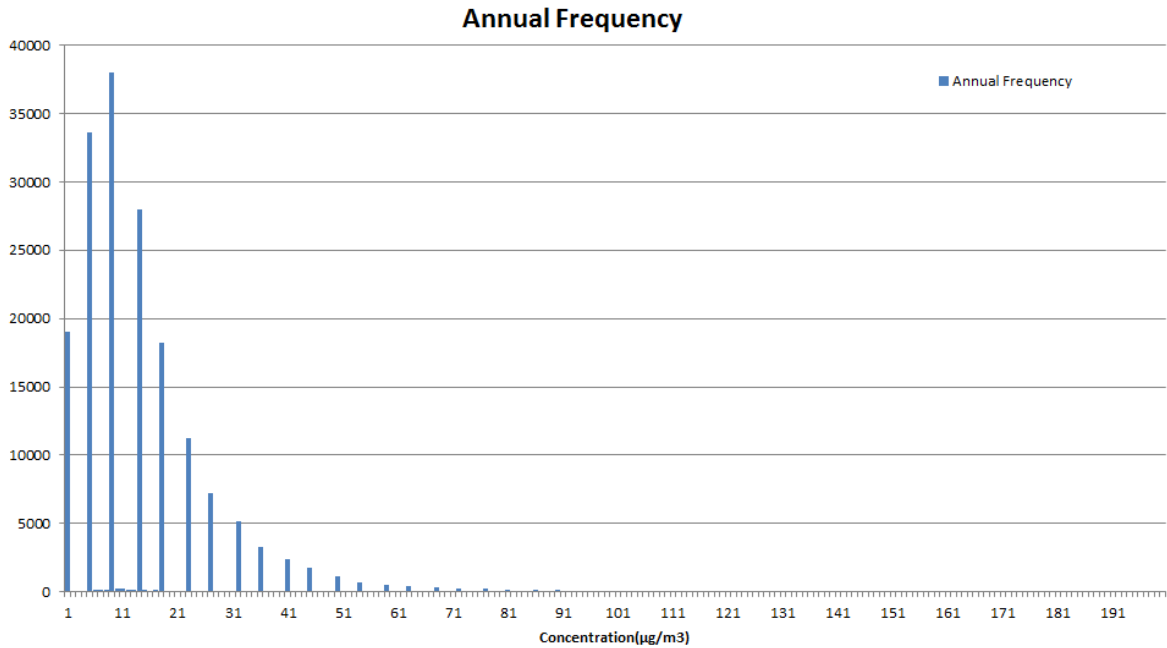


Figure 35. Histogram of dust concentration in 12-month monitoring period

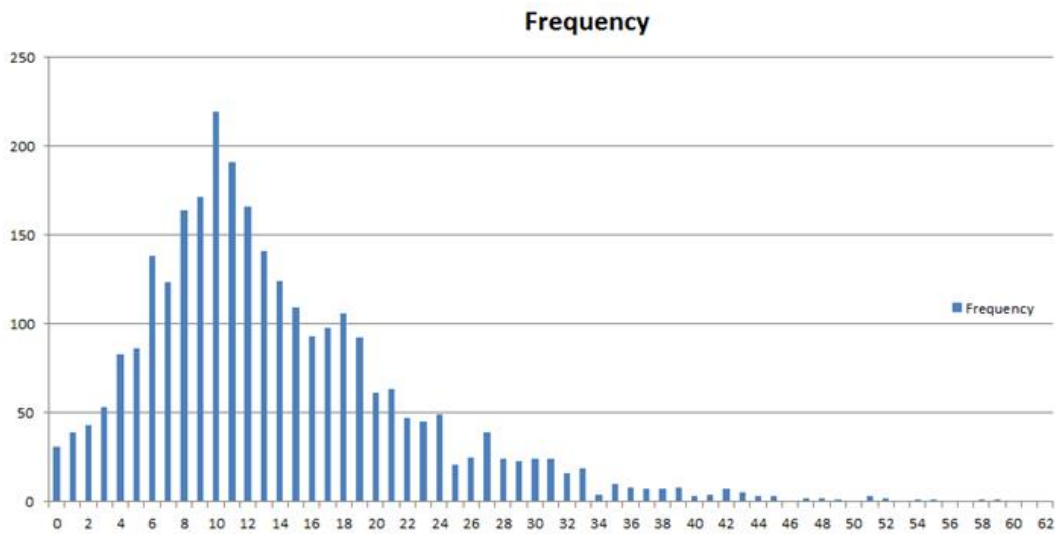


Figure 36. Histogram of dust concentration in April 2014

The histogram of wind speed collected in one-year period is plotted in Figure 37 and Figure 38 shows the occurrence of wind speed in the last week of April 2014.

Over 90% of wind speeds are lower than 5 m/s during one-year monitoring period as Figure 37 shows. The average wind speed during the one-year monitoring period was about 2m/s and the mean wind speed was 1.9m/s in April 2014.

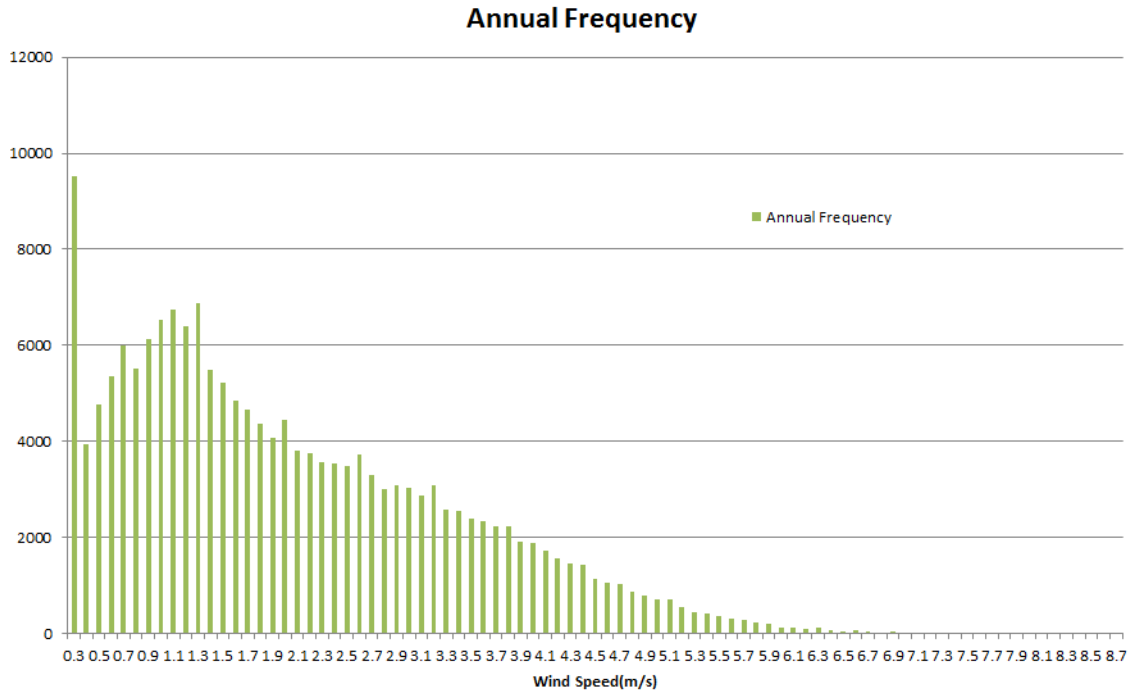


Figure 37. Histogram of Wind Speed in 12-month monitoring period

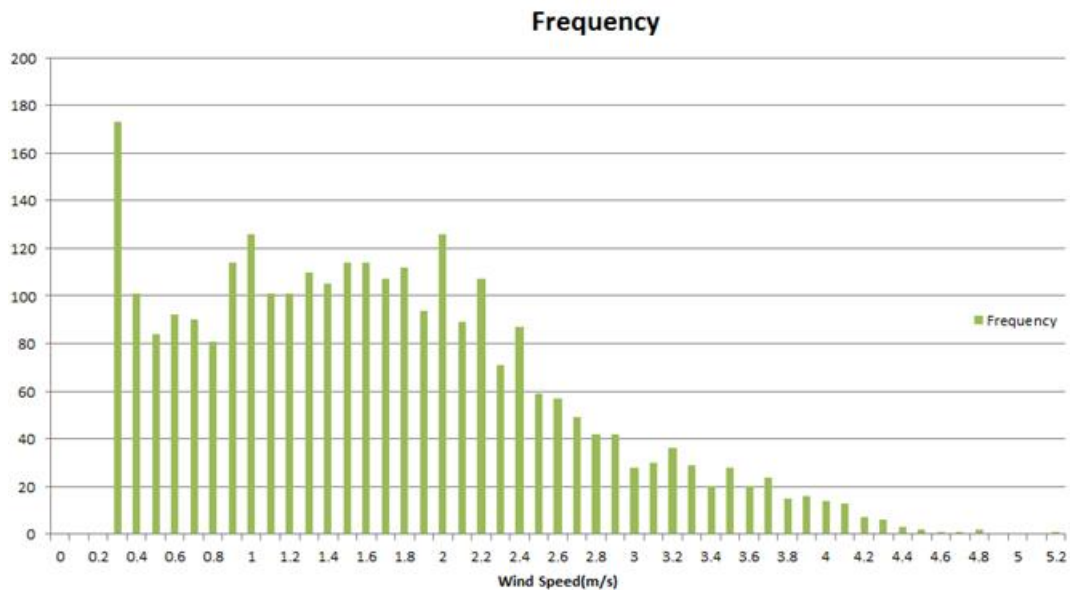


Figure 38. Histogram of Wind Speed in April 2014

Figure 39 shows annual frequency of wind direction. The high occurrences of wind direction were from the directions between 90° to 180° (South-East wind). Figure 40 plots the frequency of wind direction with April's data. It is clear to see that most winds are South-East wind, which is a favour direction with regarding to the Collinsville open-cut coal mine.

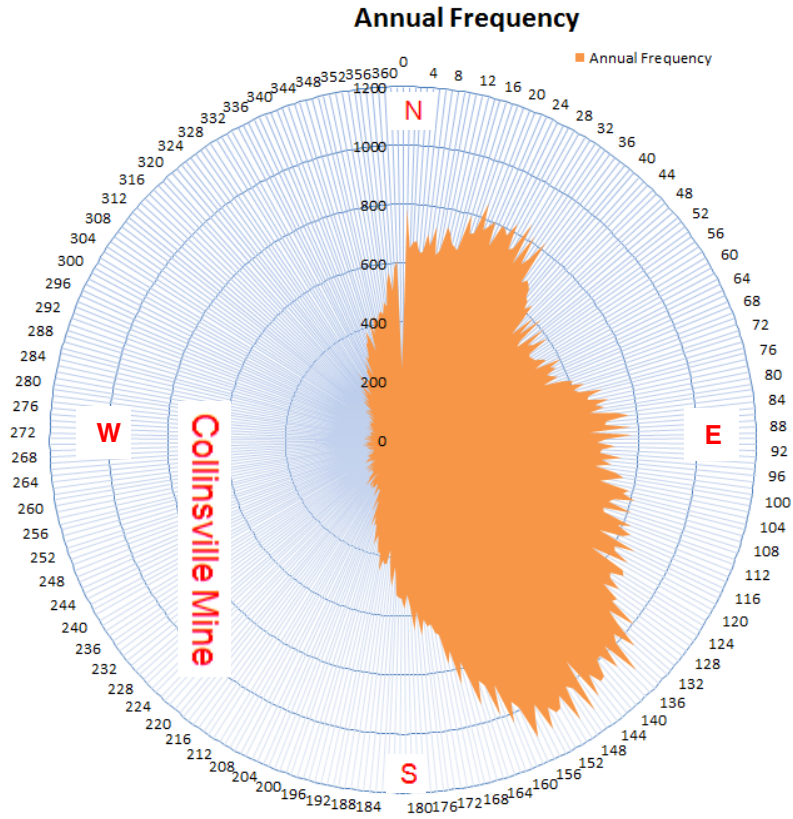


Figure 39. Histogram of Wind Direction in 12-month monitoring period

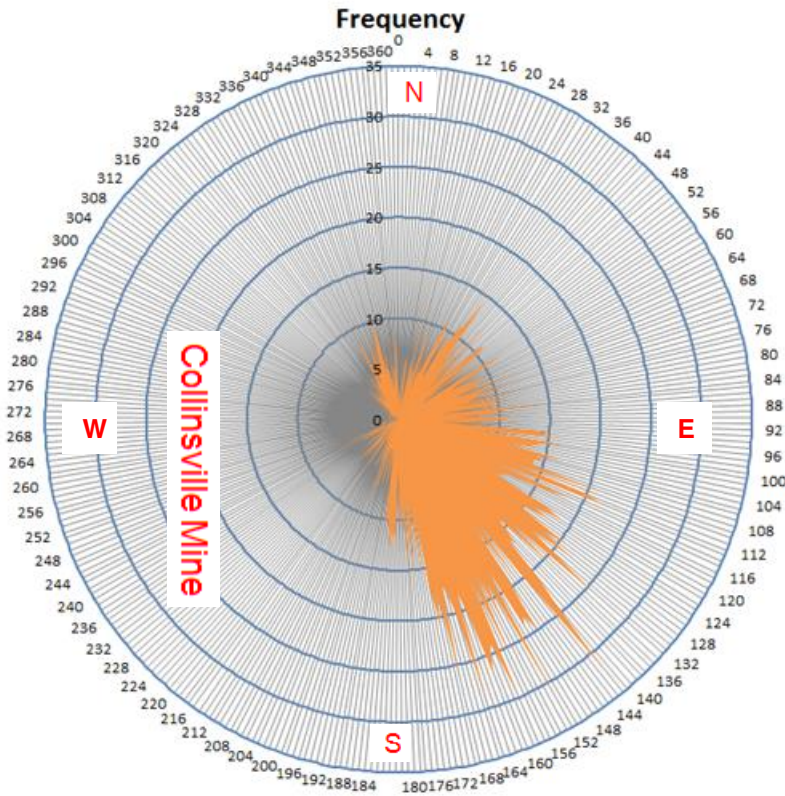


Figure 34. Histogram of Wind Direction in April 2014

Figure 41 plots the relation between the wind speed (Y-axis) and wind direction (X-axis) using the last week data of April 2014. It demonstrated that the high wind speed (>3m/s) were either Southeast or Northeast wind.

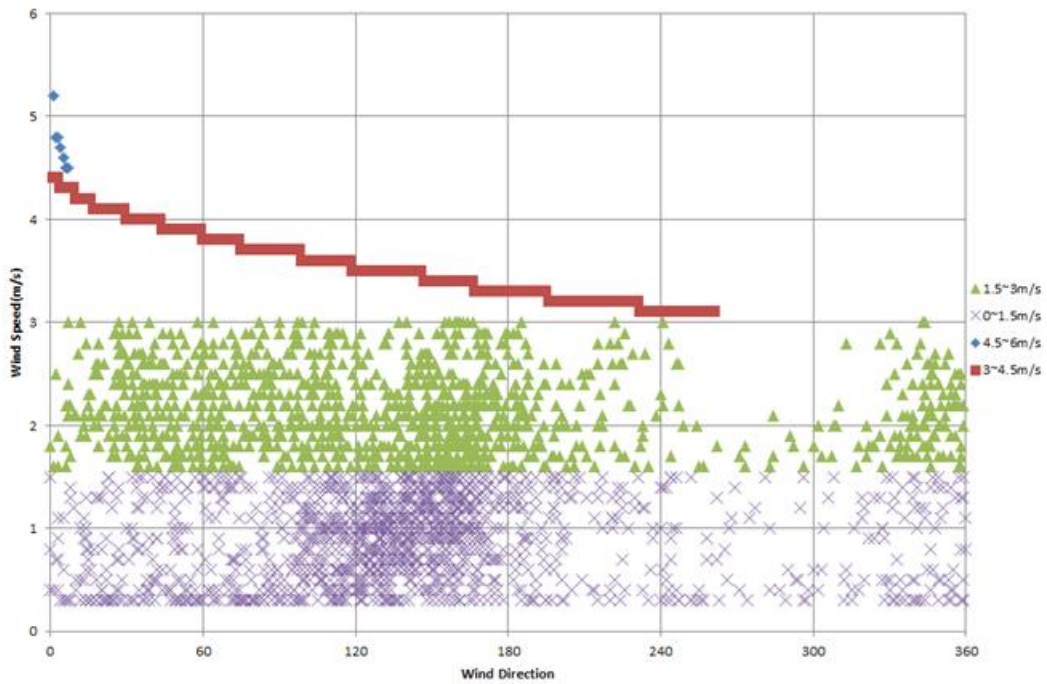


Figure 35. Distribution of wind speed in April 2014

From the monthly average dust concentration plotted in Figure 32b, one can find that the lowest and highest average dust concentration appeared in May 2013 and October 2013 respectively during one-year monitoring period. Therefore, the correlation of dust concentration with the wind speed and direction are presented in Figures 42, 43, 42 and 44 using the data collected in these two periods. Figures 42 and 43 shown the dust concentration related to the wind speed. In October, dust was distributed uniformly across the whole wind speed, which indicated that the wind speed has no effect on the dust concentration. In May, higher dust concentration appeared in lower wind speed. In fact, higher occurrence of dust concentrations over $100\mu\text{g}/\text{m}^3$ were detected in May, but much more concentrations below $15\mu\text{g}/\text{m}^3$ appeared in the same month also. It is the reason that October had higher average of dust concentration than May.

Figures 44 and 45 show the correlation of dust concentration with the wind direction. In October, most higher dust events ($>50\mu\text{g}/\text{m}^3$) were from $50^\circ - 120^\circ$ (East wind). This is not the case in May.

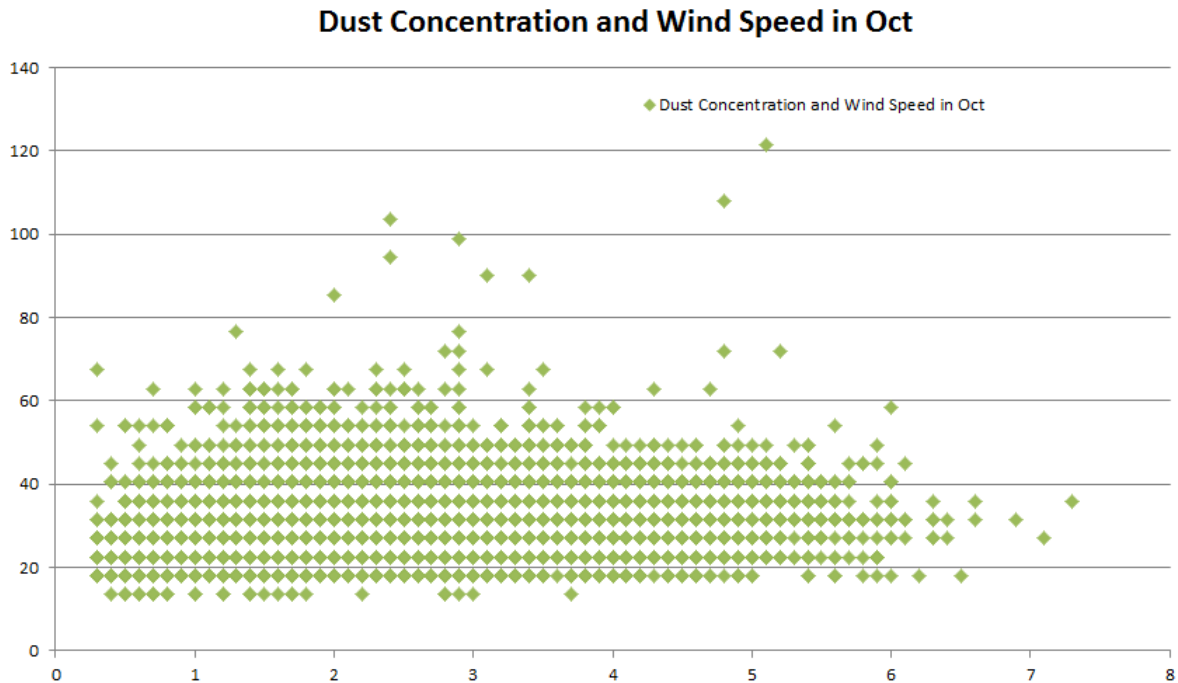


Figure 36. Relations of dust concentration and wind speed in October 2013

Dust Concentration and Wind Speed in May

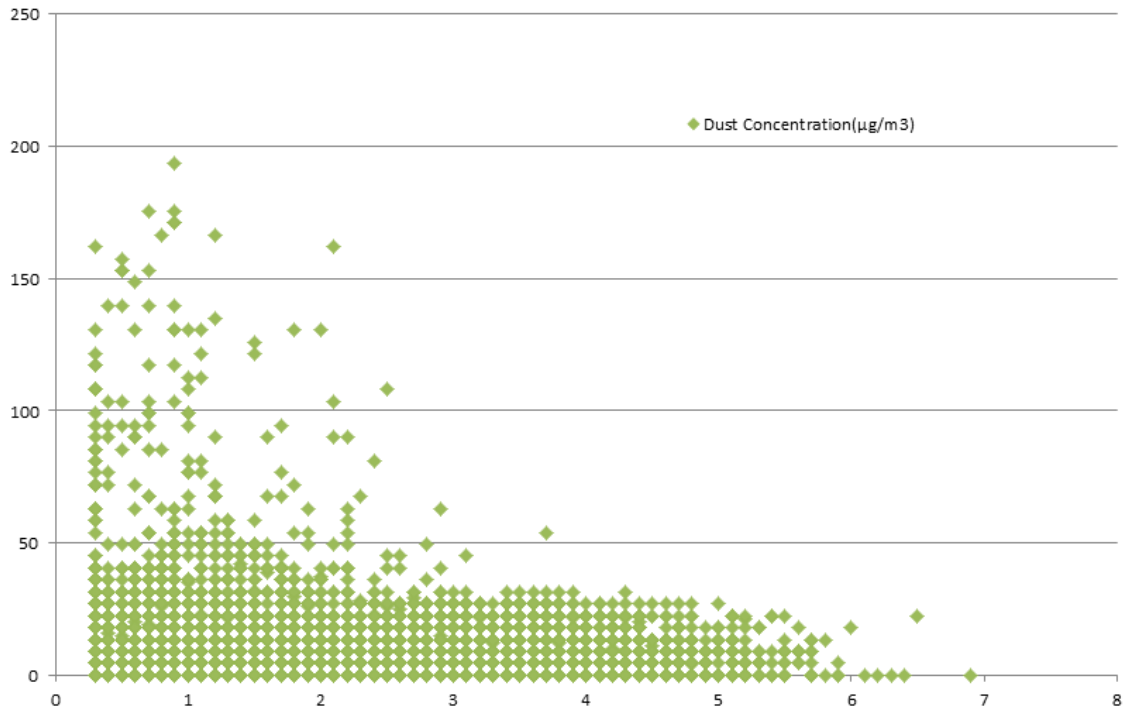


Figure 43. Relations of dust concentration and wind speed in May 2013

Dust Concentration and Wind Direction in Oct

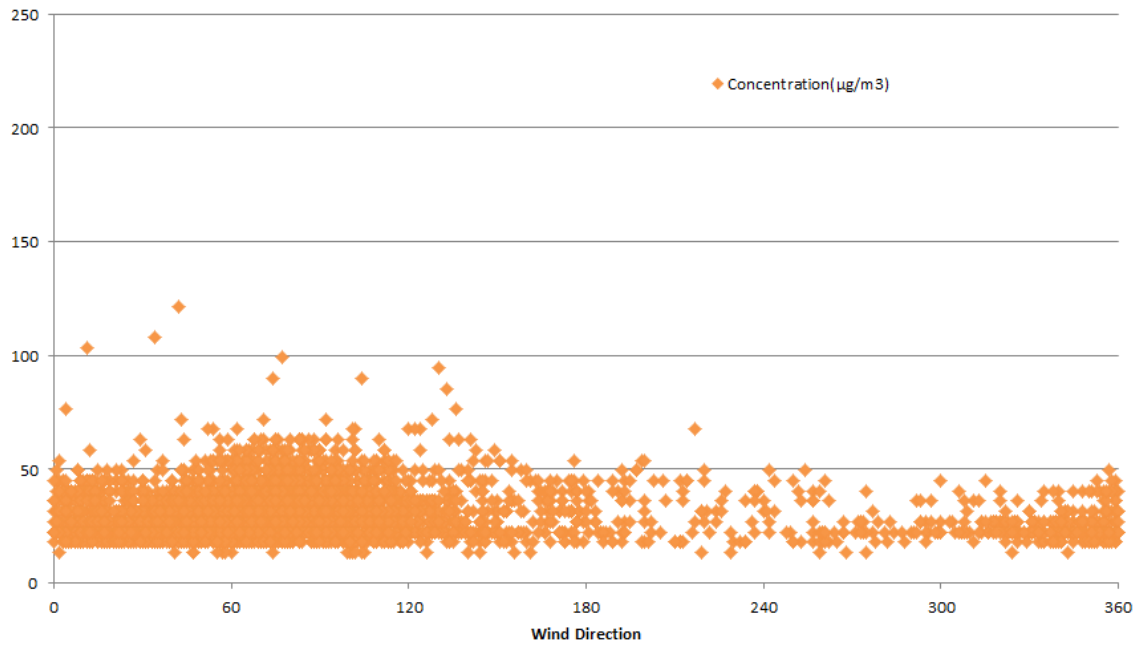


Figure 37. Relations of dust concentration and wind direction in October 2013

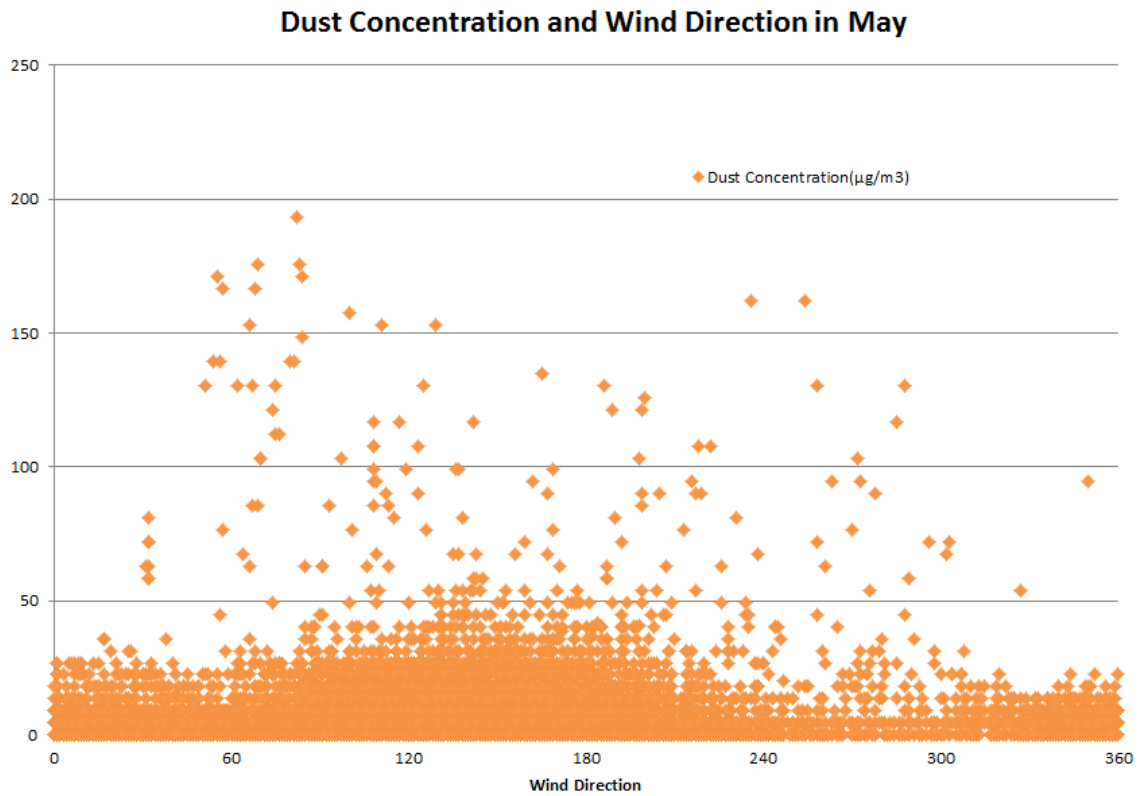


Figure 38. Relations of dust concentration and wind direction in May 2013

5.3 Estimated source (origin) of dust

This section aims to identify the source of dust based on the dust’s relation to the wind speed and direction. If higher concentrations are always from certain directions, there is a possibility of dust source exist in that direction. Hence, only high concentrations are focused on in this section. It is defined that dust concentrations higher than annual average concentration of $15\mu\text{g}/\text{m}^3$ are all expressed as high concentration in this report.

To find out the common features of high dust concentrations, three months having the average dust concentration higher than the annual average are selected for the analysis. The selected three months are September 2013 ($23\mu\text{g}/\text{m}^3$), October 2013 ($32\mu\text{g}/\text{m}^3$) and December 2013 ($22\mu\text{g}/\text{m}^3$) respectively.

The relationship of the wind speed and the dust concentration of larger than $15\mu\text{g}/\text{m}^3$ in September, October and December 2013 are plotted in Figures 46, 47 and 48. Again, it seems that the wind speed has no effect on the dust concentration.

High Concentration and Wind Speed in Sep (>15µg/m³)

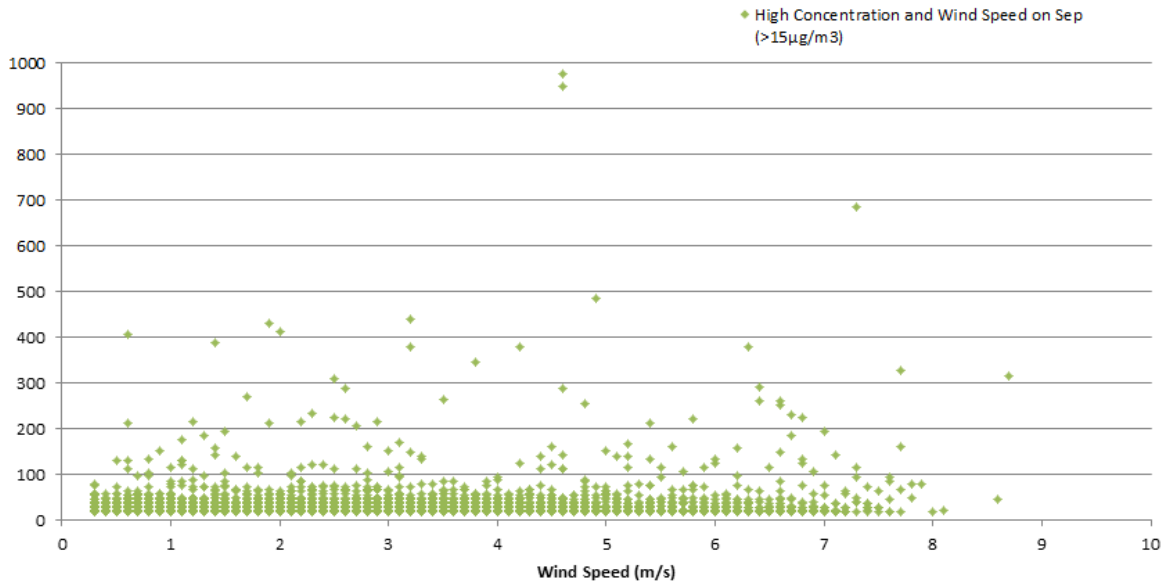


Figure 39. Relation of wind speed and high concentration in September 2013

High Concentration and Wind Speed (>15µg/m³) in Oct

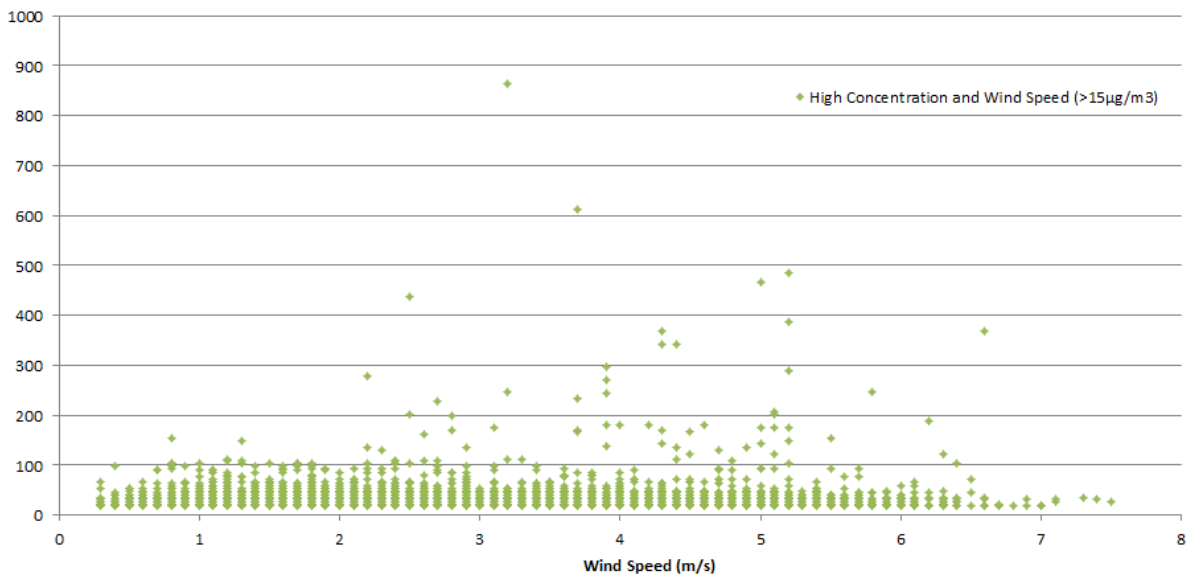


Figure 40. Relation of wind speed and high concentration in October 2013

High Concentration and Wind Speed in Dec (>15µg/m³)

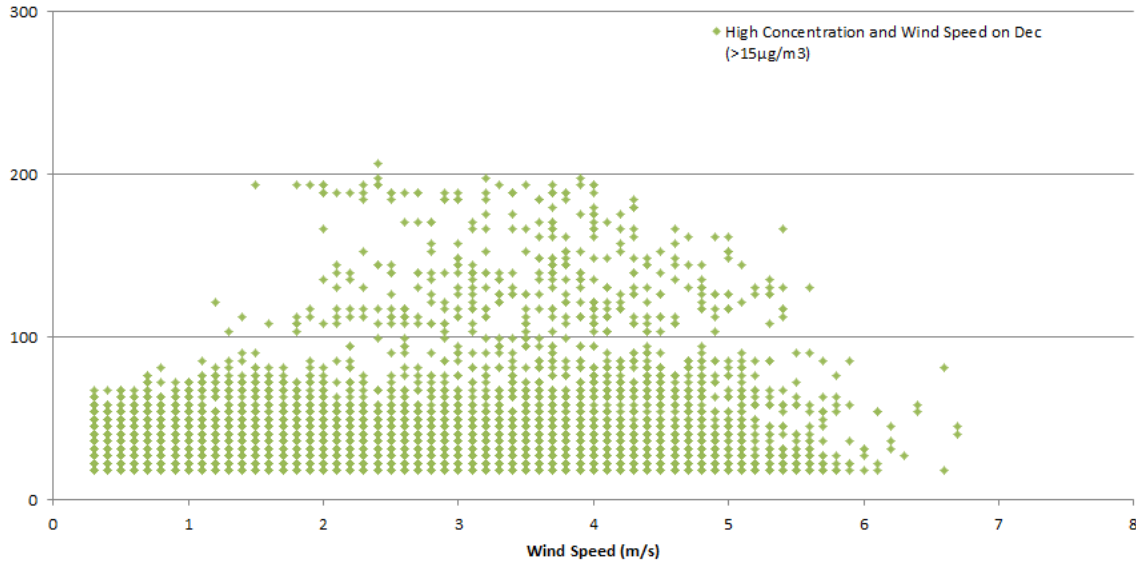


Figure 41. Relation of wind speed and high concentration in December 2013

The relationships of dust concentration (higher than 15µg/m³) with the wind direction in these three months are shown in Figures 49, 50 and 51. Figure 49 shows that the dust concentration higher than 100µg/m³ in September occurred around the directions of 120° and 300°. In October, the higher dust concentration (>100µg/m³) mainly concentrated at the wind directions of 120°. In December, the higher dust concentration (>100µg/m³) mainly concentrated at the wind directions of 60°.

High Concentration and Wind Direction in Sep (>15µg/m³)

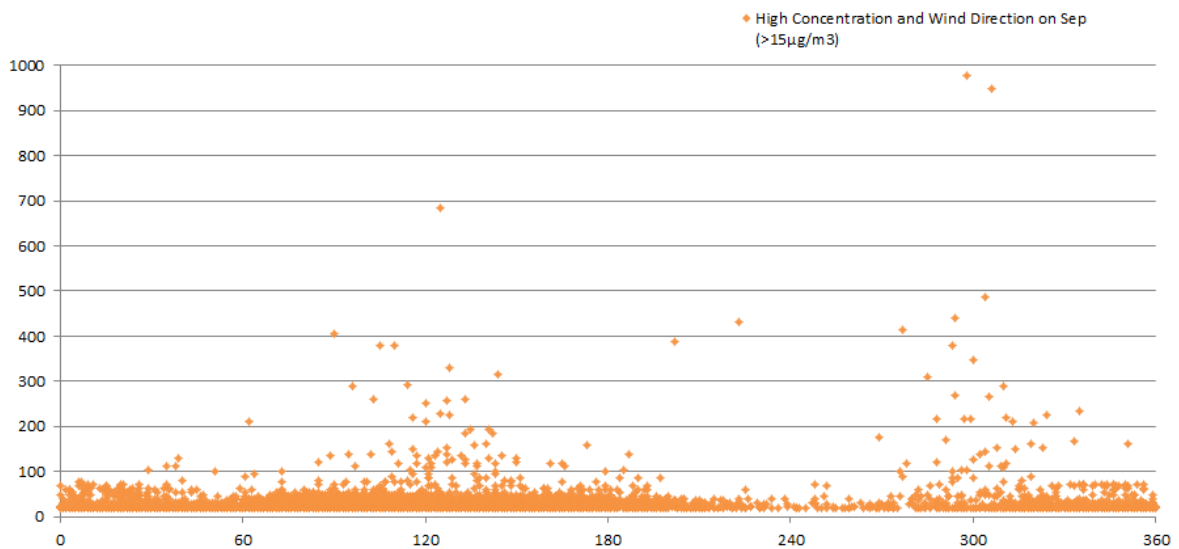


Figure 42. Relation of wind direction and high concentration in September 2013

High Concentration and Wind Direction (>15µg/m³) in Oct

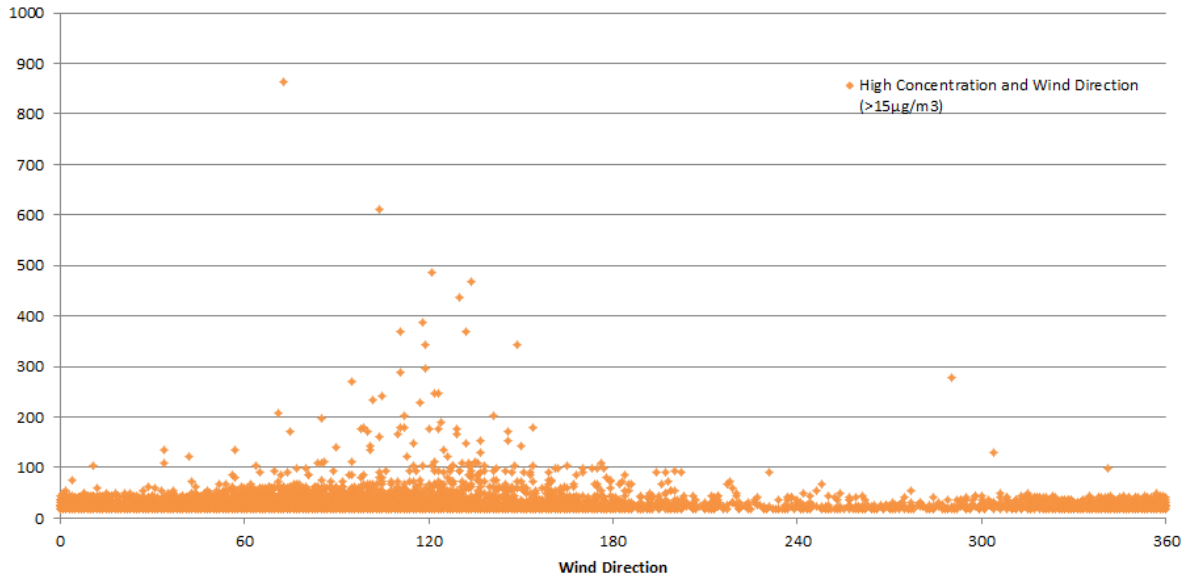


Figure 43. Relation of wind direction and high concentration in October 2013

High Concentration and Wind Direction in Dec (>15µg/m³)

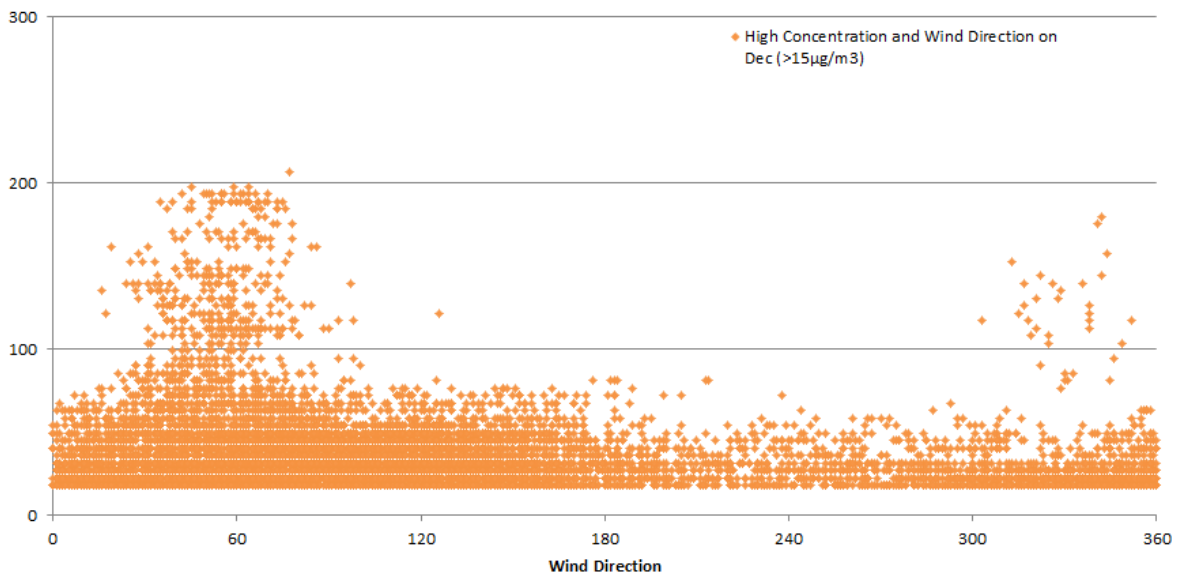


Figure 44. Relation of wind direction and high concentration in December 2013

To explore more characterisations of winds in these three months, the frequencies of wind direction related to the dust concentration larger than 15µg/m³ are plotted in Figures 52, 53 and 54. While the majority of winds in September (Figure 52) were from the directions between 80° to 140°, the higher dust concentrations (>100µg/m³) were mainly from the directions around 120° and 300° (Figure 49). The high occurrences of wind direction in October were mainly between 0° to 100° (Figure 53), but the higher dust concentrations (>100µg/m³) were concentrated at around 120° (Figure 48) even the occurrence of the direction was low. The high occurrence of wind direction in December were from 40° to 120° and the higher dust concentrations (>100µg/m³) were also in these range at around 60°

From the above analysis, the high dust concentrations mainly come from east side. Figure 55 indicates the feature of surrounding environment of our dust monitor. Most of east winds bring more soiling dust particles. However, this conclusion will be verified by analysing the composition of dust particles collected on the 47mm filters.

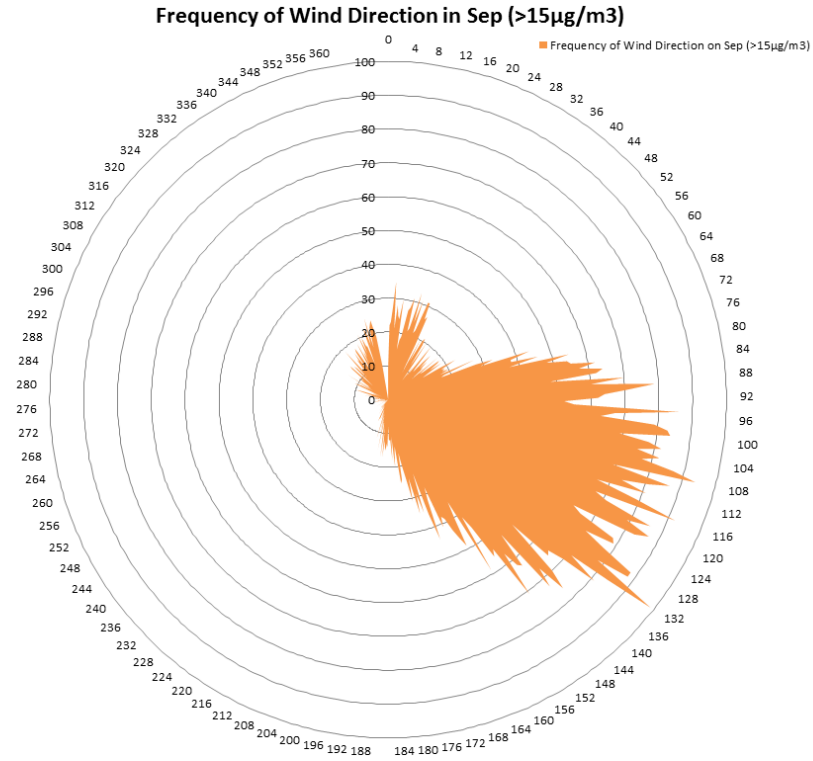


Figure 45. Frequency of wind direction in September 2013 (>15µg/m³)

Frequency of Wind DIRECTION in Oct (>15 $\mu\text{g}/\text{m}^3$)

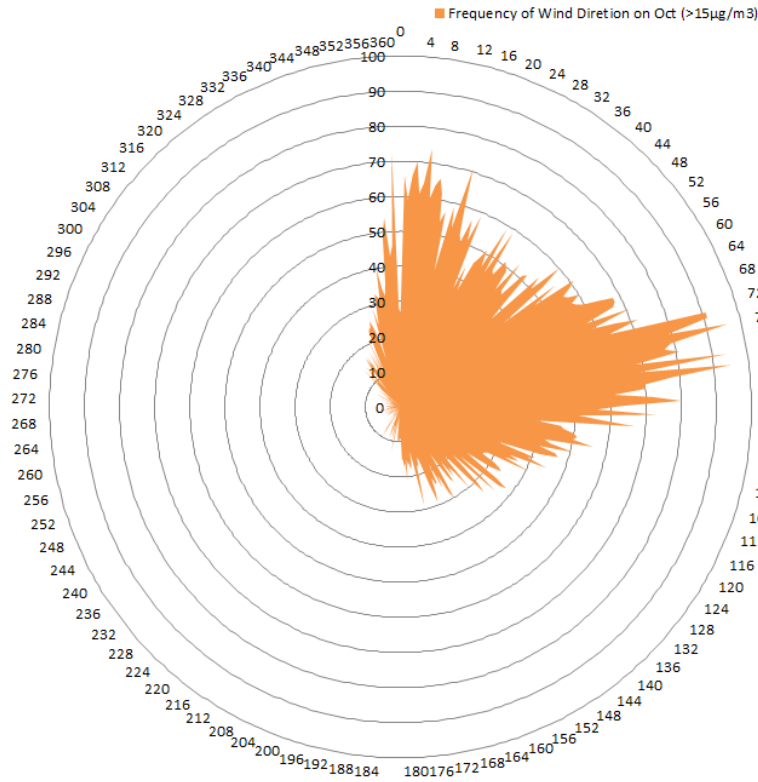


Figure 46. Frequency of wind direction in October 2013 (>15 $\mu\text{g}/\text{m}^3$)

Frequency of Wind DIRECTION in Dec (>15 $\mu\text{g}/\text{m}^3$)

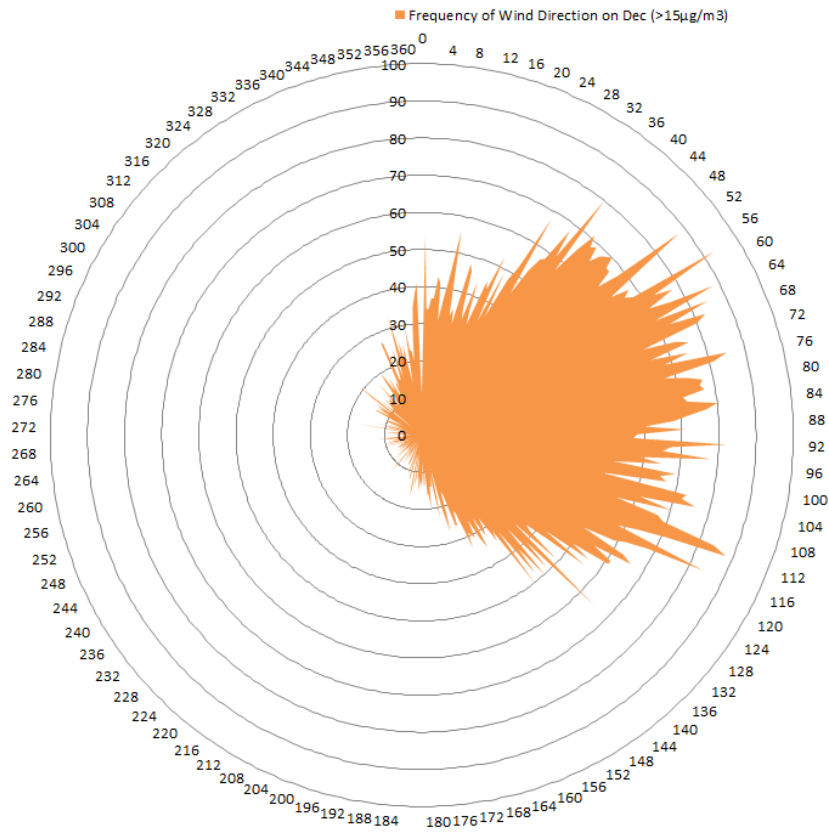


Figure 47. Frequency of wind direction in December 2013 (>15 $\mu\text{g}/\text{m}^3$)

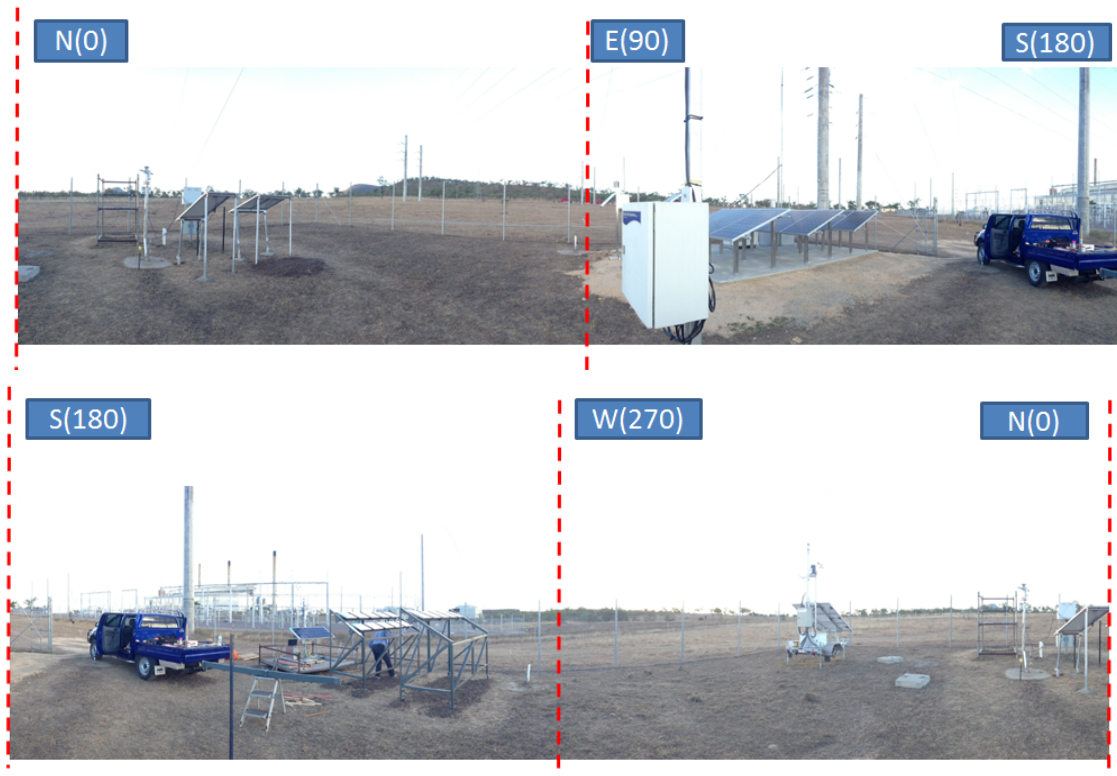


Figure 48. Surrounding environment of dust monitor

5.4 Dust particle size and properties

The dust samples collected from Collinsville on the four filters are shown in Figure 56 and were analysed in QUT lab with the equipment SEM. The filter may be polluted before installed into the monitor, therefore an unused filter was analysed first. There were no obvious dust particles on the new filter as shown in Figure 57, and about 86% in weight are fluorine as listed in Table4, since the material of the filters is polytetrafluoroethylene. Also, aluminium, silicon and sulphur element were detected.

Based on the operation requirement of SEM, all samples should be coated by carbon before the analysis. Hence, fluorine and carbon, even in high value shown in the relative table, will not be mentioned any more in the analysis of the four dust samples. All typical dust particulates will be analysed based on their characteristic shapes, such as stick, cube and uneven.

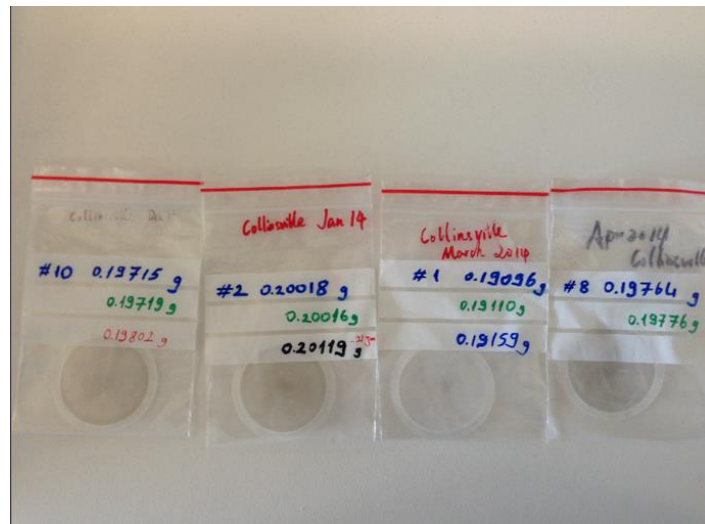


Figure 49. Dust samples for property analysis

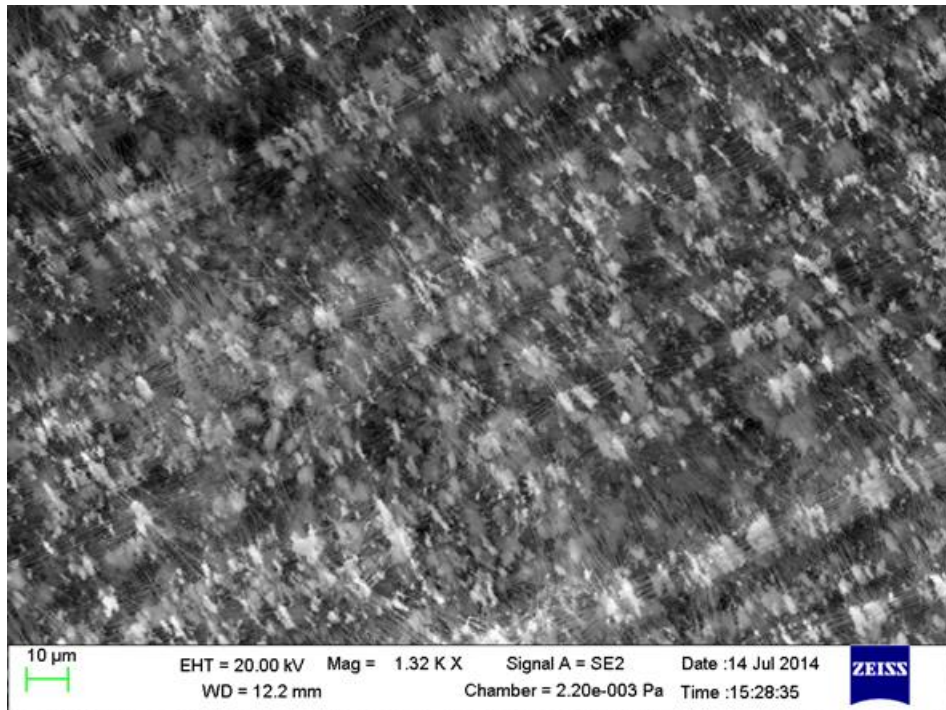


Figure 50. Electron image of the unused filter

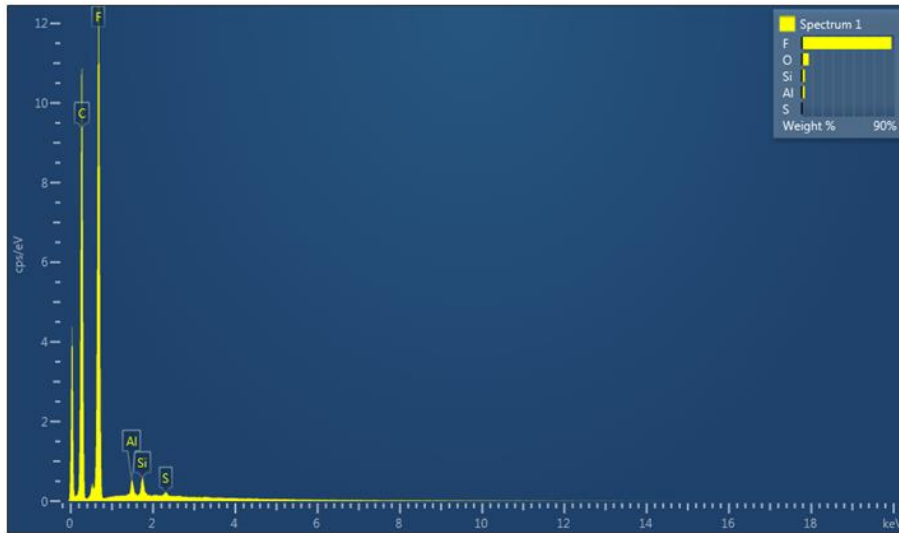


Table 4. Composition of the unused filter

| Element | Line Type | Apparent Concentration | k Ratio | Wt% | Wt% Sigma | Standard Label | Factory Standard |
|---------|-----------|------------------------|---------|-------|-----------|----------------|------------------|
| F | K series | 179.61 | 0.35267 | 86.83 | 0.22 | CaF2 | Yes |
| Al | K series | 1.17 | 0.00839 | 2.80 | 0.11 | Al2O3 | Yes |
| Si | K series | 1.39 | 0.01098 | 2.92 | 0.10 | SiO2 | Yes |
| S | K series | 0.37 | 0.00315 | 0.65 | 0.07 | FeS2 | Yes |

Figure 58 and Table 5 illustrate both physical and chemical properties of dust samples collected in December 2013. The average of dust particle size is around 10µm and the major compositions of the dust are sodium and silicon. Therefore, most particles are albite or silicon dioxide in December 2013.

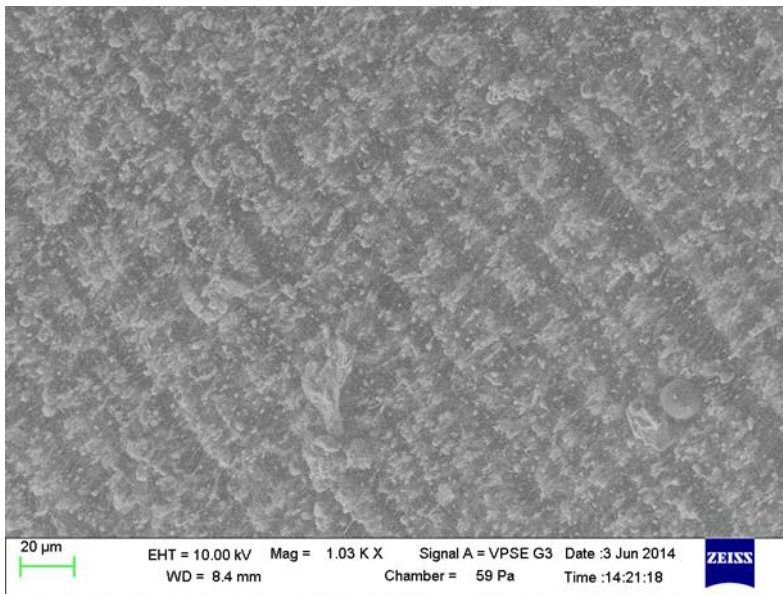


Figure 51. Electron image of filter from December 13

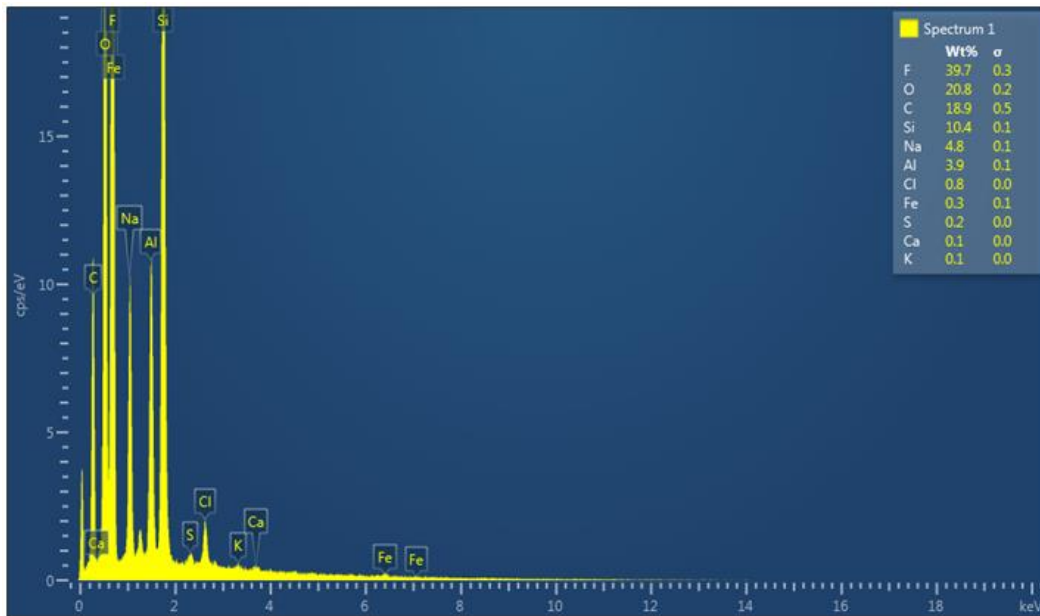


Table 5. Dust composition in December 2013

| Element | Line Type | Apparent Concentration | k Ratio | Wt% | Wt% Sigma | Standard Label | Factory Standard |
|---------|-----------|------------------------|---------|-------|-----------|--------------------------------|------------------|
| Na | K series | 4.74 | 0.01998 | 4.84 | 0.08 | Albite | Yes |
| Al | K series | 3.45 | 0.02479 | 3.91 | 0.06 | Al ₂ O ₃ | Yes |
| Si | K series | 9.39 | 0.07439 | 10.38 | 0.11 | SiO ₂ | Yes |
| S | K series | 0.15 | 0.00125 | 0.16 | 0.03 | FeS ₂ | Yes |
| Cl | K series | 0.73 | 0.00642 | 0.82 | 0.04 | NaCl | Yes |
| K | K series | 0.09 | 0.00079 | 0.09 | 0.03 | KBr | Yes |
| Ca | K series | 0.13 | 0.00113 | 0.13 | 0.03 | Wollastonite | Yes |
| Fe | K series | 0.23 | 0.00227 | 0.29 | 0.07 | Fe | Yes |

Figure 59 shows the SEM results based on the dust sample collected in January 2014. More than half of the particulates are over 10µm and some particle sizes are over 20µm. The average particle size in January 2014 is approximately 15µm.

As indicated in Table 5, sodium and chlorine are the major composition of the cubic dust particle and occupy more than 90% of the weight of the dust. For stick particle as shown in Table 7, the percentage of sodium, magnesium and chlorine are higher than other elements.

To clarify other uneven particulates, composition was analysed and listed in Table 8. The main elements of those particles are silicon and aluminium.

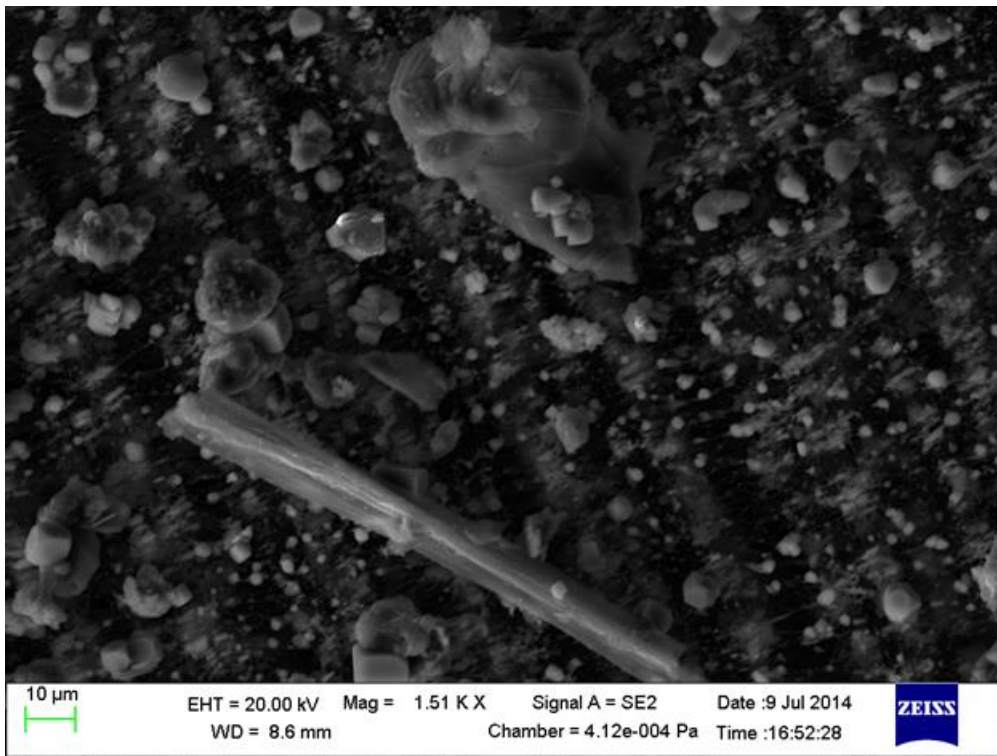


Figure 52. Electron image of filter from January 2014

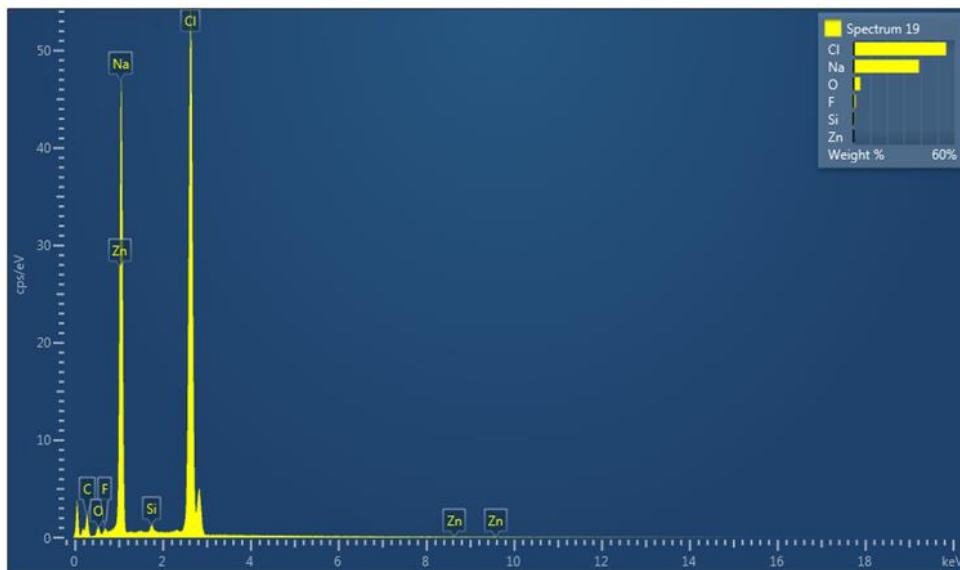


Table 6. Composition of cubic dust particles collected in January 2014

| Element | Line Type | Apparent Concentration | k Ratio | Wt% | Wt% Sigma | Standard Label | Factory Standard |
|---------|-----------|------------------------|---------|-------|-----------|------------------|------------------|
| Na | K series | 46.30 | 0.19539 | 38.84 | 0.24 | Albite | Yes |
| Si | K series | 0.48 | 0.00381 | 0.66 | 0.05 | SiO ₂ | Yes |
| Cl | K series | 46.92 | 0.41006 | 54.97 | 0.27 | NaCl | Yes |
| Zn | K series | 0.01 | 0.00007 | 0.01 | 0.12 | Zn | Yes |

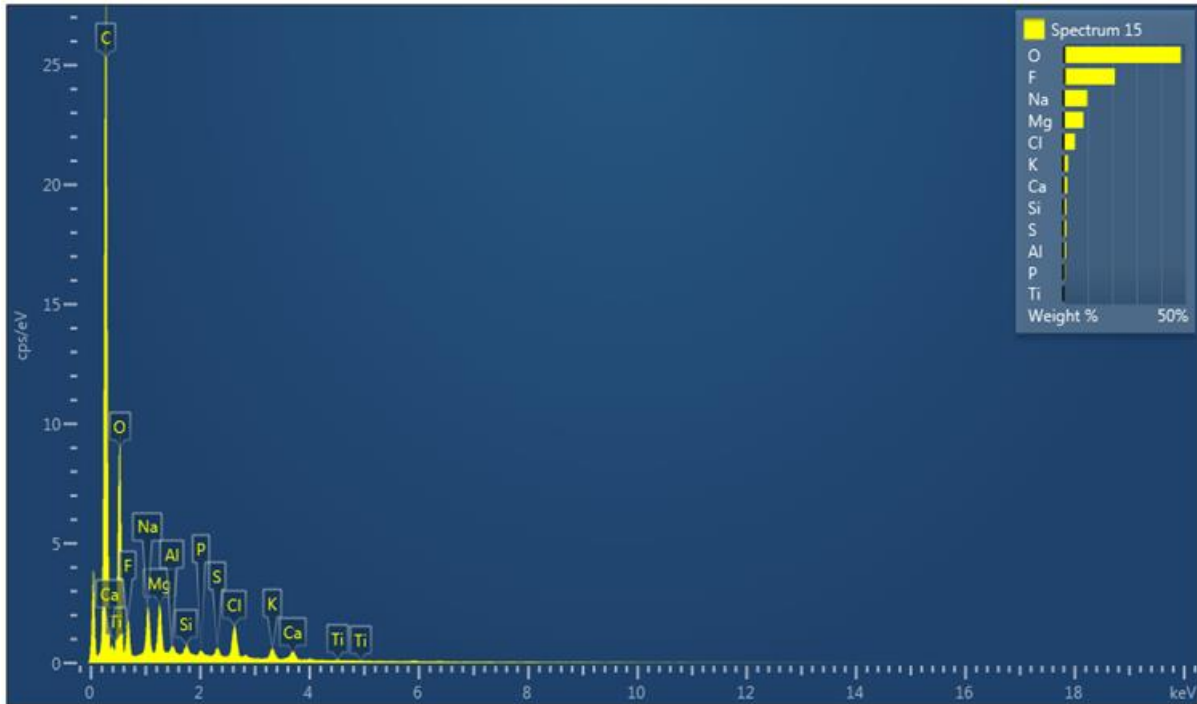


Table 7. Composition of stick dust particles collected in January 2014

| Element | Line Type | Apparent Concentration | k Ratio | Wt% | Wt% Sigma | Standard Label | Factory Standard |
|---------|-----------|------------------------|---------|------|-----------|--------------------------------|------------------|
| Na | K series | 5.13 | 0.02165 | 9.76 | 0.21 | Albite | Yes |
| Mg | K series | 3.50 | 0.02319 | 8.24 | 0.18 | MgO | Yes |
| Al | K series | 0.51 | 0.00363 | 1.11 | 0.10 | Al ₂ O ₃ | Yes |
| Si | K series | 0.65 | 0.00518 | 1.24 | 0.09 | SiO ₂ | Yes |
| P | K series | 0.57 | 0.00317 | 0.67 | 0.08 | GaP | Yes |
| S | K series | 0.76 | 0.00652 | 1.21 | 0.08 | FeS ₂ | Yes |
| Cl | K series | 3.01 | 0.02634 | 4.78 | 0.11 | NaCl | Yes |
| K | K series | 1.36 | 0.01148 | 1.94 | 0.08 | KBr | Yes |
| Ca | K series | 1.14 | 0.01017 | 1.66 | 0.08 | Wollastonite | Yes |
| Ti | K series | 0.16 | 0.00157 | 0.27 | 0.08 | Ti | Yes |

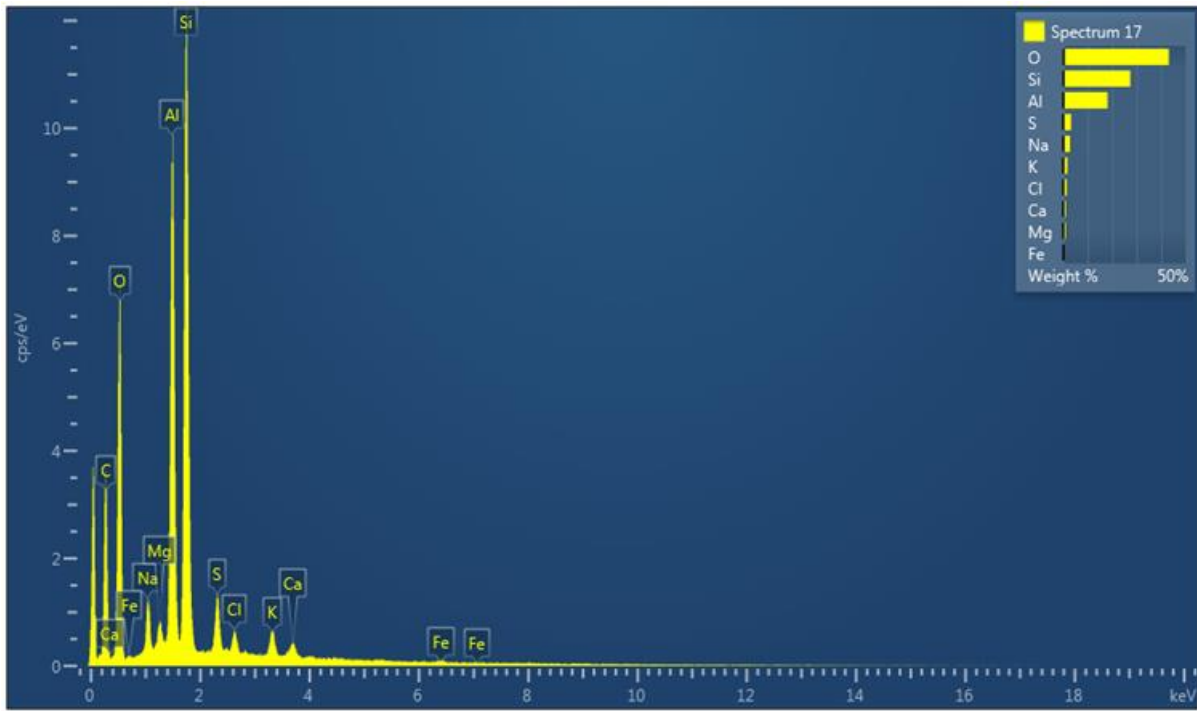


Table 8. Composition of other uneven dust particles in January 2014

| Element | Line Type | Apparent Concentration | k Ratio | Wt% | Wt% Sigma | Standard Label | Factory Standard |
|---------|-----------|------------------------|---------|-------|-----------|--------------------------------|------------------|
| Na | K series | 2.85 | 0.01203 | 2.79 | 0.09 | Albite | Yes |
| Mg | K series | 0.84 | 0.00557 | 0.97 | 0.06 | MgO | Yes |
| Al | K series | 17.12 | 0.12298 | 18.12 | 0.15 | Al ₂ O ₃ | Yes |
| Si | K series | 21.69 | 0.17188 | 27.44 | 0.19 | SiO ₂ | Yes |
| S | K series | 2.36 | 0.02034 | 3.18 | 0.08 | FeS ₂ | Yes |
| Cl | K series | 1.03 | 0.00900 | 1.34 | 0.07 | NaCl | Yes |
| K | K series | 1.60 | 0.01355 | 1.73 | 0.07 | KBr | Yes |
| Ca | K series | 0.92 | 0.00825 | 0.99 | 0.07 | Wollastonite | Yes |
| Fe | K series | 0.28 | 0.00284 | 0.34 | 0.09 | Fe | Yes |

Figure 60 shows particles analysis on the dust sample collected in March 2014 and the particles' size are very large and some of them are over 10µm. It is correlated that the average of dust concentration is 14µg/m³ in this period, which is also not very high. However, some particulates are accumulated together to form a large particle, which is larger than 100µm. The composition of the dust sample was listed in Table 9. Based on their higher weight percentage, sodium chloride and carnallite are the major composite of the dust.

Table 10 shows composition of cubic particles of the dust collected in March 2014. Chlorine and sodium take up over 75% of all elements of cube. Two sticks particles are also measured with about 144 μ m length and are listed in Table 11. Chlorine, sodium and magnesium are the major compositions of those stick particulates. The other uneven particles size are listed in Table 12. It is clear to see that the percentage of silicon (25.48%) is much higher than other elements, and most of those particulates are silicon dioxide.

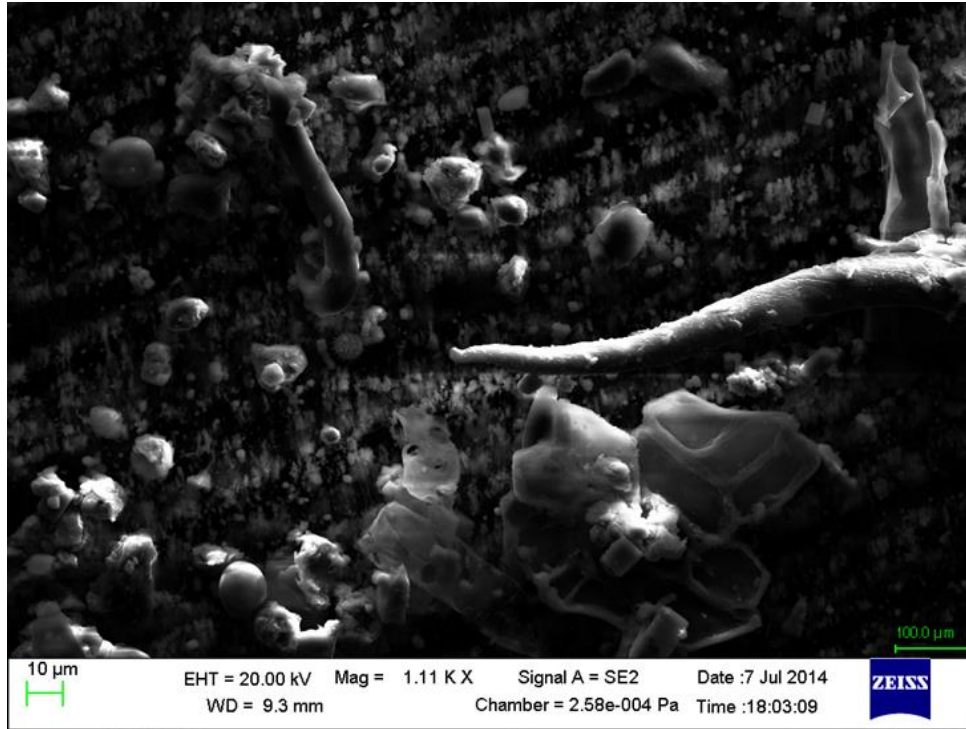


Figure 53. Electron image of dust collected in March 2014

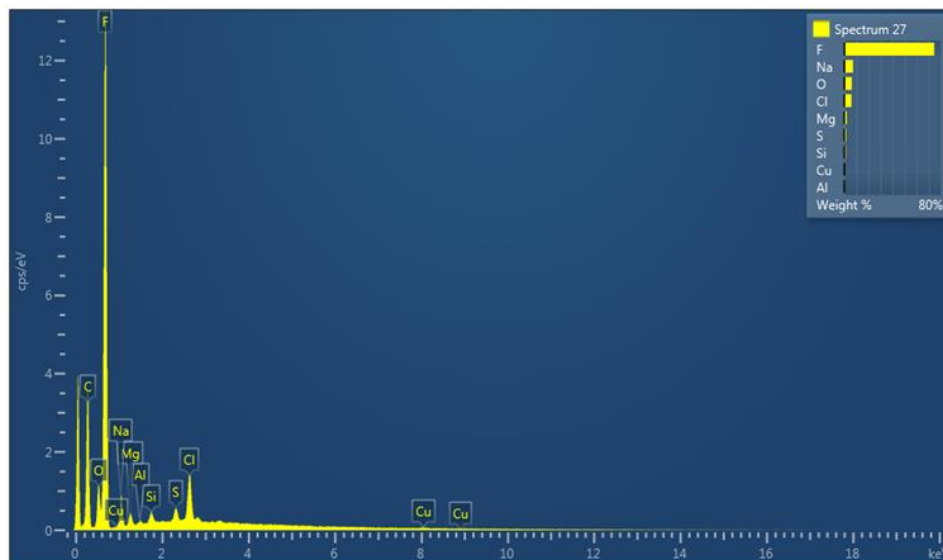


Table 9. Composition of large particle size based on the dust sample collected in March 2014

| Element | Line Type | Apparent Concentration | k Ratio | Wt% | Wt% Sigma | Standard Label | Factory Standard |
|---------|-----------|------------------------|---------|------|-----------|--------------------------------|------------------|
| Na | K series | 3.44 | 0.01450 | 7.25 | 0.18 | Albite | Yes |
| Mg | K series | 0.85 | 0.00567 | 2.04 | 0.10 | MgO | Yes |
| Al | K series | 0.20 | 0.00147 | 0.40 | 0.07 | Al ₂ O ₃ | Yes |
| Si | K series | 0.70 | 0.00555 | 1.16 | 0.07 | SiO ₂ | Yes |
| S | K series | 1.14 | 0.00983 | 1.56 | 0.08 | FeS ₂ | Yes |
| Cl | K series | 4.40 | 0.03844 | 5.99 | 0.11 | NaCl | Yes |
| Cu | K series | 0.53 | 0.00531 | 0.80 | 0.19 | Cu | Yes |

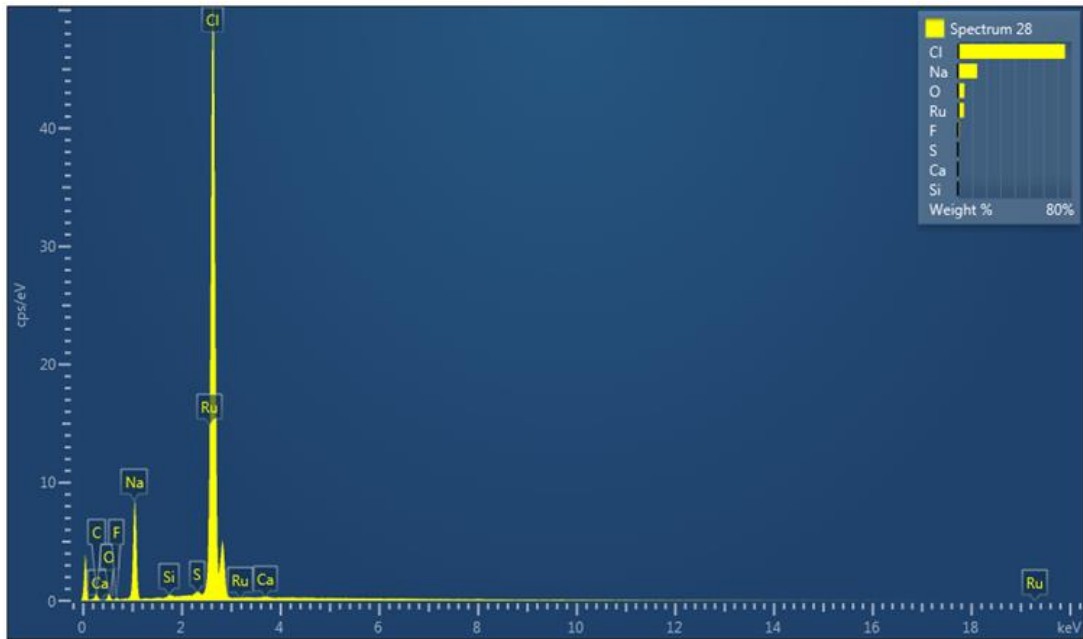


Table 10. Composition of cubic particles of the dust collected in March 2014

| Element | Line Type | Apparent Concentration | k Ratio | Wt% | Wt% Sigma | Standard Label | Factory Standard |
|---------|-----------|------------------------|---------|-------|-----------|----------------|------------------|
| Na | K series | 12.39 | 0.05229 | 13.71 | 0.16 | Albite | Yes |
| Si | K series | 0.18 | 0.00142 | 0.22 | 0.04 | SiO2 | Yes |
| S | K series | 0.41 | 0.00354 | 0.44 | 0.05 | FeS2 | Yes |
| Cl | K series | 63.68 | 0.55652 | 75.35 | 0.49 | NaCl | Yes |
| Ca | K series | 0.16 | 0.00144 | 0.25 | 0.07 | Wollastonite | Yes |
| Ru | L series | 3.20 | 0.03197 | 4.39 | 0.50 | Ru (v) | Yes |

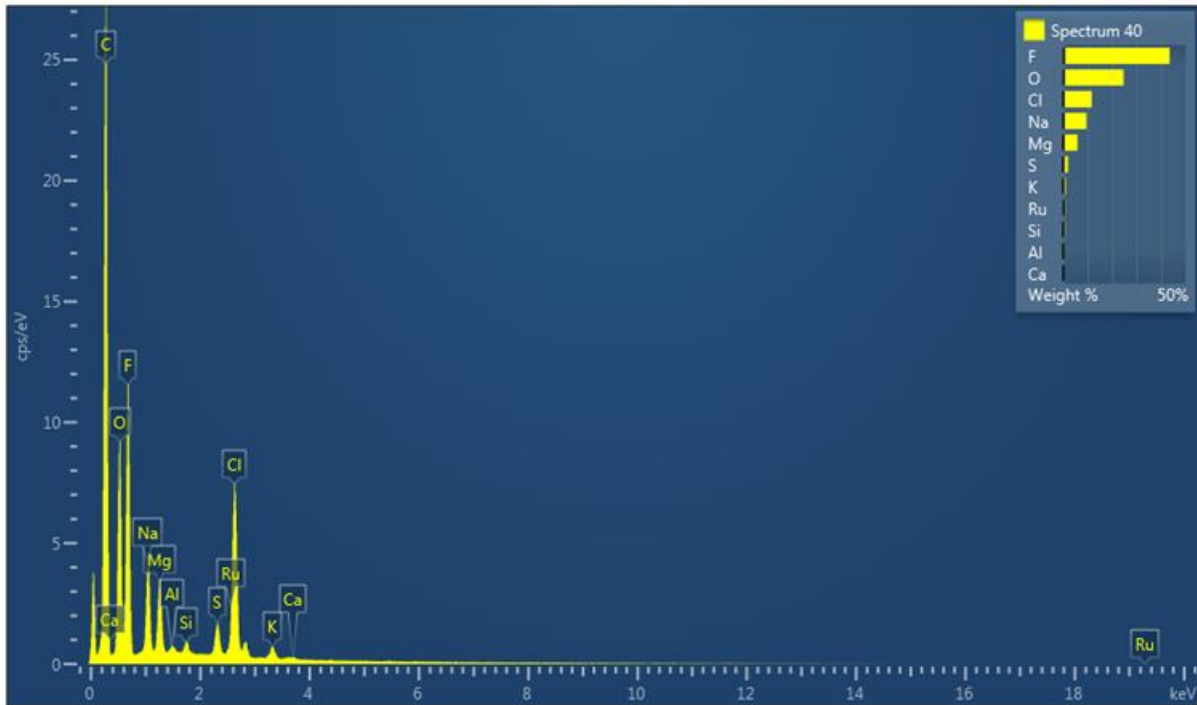


Table 11. Composition of the stick particles based on the dust sample collected in March 2014

| Element | Line Type | Apparent Concentration | k Ratio | Wt% | Wt% Sigma | Standard Label | Factory Standard |
|---------|-----------|------------------------|---------|-------|-----------|--------------------------------|------------------|
| Na | K series | 7.17 | 0.03025 | 9.48 | 0.16 | Albite | Yes |
| Mg | K series | 3.62 | 0.02399 | 5.80 | 0.12 | MgO | Yes |
| Al | K series | 0.28 | 0.00198 | 0.39 | 0.06 | Al ₂ O ₃ | Yes |
| Si | K series | 0.57 | 0.00450 | 0.69 | 0.05 | SiO ₂ | Yes |
| S | K series | 1.91 | 0.01648 | 1.93 | 0.06 | FeS ₂ | Yes |
| Cl | K series | 11.43 | 0.09990 | 11.63 | 0.13 | NaCl | Yes |
| K | K series | 1.02 | 0.00863 | 0.98 | 0.05 | KBr | Yes |
| Ca | K series | 0.18 | 0.00164 | 0.18 | 0.04 | Wollastonite | Yes |
| Ru | L series | 0.71 | 0.00710 | 0.84 | 0.26 | Ru (v) | Yes |

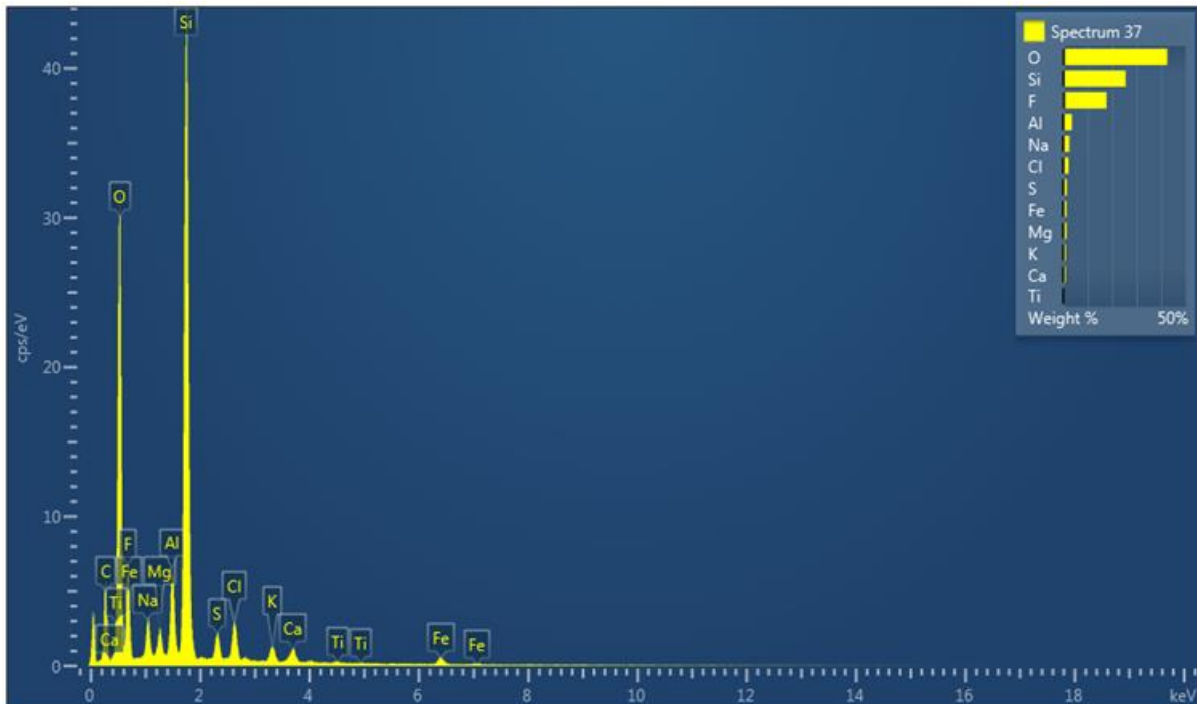


Table 12. Composition of the uneven particles based on the dust sample collected in March 2014

| Element | Line Type | Apparent Concentration | k Ratio | Wt% | Wt% Sigma | Standard Label | Factory Standard |
|---------|-----------|------------------------|---------|-------|-----------|----------------|------------------|
| F | K series | 22.71 | 0.04458 | 17.71 | 0.31 | CaF2 | Yes |
| Na | K series | 2.90 | 0.01222 | 2.50 | 0.08 | Albite | Yes |
| Mg | K series | 1.34 | 0.00888 | 1.29 | 0.05 | MgO | Yes |
| Al | K series | 4.15 | 0.02981 | 3.50 | 0.07 | Al2O3 | Yes |
| Si | K series | 31.91 | 0.25284 | 25.48 | 0.17 | SiO2 | Yes |
| S | K series | 1.66 | 0.01429 | 1.46 | 0.05 | FeS2 | Yes |
| Cl | K series | 2.54 | 0.02220 | 2.15 | 0.05 | NaCl | Yes |
| K | K series | 1.42 | 0.01204 | 1.03 | 0.04 | KBr | Yes |
| Ca | K series | 1.31 | 0.01172 | 0.95 | 0.04 | Wollastonite | Yes |
| Ti | K series | 0.18 | 0.00177 | 0.15 | 0.04 | Ti | Yes |
| Fe | K series | 1.57 | 0.01569 | 1.30 | 0.07 | Fe | Yes |

Figure 61 shows the dust particulates collected in April 2014. Some dust particles are over 20µm. The compositions of these larger particles are listed in Table 13. Silicon and aluminium have much higher weight percentage than other elements. Consequently, these large dust particulates are mainly of silicon dioxide and aluminium. Furthermore, elements of some fine particles are listed in Table 14. More than 36% of those particulate contents are silicon.



Figure 54. Electron image based on the dust sample collected in April 14

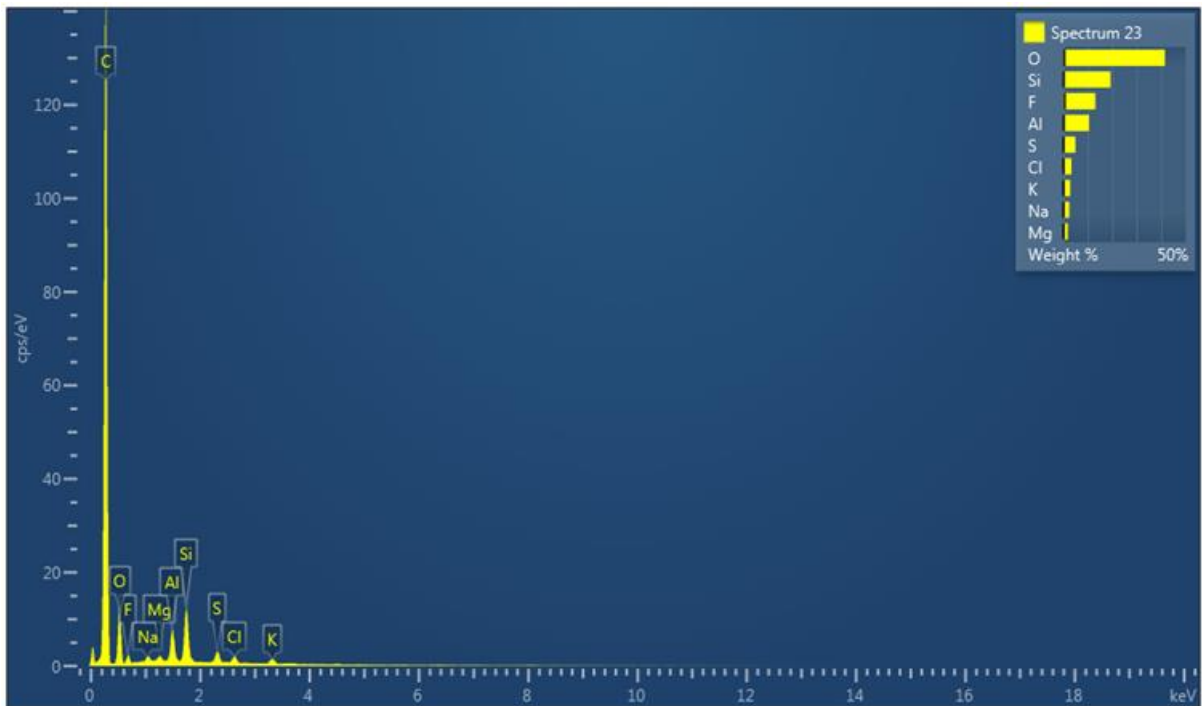


Table 13. Composition of large particles based on the dust sample collected in April 2014

| Element | Line Type | Apparent Concentration | k Ratio | Wt% | Wt% Sigma | Standard Label | Factory Standard |
|---------|-----------|------------------------|---------|-------|-----------|--------------------------------|------------------|
| Na | K series | 0.79 | 0.00332 | 2.51 | 0.22 | Albite | Yes |
| Mg | K series | 0.51 | 0.00338 | 1.85 | 0.17 | MgO | Yes |
| Al | K series | 3.24 | 0.02329 | 10.55 | 0.23 | Al ₂ O ₃ | Yes |
| Si | K series | 5.67 | 0.04491 | 19.31 | 0.29 | SiO ₂ | Yes |
| S | K series | 1.44 | 0.01245 | 4.99 | 0.18 | FeS ₂ | Yes |
| Cl | K series | 0.96 | 0.00836 | 3.30 | 0.16 | NaCl | Yes |
| K | K series | 0.97 | 0.00819 | 2.86 | 0.16 | KBr | Yes |

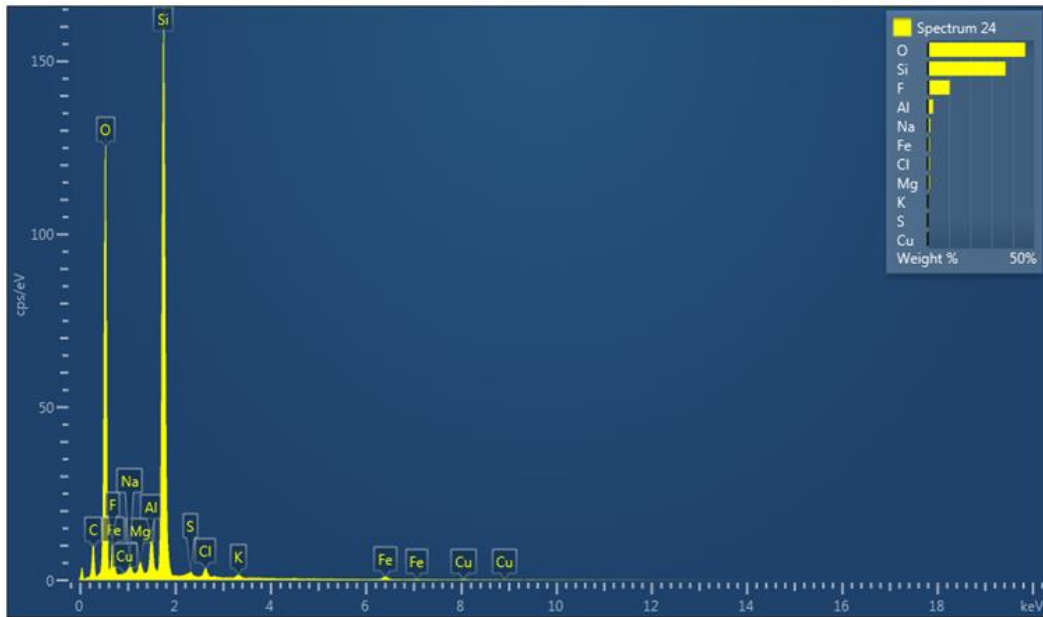


Table 14. Composition of fine particles based on the dust sample collected in April 2014

| Element | Line Type | Apparent Concentration | k Ratio | Wt% | Wt% Sigma | Standard Label | Factory Standard |
|---------|-----------|------------------------|---------|-------|-----------|--------------------------------|------------------|
| Na | K series | 1.18 | 0.00499 | 1.18 | 0.08 | Albite | Yes |
| Mg | K series | 0.83 | 0.00547 | 0.91 | 0.05 | MgO | Yes |
| Al | K series | 2.59 | 0.01863 | 2.54 | 0.06 | Al ₂ O ₃ | Yes |
| Si | K series | 38.96 | 0.30875 | 36.50 | 0.20 | SiO ₂ | Yes |
| S | K series | 0.27 | 0.00232 | 0.31 | 0.04 | FeS ₂ | Yes |
| Cl | K series | 0.83 | 0.00730 | 0.92 | 0.05 | NaCl | Yes |
| K | K series | 0.40 | 0.00343 | 0.37 | 0.04 | KBr | Yes |
| Fe | K series | 0.89 | 0.00885 | 0.92 | 0.07 | Fe | Yes |
| Cu | K series | 0.27 | 0.00265 | 0.29 | 0.08 | Cu | Yes |

For a comparison, we also have a dust monitor located in the UQ St Lucia campus and a filter was installed to collect the dust sample in this region. This dust sample was analysed and the result is shown in Figure 62. Table 15 shows the composition of a cubic particulate which calcium takes up over 57% of weight, so the primary composition of this particle is wollastonite. Furthermore, based on the largest particle presented in this filter (over 20µm) the majority of element is titanium as shown Table 16. Other uneven particulates are listed in Table 17. The percentage of silicon is much higher than other elements in these uneven particles.

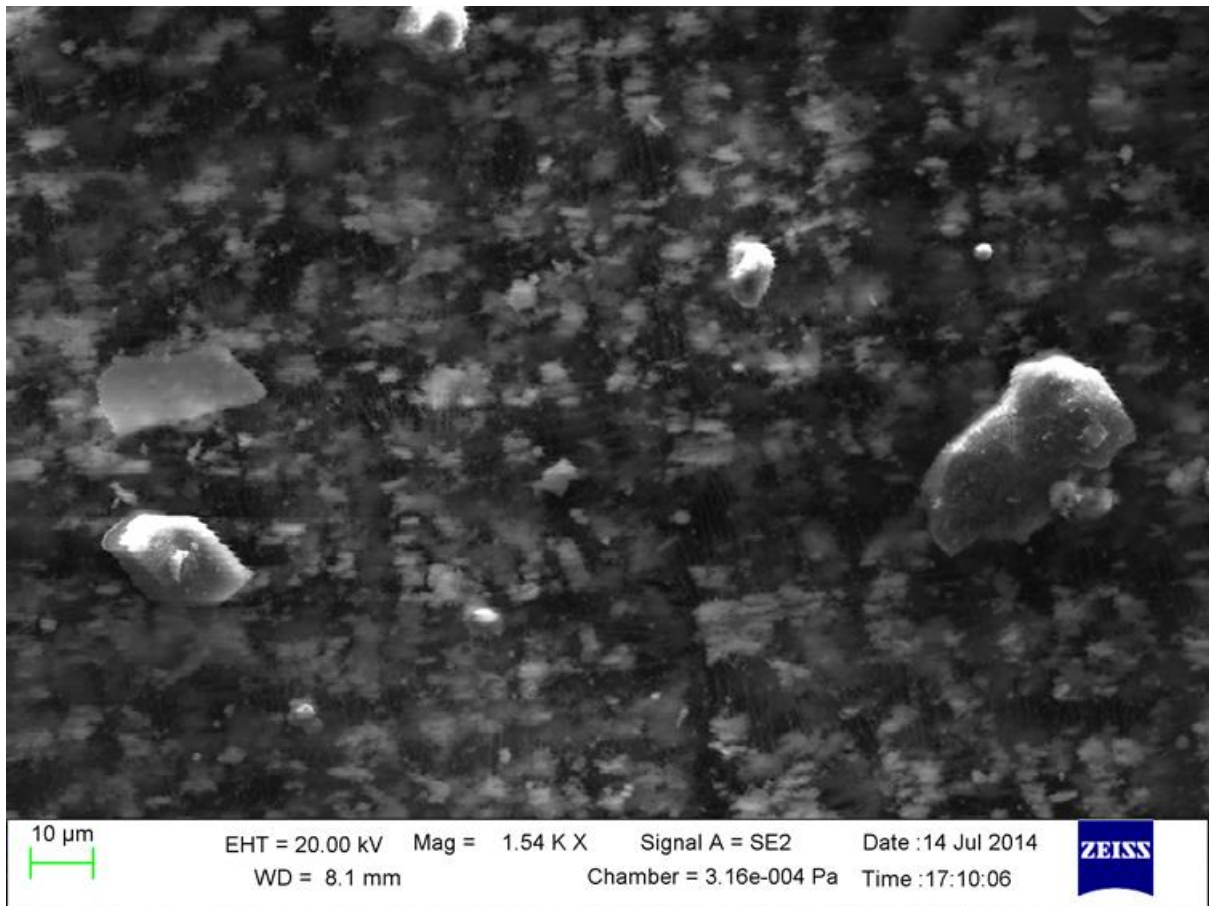


Figure 55. Electron image of dust sample from UQ monitor

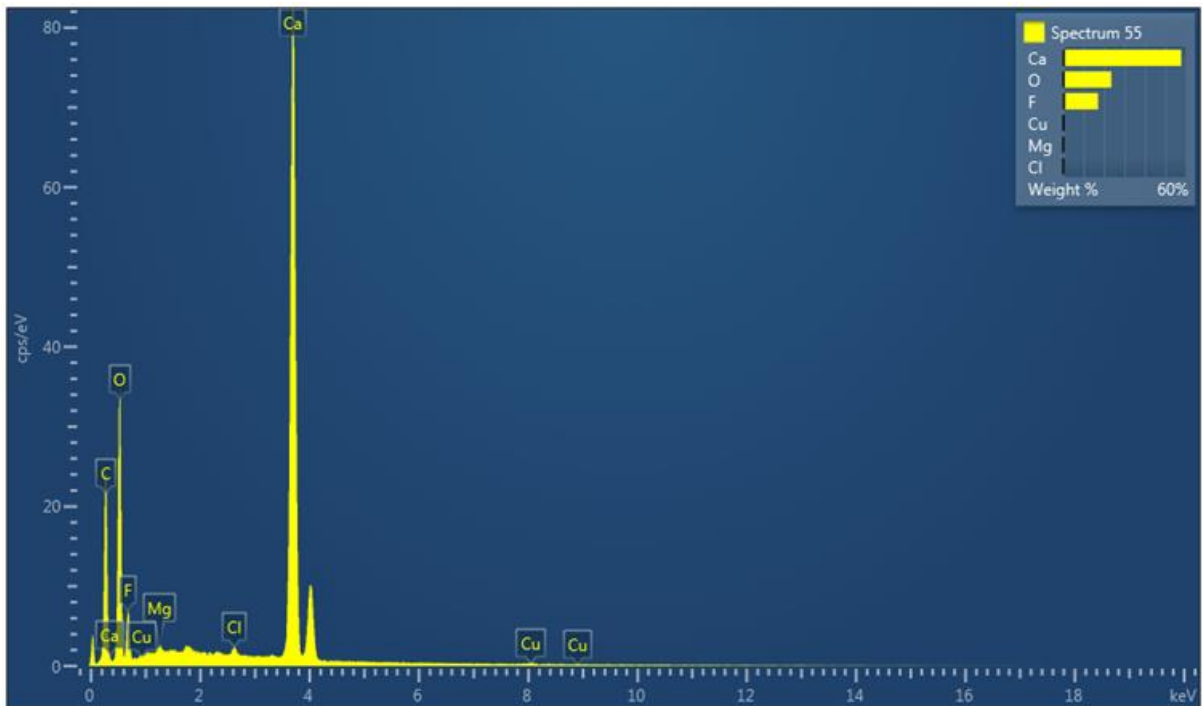


Table 15. Composition of cube particle with the dust sample collected in UQ monitor

| Element | Line Type | Apparent Concentration | k Ratio | Wt% | Wt% Sigma | Standard Label | Factory Standard |
|---------|-----------|------------------------|---------|-------|-----------|----------------|------------------|
| Mg | K series | 0.29 | 0.00195 | 0.48 | 0.08 | MgO | Yes |
| Cl | K series | 0.48 | 0.00423 | 0.48 | 0.05 | NaCl | Yes |
| Ca | K series | 60.07 | 0.53675 | 57.83 | 0.34 | Wollastonite | Yes |
| Cu | K series | 0.49 | 0.00486 | 0.62 | 0.13 | Cu | Yes |

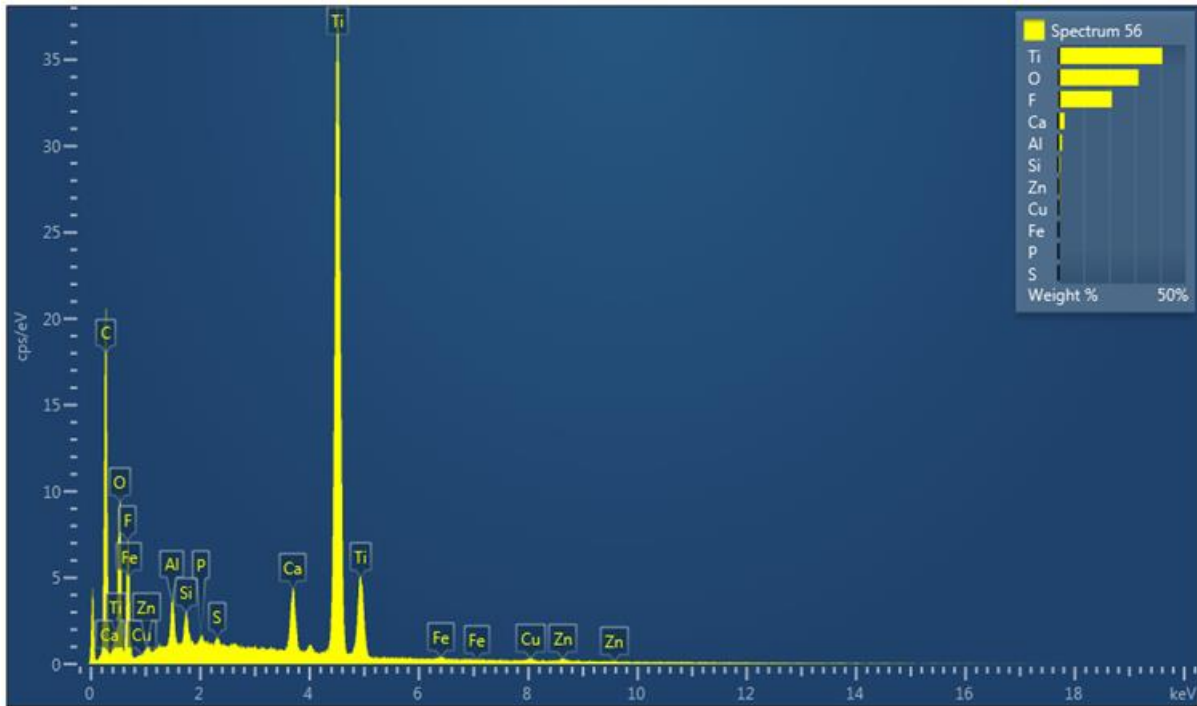


Table 16. Composition of the largest particle with the dust sample collected in UQ monitor

| Element | Line Type | Apparent Concentration | k Ratio | Wt% | Wt% Sigma | Standard Label | Factory Standard |
|---------|-----------|------------------------|---------|-------|-----------|--------------------------------|------------------|
| Al | K series | 1.55 | 0.01115 | 1.47 | 0.05 | Al ₂ O ₃ | Yes |
| Si | K series | 1.02 | 0.00805 | 0.84 | 0.04 | SiO ₂ | Yes |
| P | K series | 0.46 | 0.00259 | 0.24 | 0.04 | GaP | Yes |
| S | K series | 0.29 | 0.00252 | 0.20 | 0.03 | FeS ₂ | Yes |
| Ca | K series | 4.28 | 0.03822 | 2.46 | 0.05 | Wollastonite | Yes |
| Ti | K series | 54.25 | 0.54251 | 40.85 | 0.24 | Ti | Yes |
| Fe | K series | 0.31 | 0.00312 | 0.25 | 0.07 | Fe | Yes |
| Cu | K series | 0.66 | 0.00661 | 0.53 | 0.10 | Cu | Yes |
| Zn | K series | 0.79 | 0.00791 | 0.64 | 0.12 | Zn | Yes |

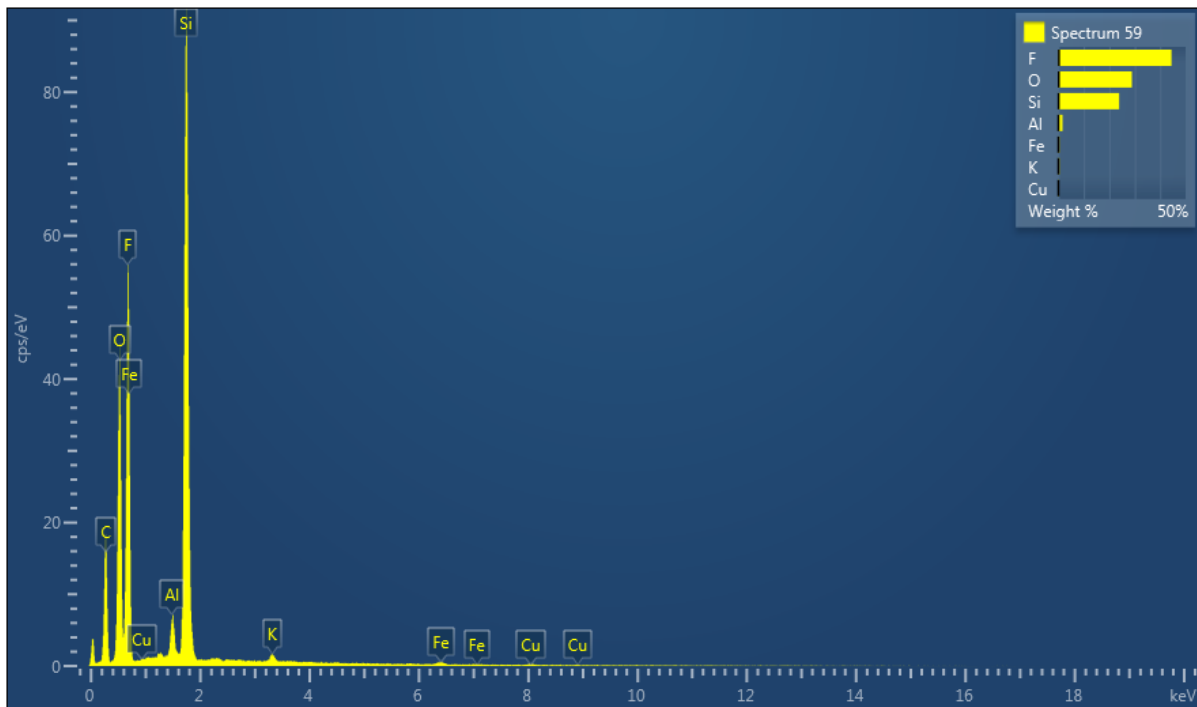


Table 17. Composition of the uneven particles with the dust sample collected in UQ monitor

| Element | Line Type | Apparent Concentration | k Ratio | Wt% | Wt% Sigma | Standard Label | Factory Standard |
|---------|-----------|------------------------|---------|-------|-----------|--------------------------------|------------------|
| Al | K series | 2.07 | 0.01488 | 1.62 | 0.05 | Al ₂ O ₃ | Yes |
| Si | K series | 33.49 | 0.26541 | 23.87 | 0.14 | SiO ₂ | Yes |
| K | K series | 0.67 | 0.00565 | 0.42 | 0.03 | KBr | Yes |
| Fe | K series | 0.58 | 0.00580 | 0.42 | 0.05 | Fe | Yes |
| Cu | K series | 0.39 | 0.00387 | 0.29 | 0.07 | Cu | Yes |

6. Discussions and conclusions

Selecting a cost-effective cleaning method and frequency for CSP plants is very site-specific since the density of the dust deposited on solar mirror depends on the rate and natural of dust accumulation, particulate size of the dust, the materials of the mirrors used, and the ambient conditions like relative humidity, rainfall, wind, and temperature. Therefore, collecting these data becomes an important first step.

Solar mirror made of different materials may respond differently to each cleaning method and may require different cleaning frequency.

Although there are several commercially available cleaning systems for the solar industry in general, automatically controlled high pressure jet washing and automatically controlled brush washing system were most widely used in solar mirror cleaning. While water pressure, water spray volume and water quality are important factor for effective cleaning, nozzle type, nozzle orientation, and nozzle distance to the solar mirror surface play important role in the system design.

On the basis of the discussions described above, the following conclusions are presented:

- Real time dust concentration in Collinsville has been quantified. The highest monthly average dust was about $31.5\mu\text{g}/\text{m}^3$ in October and the highest frequency was 898 for the density of $23\mu\text{g}/\text{m}^3$. In average, the dust was about $11\mu\text{g}/\text{m}^3$ in Summer, $13\mu\text{g}/\text{m}^3$ in Winter, $14\mu\text{g}/\text{m}^3$ in Autumn and $18\mu\text{g}/\text{m}^3$ in Spring.
- Ambient weather data including wind speed, wind direction, humidity and temperature have been monitored and recorded to gain an understanding of the processes which govern the dispersion and transport of dust from nearby sources.
- The interaction of dust with different mirror materials needed to be quantified in the future work.
- The average size of dust particles is generally around $15\mu\text{m}$ in Collinsville, and the composition of the dust are mainly albite and silicon dioxide. Also, some typical particulates (sodium chloride; carnallite; aluminium oxide) were detected.
- Future study on the most widely used high pressure jet washing system should be focused on the optimum selection of parameters such as water pressure, water flow rate and nozzle type etc.

7. Suggestions for future work

The data collected from the monitor and the dust sample from the 47mm filters are the air suspension dusts. To determine how these dusts deposit on solar surface, what is the effect on the mirror performance and how to optimise the mirror cleaning, research will be carried out by the Masters student, Shengzhe Yu.

7.1 Interaction of Dust and Mirror surface degradation

The deposition of dust on different mirror materials will be studied and the reflectance of each mirror will be measured. A metallic test bench has been built and installed in Collinsville. Figure 63 illustrates that five different types of mirrors have been prepared and placed on the bench. 10 samples with the size of 400×400 mm (0.5mm thickness) are arranged in 2 rows and 5 columns. The first row of the mirrors are to be left for dust

accumulation for a certain time period, and they will be used as the test samples for spray cleaning in wind tunnel. The second row of surfaces will be cleaned regularly and their reflectance will be measured before and after each leaning.



Figure 63. The test bench for dust collection on different mirrors installed at Collinsville

A reflectance meter, 410-Solar, will be used for measuring the reflectance of the mirrors and is shown in Figure 64. The reflectance measurement will be carried out each time before and after the mirror wash. By doing this, the mirror surface degradation due to the dust deposition and the effectiveness of mirror washing can be identified.

When washing each mirror, dust will be collected by collecting both the water and dust. After drying out the water, dust will be characterised to determine the interaction between dust and mirror materials.



Figure 64. 410-Solar reflectometer

6.2 Optimising water spray cleaning

After the dust characterisation and its interaction with different mirrors have been identified, effective cleaning method can be determined. Although there are several commercially available cleaning systems for the solar industry in general, automatically controlled high-pressure jet washing are one of the mostly suitable for solar mirror cleaning. While water pressure, water spray volume and water quality are important factor for effective cleaning, nozzle type, nozzle orientation, and nozzle distance to the solar mirror surface play important role in the system design.

UQ's Gatton wind tunnel (Figure 65) is an excellent testing facility for optimising solar mirror cleaning by high pressure jet washing. During the tests, each mirror sample will be fouled with dust either by simulating the dust on mirror surface or by exposing the mirror on site for required time. The fouled mirrors are tested in the wind tunnel by various parameter selections and the effectiveness of the cleaning can be measured by the 410-Solar reflectometer.

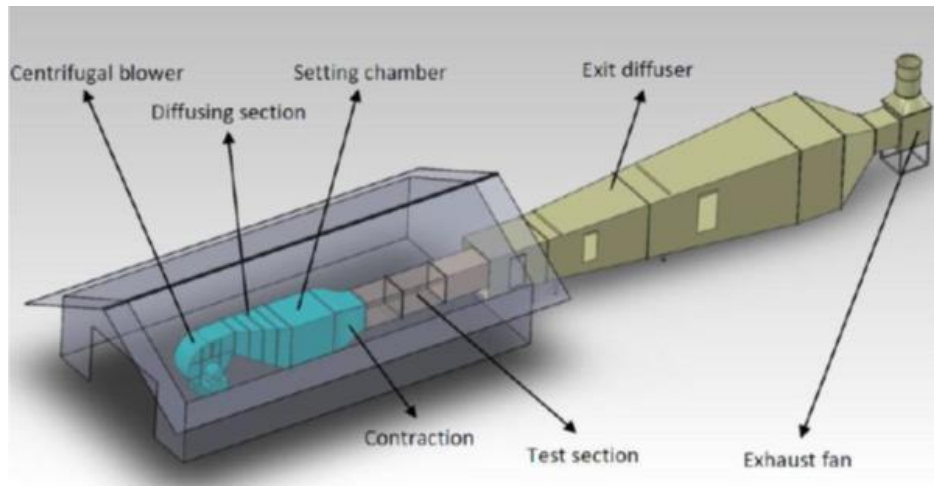


Figure 65. Gatton wind tunnel

During the test, the mirror is placed in the test section of the wind tunnel as shown in Figure 66. Different nozzle types, orientations of the nozzle, water flow rates, and water pressures will be selected to compare their effectiveness. The water droplet size and droplet speed will be measured by Phase Doppler Particle Analyzer (PDPA) to study the shear forces of the water to remove the dust.

Figure 67 shows the PDPA in Gatton wind tunnel.

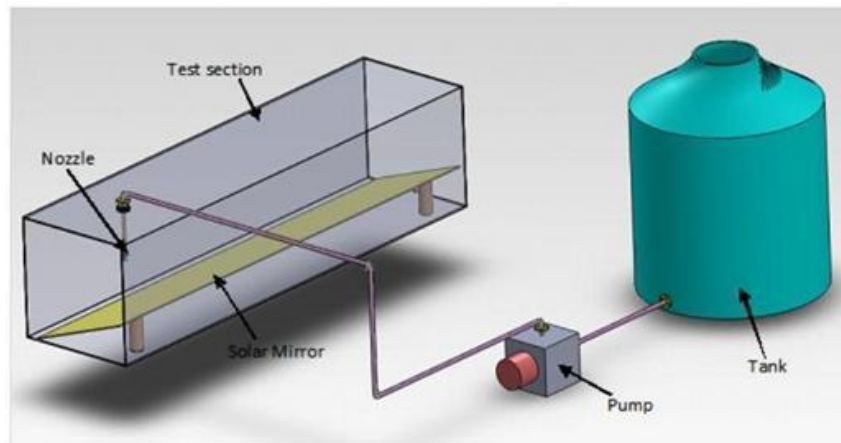


Figure 56. Proposed mirror cleaning test in Gatton wind tunnel



Figure 57. PDPA located in Gatton wind tunnel

8. References

- Bergeron, B K and Freese, J M "Cleaning Strategies for Parabolic-Trough Solar- Collector Fields; Guidelines for Decisions", SAND81-0385, 1981.
- Carbon Monitoring for Action, <http://carma.org/plant/detail/9067>
- RATCH-Australia Collinsville Energy Park,
<http://wmdl.com.au/Portals/3/Documents/Events/23%20-%20Thursday%20-%20Geoff%20Dutton%20-%20RATCH.pdf>
- Aránzazu, F.-G., E. C.-S. Maria, L. Javier and L.-M. Rafael (2013). Optimization of some aspects of CSP plants SolarPACES 2013 Conference. Las Vegas.
- McTainsh, G. and J. Pitblado (1987). "Dust storms and related phenomena measured from meteorological records in Australia." *Earth Surface Processes and Landforms* 12(4): 415-424.
- McEwan, I. K. and B. B. Willetts (1993). "Sand transport by wind: a review of the current conceptual model." *Geological Society, London, Special Publications* 72(1): 7-16.
- Hagen, L., S. Van Pelt and B. Sharratt (2010). "Estimating the saltation and suspension components from field wind erosion." *Aeolian Research* 1(3): 147-153.
- Shao, Y. (2008). *Physics and modelling of wind erosion*, Springer.
- Hamdy K. Elminir, Ahmed E. Ghitas, R.H. Hamid, F. El-Hussainy, M.M. Beheary, Khaled M. Abdel-Moneim, Effect of dust on the transparent cover of solar collectors, *Energy Conversion and Management* 47 (2006) 3192–3203
- Hottel, H. and B. Woertz (1942). "The performance of flat plate solar heat collectors " *ASME Transactions* 64: 91-104
- Dietz, A. (1963). "Diathermanous materials and properties of surfaces." *Zareem AM*: 59-86.
- Garg H. P. (1974) Effect of dirt on transparent covers in flat-plate solar energy collectors. *Solar Energy* 15, 299.
- Nimmo, B. and S. Saed (1979). "Effects of dust on the performance of thermal and photovoltaic flat collectors in Saudi Arabia." *Alternative Energy Sources* 2(145): 52.
- Sayigh, A. (1978). Effect of dust on flat plate collectors. *Sun: mankind's future source of energy*.
- Sayigh, A., S. Al-Jandal and H. Ahmed (1985). Dust effect on solar flat surfaces devices in Kuwait. Trieste, Italy, ICTP.
- Said, S. (1990). "Effects of dust accumulation on performances of thermal and photovoltaic flat-plate collectors." *Applied Energy* 37(1): 73-84.

- El-Nashar, A. M. (1994). "The effect of dust accumulation on the performance of evacuated tube collectors." *Solar Energy* 53(1): 105-115.
- Niknia, I, Yaghoubi M. & Hessami R. (2012): "A novel experimental method to find dust deposition effect on the performance of parabolic trough solar collectors", *International Journal of Environmental Studies*, DOI:10.1080/00207233.2012.664810
- Lovegrove K and Stein, W "Concentrating Solar Power Technology", Woodhead Publishing Limited, 2012.
- Strachan, J W. and Houser, R M. "Testing and Evaluation of Large-Area Heliostats for Solar Thermal Applications", SAND92-1381, 1993.
- Blackmon, J. B. and M. Curcija (1978). Heliostat reflectivity variations due to dust build up under desert conditions. Seminar on Testing Solar Energy Materials and Systems. M. Gaithersburg. Mt. Prospect, Ill., Institute of Environmental Sciences: 169-183.
- Deffenbaugh, D, Green, S and Svedeman, S "The Effect of dust accumulation on line-focus parabolic trough collector", *Solar Energy* Vol. 36, No. 2, pp. 139-146, 1986
- Morris, V "Cleaning agents and techniques for concentrating solar collectors" *Solar Energy Materials* 3 (1980) 35-55
- Roth, E. P. and Anaya, A.J. "The Effect of Natural Soiling and Cleaning on the Size Distribution of Particles Deposited on Glass Mirrors", *Journal of Solar Energy Engineering*, NOVEMBER 1980, Vol. 102 / 251.
- Fernández-García, A., L. Álvarez-Rodríguez, L. Martínez-Arcos, R. Aguiar and J. Márquez-Payés (2013). Study of different cleaning methods for solar reflectors used in CSP plants. *SolarPACES 2013 Conference*. Las Vegas.
- Aránzazu, F.-G., E. C.-S. María, L. Javier and L.-M. Rafael (2013). Optimization of some aspects of CSP plants *SolarPACES 2013 Conference*. Las Vegas.
- Burgaleta, J, Ternero, A, Vindel, D, Salbidegoitia, I and Azcarraga, G, "GEMASOLAR, key points for the operation of the plant", *Solar Paces 2012*
- SENER, PARIS-Autonomous cleaning system for Parabolic Troughs, www.sener.es.
- Dave Levitan, <http://spectrum.ieee.org/energywise/green-tech/solar/how-do-you-clean-258048-solar-thermal-mirrors-trucks-with-robot-arms>
- CSP O&M: Dust-proof solar fields, <http://social.csptoday.com/technology/csp-om-dust-proof-solar-fields>
- <http://latusolar.com/en/>
- www.novatec-biosol.com
- Mostafa Abdel Moneim, Integrated Solar Combined Cycle of Kuraymat, NREA
- Self-Cleaning CSP Collectors, <http://www.nrel.gov/docs/fy12osti/55448.pdf>

Cuddihy, E "Surface soiling: theoretical mechanisms and evaluation of low-soiling coatings"
Jet Propulsion Laboratory, California Institute of Technology, Pasadena, California 91109

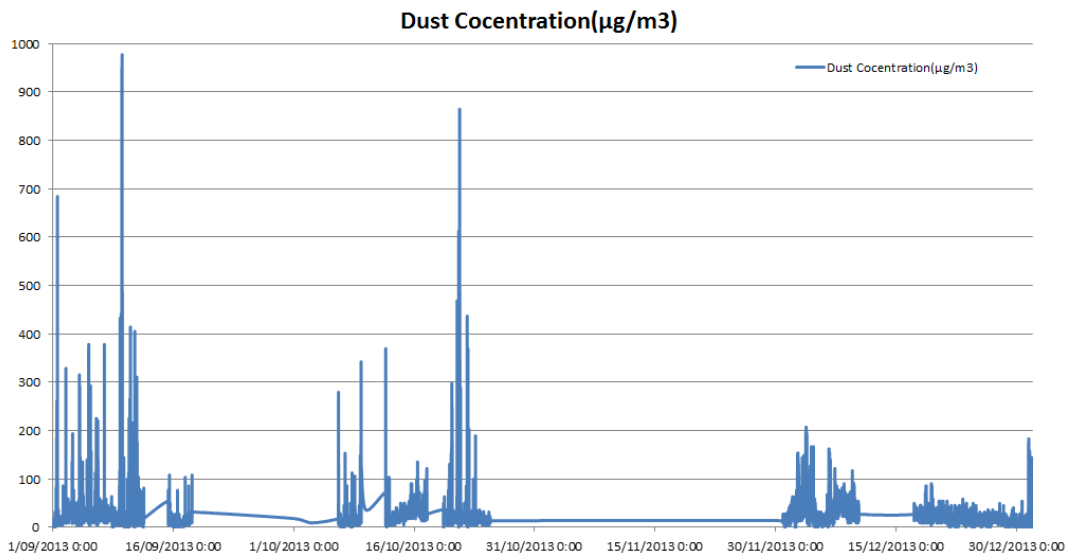
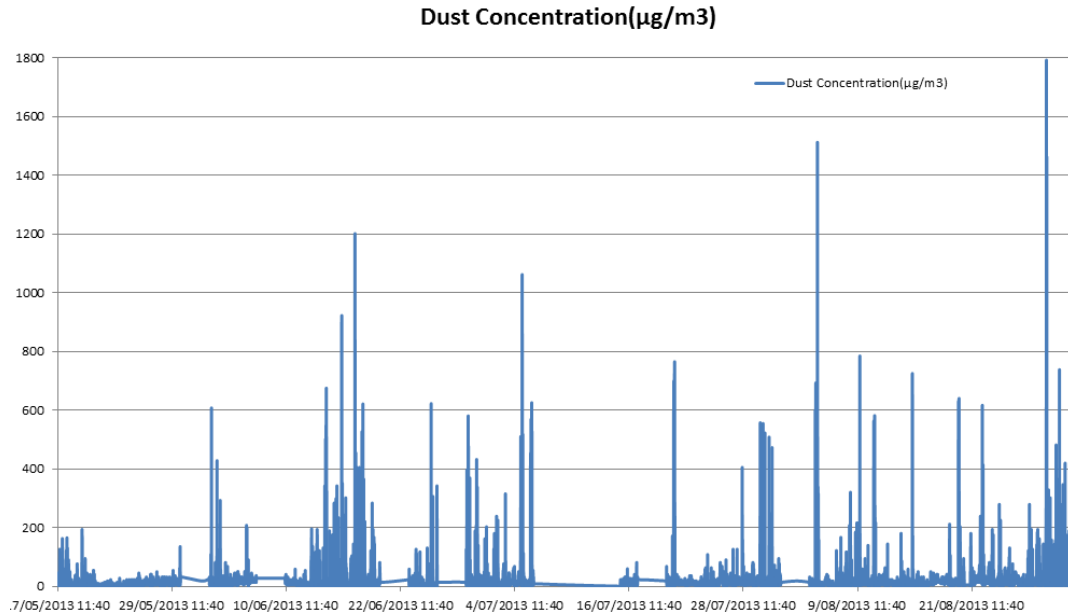
Kattke, K and Vant-Hull, L, Optimum target reflectivity for heliostat washing,
<http://cms.solarpaces2012.org/proceedings/paper/7b0145bef98>.

Pluschke, A. E., 2011, The development of a dust monitoring system for a geothermal power plant at Innamincka of South Australia, Bachelor of engineering thesis of the University of Queensland.

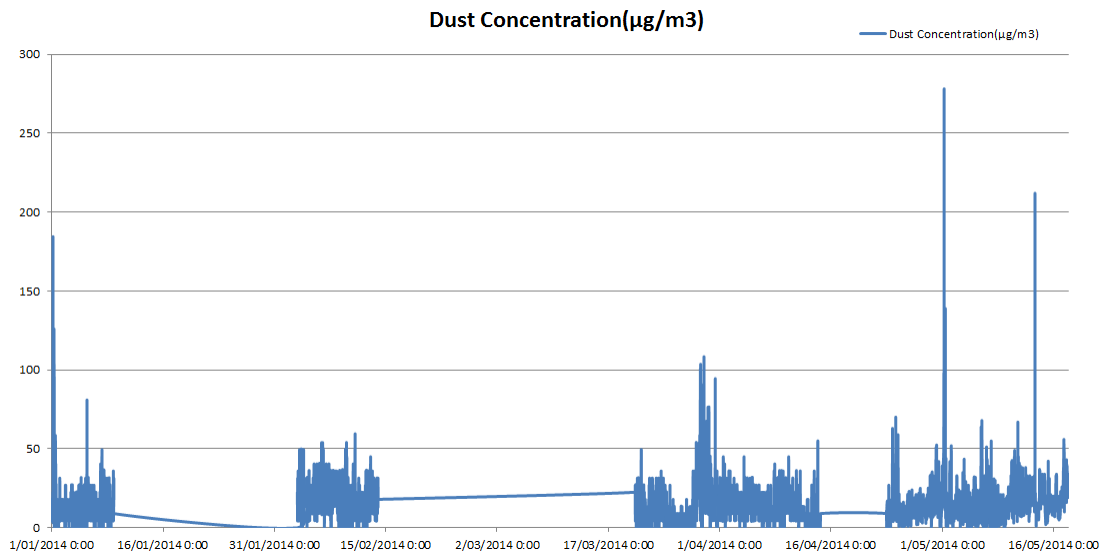
Met One Instruments, Inc., E-SAMPLER Particulate Monitor Operation Manual, 2011.

Appendix A: Time History of Dust Concentration

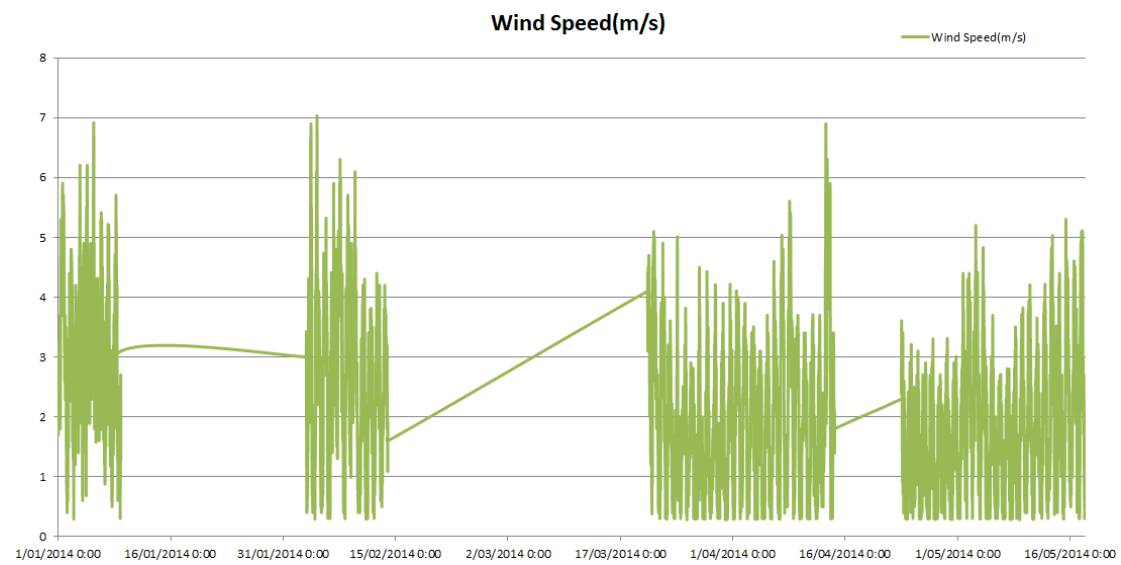
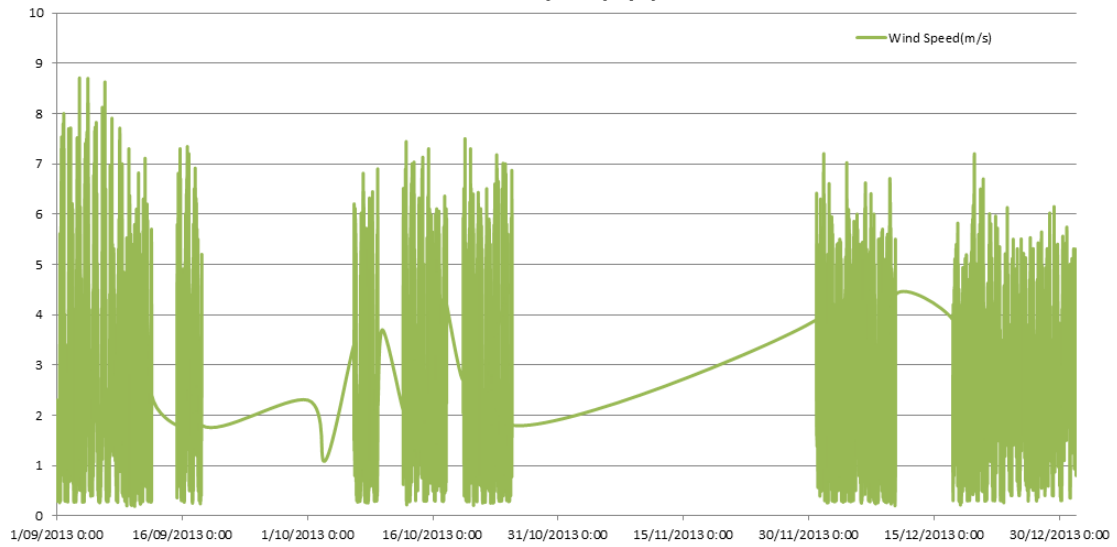
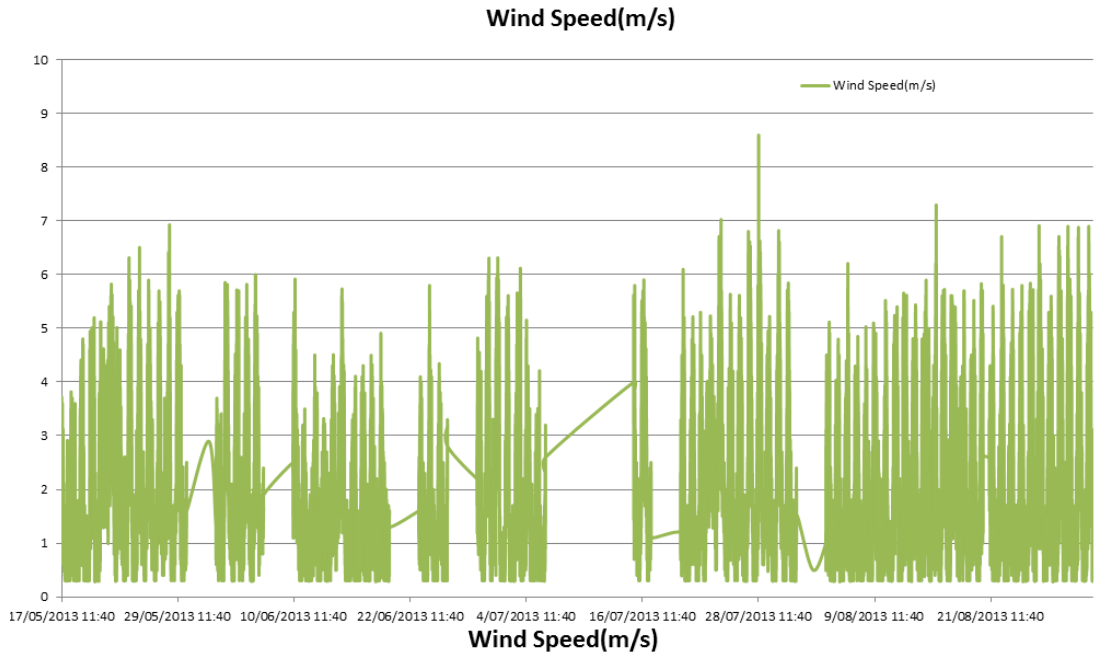
Due to the Telstra SIM card issues as mentioned before, manual downloads were conducted during the periods from November 2013 to March 2014 with some data lost. The manual downloaded data included: only one day data in November which was 30/11/2013; a full month data in December (from 01/12/13 to 31/12/13); nine days data in January (01/01/2014 to 09/01/14); about two weeks data in February (03/02/2014 to 14/02/14); and about 10 days data in March (20/03/14 to 31/03/14). From 23/04/14, new SIM card was installed and the data was downloaded through internet.



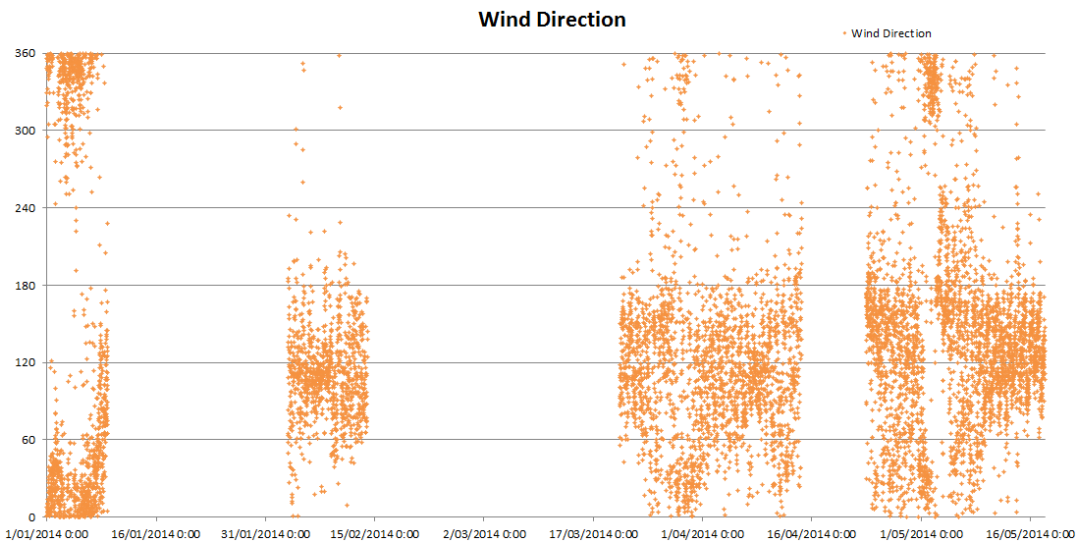
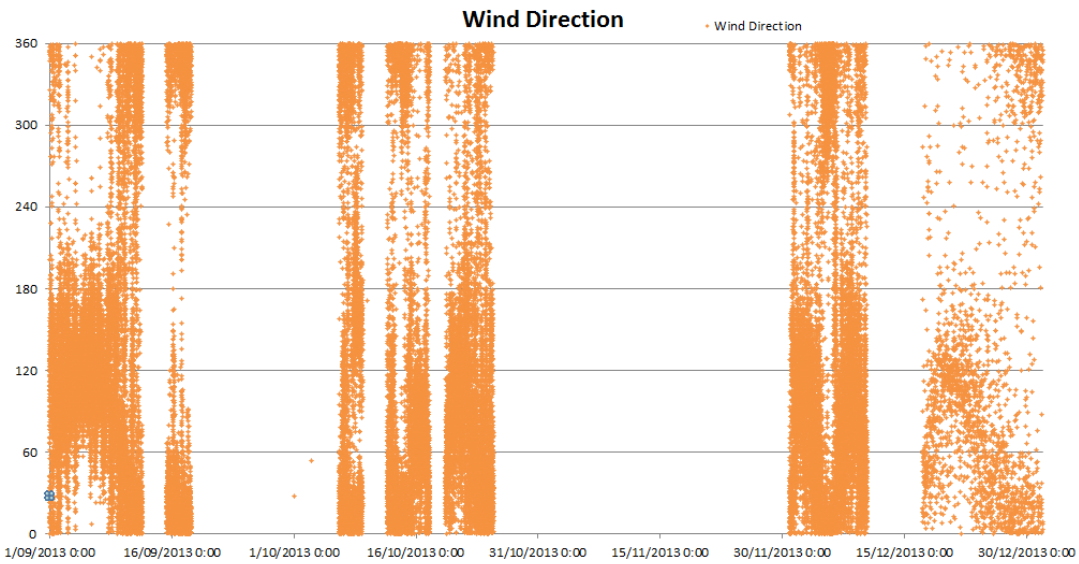
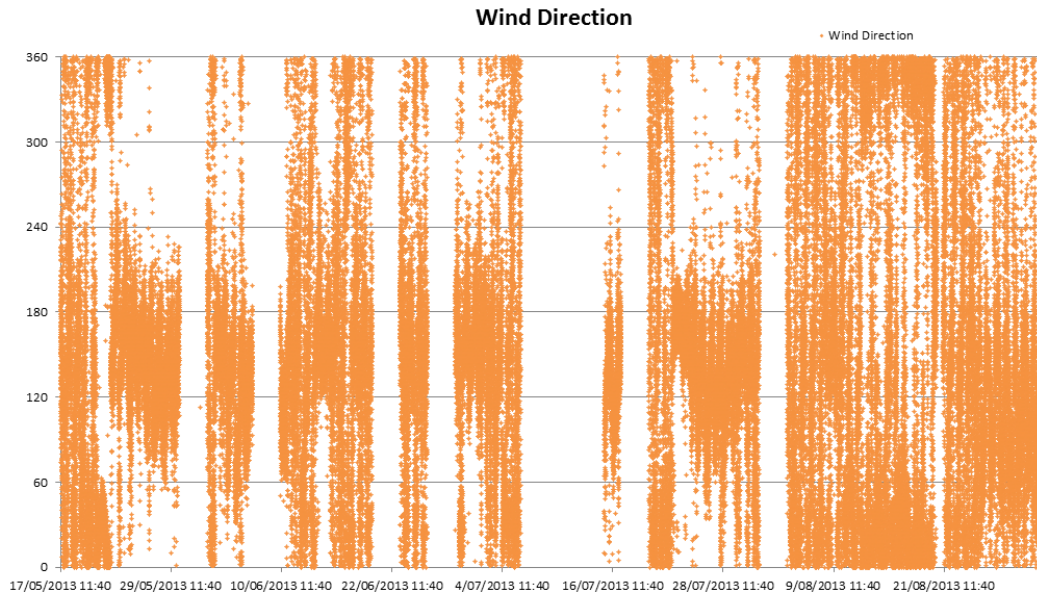
Collinsville Solar Thermal Project: Solar Mirror Cleaning Requirements



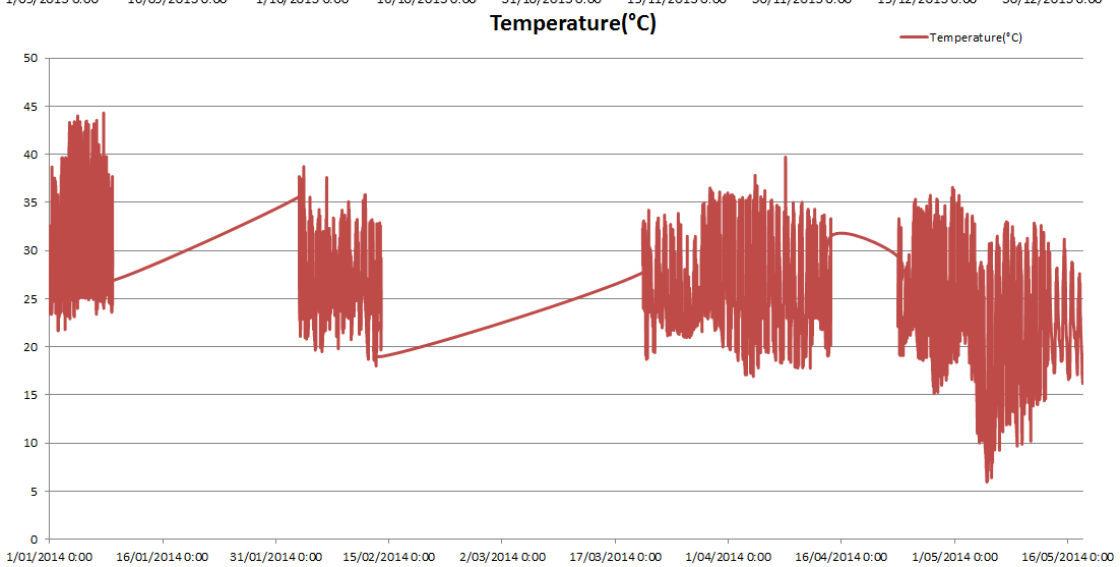
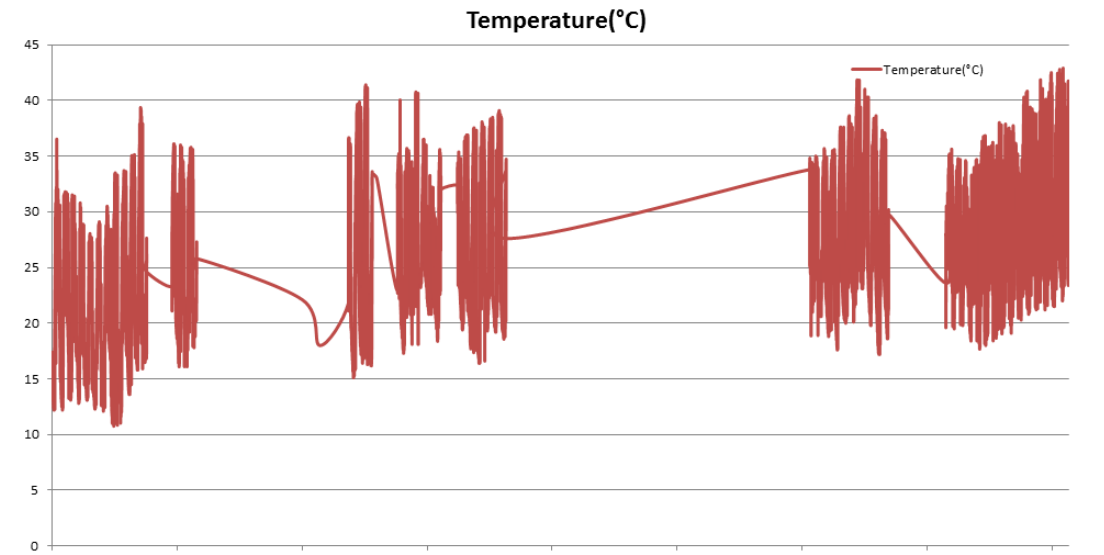
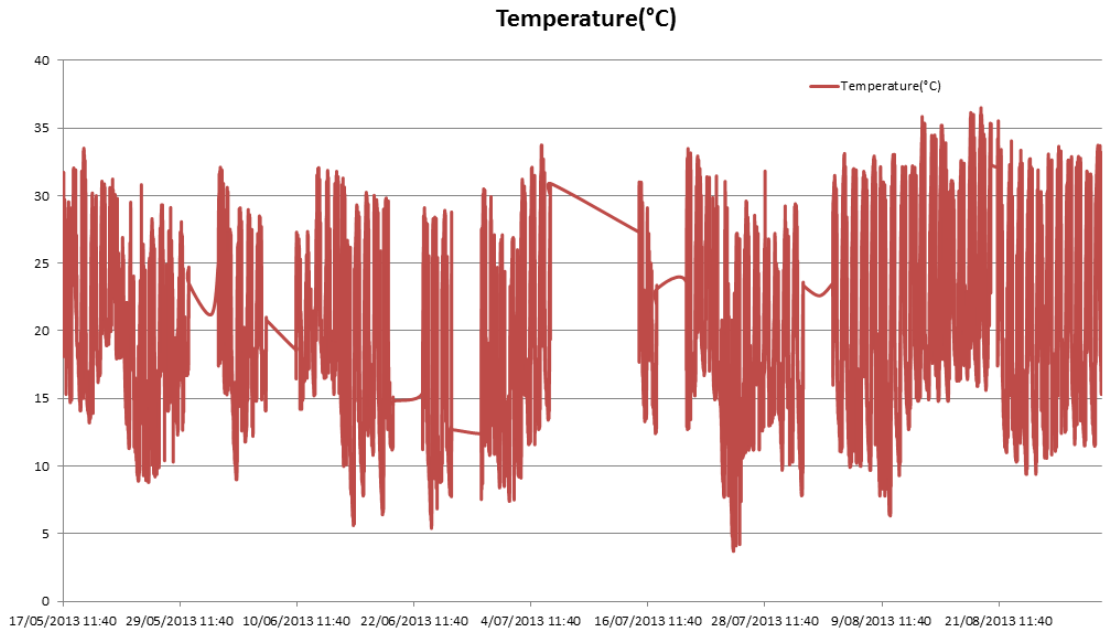
Appendix B: Time History of Wind Speed



Appendix C: Time History of Wind Direction



Appendix D: Time History of Temperature



**About the
Global Change Institute**

The Global Change Institute at The University of Queensland, Australia, is an independent source of game-changing research, ideas and advice for addressing the challenges of global change. The Global Change Institute advances discovery, creates solutions and advocates responses that meet the challenges presented by climate change, technological innovation and population change.

This technical report is published by the Global Change Institute at The University of Queensland.

T: (+61 7) 3443 3100 / E: gci@uq.edu.au
Global Change Institute (Bldg. 20)
Staff House Road
The University of Queensland
St Lucia QLD 4072, Australia

www.gci.uq.edu.au

